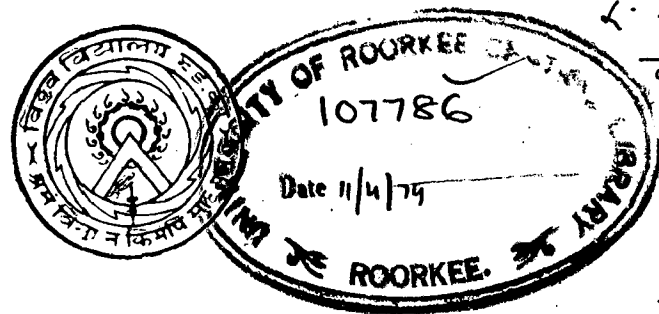


(T) ✓ C-73
NAN

**LATTICE DYNAMICAL ASPECTS OF
MÖSSBAUER PARAMETERS**

**Thesis Submitted to
UNIVERSITY OF ROORKEE
FOR THE AWARD OF THE DEGREE OF
DOCTOR OF PHILOSOPHY
IN
PHYSICS**

by
SHYAM SUNDER NANDWANI



**DEPARTMENT OF PHYSICS
UNIVERSITY OF ROORKEE
ROORKEE (India)
July, 1973**

CERTIFICATE

Certified that the thesis entitled ' LATTICE DYNAMICAL ASPECTS OF MOSSBAUER PARAMETERS' which is being submitted by Shri S.S.Nandwani in fulfilment for the award of the Degree of Doctor of Philosophy in Physics of University of Roorkee, Roorkee is a record of his own work carried out by him under my supervision and guidance since September 1969.

The matter embodied in this thesis has not been submitted for the award of any other Degree.

Dated July 31st, 1973.

S.P. Puri
(S.P. Puri)

A C K N O W L E D G E M E N T S

It is indeed a matter of great pleasure to express my deep sense of gratitude to Prof. S.P.Puri, Department of Physics, Punjab Agricultural University, Ludhiana (formerly at University of Roorkee, Roorkee), for the inspiration, encouragement and valuable guidance throughout this work.

The author also acknowledges with great pleasure the cooperation and understanding which he received from Dr. Deo Raj.


I feel beholden to Prof. S.K.Joshi, Head of Physics Department, University of Roorkee, for his interest and encouragement throughout the progress of this work. I sincerely appreciate the help extended to me by Dr. N.C. Varshneya.

Furthermore, I express my deep appreciation to Dr. R.Ingalls (Washington, U.S.A.) for sending the numerical values of $|\Psi(o)|^2$ at various volumes, Dr. W.Bührer (Würenlingen, Germany) for supplying the numerical value of phonon frequency distribution function, measured by them, for CsI lattice and Dr. Daniel L.Decker for sending the relevant zerox of the results of Mössbauer fraction versus pressure ($\text{Fe}^{57}:\text{Pt}$) measurements, from the doctoral thesis of Dr. John L. Stokes.

The author takes this an opportunity to express his gratefulness to his colleagues, especially to Messrs Vishwamittar, V.K. Agarwal, S.K.Mitra, M.P.Das, M.L. Sachdeva and G.C. Shukla for cooperation and useful discussions throughout the work.

The help from Director, Computer Centre, Structural Engineering Research Centre, Roorkee, is deeply acknowledged. Lastly, the author feels highly obliged to Council of Scientific and Industrial Research, New Delhi (India) and University Grants Commission, New Delhi (India) for the award of research fellowship. The financial support took the worry out of mind and enabled me to pursue my work with single mindedness.

Dated July 31, 1973


(S.S. Nandwani)

R E S U M E

Like the optical and acoustical resonance, Mössbauer effect may be defined as recoilless gamma resonance (emission, absorption or scattering) i.e. no part of the energy is expended in the recoil of the nucleus emitting or absorbing the gamma quanta. The probability f for the emission of gamma rays from radioactive atoms without energy exchange with the lattice vibrations of the crystal in which these are embedded, depends upon the strength of the interatomic forces between these atoms and the crystal. In this way Mössbauer effect offers a unique tool in its ability to look upon an impurity atom selectively. Precision measurements of the temperature dependent ' f ' yield the temperature dependence of the mean square displacement of the atom $\langle x^2 \rangle$ along the direction of gamma ray emission, through the relation, $f = \exp(-\frac{\langle x^2 \rangle}{\lambda^2})$. Another dynamical parameter of great significance is the mean square velocity $\langle v^2 \rangle$ of the Mössbauer atom which contributes partly to the shifts of the emission and absorption lines. The different lattice dynamical aspects which can profitably be studied from these parameters include: phonon spectra, **anisotropy of the atomic binding forces**, anharmonicity of the motion of the vibrating atom,

the evidence of the force constant change of the impurity-host to host-host coupling etc. The present work comprises of the following nine chapters.

Chapter I- After a brief introduction of the phenomenon of recoilless emission, absorption and discussion of the conditions under which it can be observed, an attempt is made to sketch briefly the various parameters of hyperfine interaction: I.S., Q.S. and magnetic splitting.

Chapter II- Herein is discussed the theoretical background for the quantitative estimation of lattice dynamical parameters: f and S.O.D. Furthermore the various solid state applications of Mössbauer effect are discussed.

Chapter III- Temperature dependence of Mossbauer fraction has been analysed in harmonic approximation for

- (i) 9.3 keV transition of Kr^{83} in solid Krypton,
- (ii) 77.3 keV transition of Au^{197} in Gold metal,
- (iii) 14.4 keV transition of Fe^{57} in natural Iron,
- (iv) 26.8 keV transition of I^{129} in Cesium Iodide lattice and
- (v) 81.0 keV transition of Cs^{133} in Cesium metal,

in the framework of real phonon frequency distribution function $g(\omega)$ (p.f.d.f.) for the host lattices.

Disagreement with the experiment for the first three cases was attributed to the presence of anharmonic effects. Nice agreement was obtained for the I^{129} transition in CsI lattice. In the case of Cs^{133} in cesium metal, although the measured $f(=5.50 \times 10^{-5})$, does not agree with the calculated $f(=0.062 \times 10^{-5})$ but in view of smallness of the measured effect, it is difficult to uphold its correctness.

Chapter IV- The analysis of recoilless fraction is improved by incorporating anharmonicity-quasiharmonic and explicit temperature dependent anharmonicity, in the calculated $f(T)$ variation in the three unexplained cases((i)-(iii)). The attempt seemed to succeed in the first two cases whereas in the case of natural iron, despite the inclusion of anharmonicity; a discrepancy between the calculation and experiment still persisted. However it was suggested that magnetic ordering in the case of ferromagnetic iron may be responsible for the residual discrepancy.

Chapter V- Based on the theory developed by Bashkirov and Selyutin, magnetic ordering contribution to $f(T)$ variation was included and good agreement with the experiment was obtained.

Chapter VI- Since the probability of Mössbauer effect increases with increase of pressure, the use of high

pressure may allow the study of Mössbauer effect for materials where it is either marginal or non-existent at zero external pressure. Using Grüneisen law, $f(P)$ at various temperatures has been calculated for

- (i) Au^{197} in Gold metal,
- (ii) I^{129} in Cesium Iodide,
- (iii) Cs^{133} in CsI and Cesium metal,
- (iv) 29.4 keV transition of K^{40} in Potassium metal,
- (v) Fe^{57} in natural Iron and
- (vi) 23.9 keV transition of Sn^{119} in white (β) Tin,

and the results are compared with available experimental data. For the first four cases where f (at $P=0$) is small even at low temperatures, we have predicted that with an impressed pressure of the order of 100-200 Kbar, one can perform the experiments with these nuclei at a relatively high temperature. In the case of Sn^{119} in white tin, good agreement with experiment is observed whereas much discrepancy still persists in the case of Fe^{57} in iron lattice. The discrepancy is qualitatively attributed to the change of polarisation of the iron lattice with pressure resulting from changes in the anisotropy and magnetostriction constants with pressure.

Chapter VII- It is generally assumed that the temperature dependence of isomeric shift (hence s-electron density at the nucleus) is negligible. We have analysed the temperature and pressure dependence of Mössbauer γ -ray

energy shift of Fe^{57} in natural iron taking into account the variation of the S.O.D. both with temperature and pressure, calculated from the experimental p.f.d.f. Data from the pressure studies has been utilized to evaluate two parameters; the proportionality constant, α , between the I.S. and $|\Psi_s(0)|^2$, and X, the number of electrons transferred with change of volume from the 4s to 3d band. It appears that in the case of magnetic lattice such as iron the temperature dependence of S.O.D. calculated from the p.f.d.f. is inadequate to explain the observed energy shift, that instead a contribution arising from magnetization seems important which is to be expected theoretically. On including a term proportional to the magnetisation, the calculated temperature variation of the I.S. ($\sim (0.60 \pm 0.03) \times 10^{-4} \text{ mm sec}^{-1} \text{ } ^\circ\text{K}^{-1}$) compares well with that determined from the pressure studies of the γ -ray energy shift ($\sim (0.55 \pm 0.09) \times 10^{-4} \text{ mm sec}^{-1} \text{ } ^\circ\text{K}^{-1}$).

Chapter VIII- Analysing the pressure variation of f for an impurity atom with Debye theory, quantitative estimation of the force constant change q'/q for impurity-host binding to host-host binding for Fe^{57} in Cu, V and Ti is calculated. This is compared with that obtained from the independent temperature studies of f and the results are discussed.

Chapter IX- Lastly in this chapter it is shown that the combined effect of high pressure and temperature can yield information regarding the force constant change, q'/q with temperature, change of the 3d-4s band electron transfer coefficient with temperature. Pressure dependence of Mössbauer intensity for Fe^{57} in Pt has been studied experimentally at two temperatures. Analysing the measurement the force constant change q'/q is found to be same (0.45) at both the temperatures. Secondly measured Mössbauer spectrum shift versus pressures at two temperatures for Fe^{57} in Cu was analysed in the framework of Debye theory to calculate the temperature dependence of I.S. with pressure. This analysis shows that at 82 Kbar the s-electron density at 298°K becomes equal to that at 1 bar and 94°K . It is also found that the electron transfer parameter X at 94°K is greater than that at 298°K by about 25%. Finally the measured $f(T)$ at two pressures for Fe^{57} in natural iron is analysed in the framework of experimental p.f.d.f. after accounting for the S.O.D. contribution for anharmonicity and magnetic ordering. The analysis leads to an interesting result that at 22°C the s-electron density at iron nucleus at 1 bar equals to that at 88 Kbar and 700°C . This has been explained qualitatively in the framework of the band structure of Iron lattice.

C O N T E N T S

<u>Chapter</u>	<u>Page No.</u>
I- <u>INTRODUCTION</u>	... 1-20
1.1 Mössbauer effect	... 1
1.2 Resonance	... 1
1.3 Factors responsible for resonance	... 2
1.4 Earlier methods to observe gamma-resonance	... 4
(i) Centrifuge	... 4
(ii) Heat	... 5
(iii) Previous recoil	... 5
1.5 Mössbauer discovery and its interpretation	... 6
1.6 A Mössbauer spectrum	11
1.7 Importance of the Mössbauer effect	... 12
1.8 Parameters of gamma-resonance spectra	... 13
(a) Dynamical parameters	... 13
(b) Electromagnetic parameters	... 14
(i) Isomer shift	... 14
(ii) Quadrupole splitting	... 17
(iii) Magnetic hyperfine splitting	... 19
II- <u>LATTICE DYNAMICAL PARAMETERS OF GAMMA RESONANCE SPECTRA</u>	... 21-41
2.1 Introductory remarks	... 21
2.2 Probability of the Mössbauer effect	... 21
2.3 Second order Doppler effect	... 27
2.4 Experimental determination of Mössbauer fraction	... 31
2.5 Applications of Mössbauer effect to the study of solid state physics	... 35
(a) Determination of $\langle x^2 \rangle$ and $\langle v^2 \rangle$... 35
(b) Evidence of force constant change and existence of localised modes for an impurity atom	... 35
(c) Anharmonicity	... 36
(d) Anisotropy	... 37
(e) Surface physics	... 37
(f) Molecular crystal	... 38
(g) Zero point root mean square velocity	... 40

<u>Chapter</u>	<u>Page No.</u>
III- <u>ANALYSIS OF MÖSSBAUER FRACTION IN THE HARMONIC APPROXIMATION</u>	... 42-53
3.1 Introduction	... 42
3.2 9.3 keV transition of Kr ⁸³ in solid Krypton	... 43
3.3 14.4 keV transition of Fe ⁵⁷ in natural Iron	... 45
3.4 77.3 keV transition of Au ¹⁹⁷ in Gold metal	... 47
3.5 26.8 keV transition of I ¹²⁹ in CsI lattice and 81.0 keV transition of Cs ¹³³ in Cs metal	... 47
IV- <u>ANALYSIS OF MÖSSBAUER FRACTION IN THE ANHARMONIC APPROXIMATION</u>	... 54-66
4.1 Introduction	... 54
4.2 9.3 keV transition of Kr ⁸³ in solid Krypton	... 60
4.3 14.4 keV transition of Fe ⁵⁷ in natural Iron	... 63
4.4 77.3 keV transition of Au ¹⁹⁷ in Gold metal	... 65
V- <u>ANALYSIS OF MÖSSBAUER FRACTION IN SPIN-ORDERED SYSTEM</u>	... 67-72
5.1 Introduction	... 67
5.2 14.4 keV transition of Fe ⁵⁷ in natural Iron	... 71
VI- <u>THE INFLUENCE OF PRESSURE ON MÖSSBAUER EFFECT</u>	... 73-82
6.1 Introduction	... 73
6.2 77.3 keV transition of Au ¹⁹⁷ in Gold metal	... 75
6.3 26.8 keV transition of I ¹²⁹ in Cesium iodide and 81.0 keV transition of Cs ¹³³ in Cesium metal	... 76
6.4 23.9 keV transition of Sn ¹¹⁹ in white Tin (β)	... 77
6.5 29.4 keV transition of K ⁴⁰ in Potassium metal	... 79
6.6 14.4 keV transition of Fe ⁵⁷ in natural Iron	... 80

<u>Chapter</u>	<u>Page No</u>
VII- <u>ANALYSIS OF MÖSSBAUER GAMMA-RAY ENERGY SHIFT</u>	... 83-95
7.1 Introduction	... 83
7.2 Energy shift due to S.O.D. in CsI, Cs, Au, K and Kr lattices	... 84
7.3 Energy shift due to S.O.D. in Fe lattice	... 85
VIII- <u>ANALYSIS OF MÖSSBAUER PARAMETERS FOR AN IMPURITY ATOM</u>	... 96-104
8.1 Introduction	... 96
8.2 Fe ⁵⁷ as an impurity in Cu lattice	... 103
8.3 Fe ⁵⁷ as an impurity in Ti lattice	... 103
8.4 Fe ⁵⁷ as an impurity in V lattice	... 103
IX- <u>COMBINED EFFECT OF TEMPERATURE AND PRESSURE ON MÖSSBAUER PARAMETERS-ANALYSIS</u>	... 105-116
9.1 Introduction	... 105
9.2 14.4 keV transition of Fe ⁵⁷ in Platinum lattice	... 105
9.3 14.4 keV transition of Fe ⁵⁷ in Copper lattice	... 106
9.4 14.4 keV transition of Fe ⁵⁷ in natural Iron	... 113
<u>REFERENCES</u>	... 117-129
<u>LIST OF PUBLICATIONS</u>	

CHAPTER I

I N T R O D U C T I O N

1.1 MOSSBAUER EFFECT- The Mössbauer effect is named after the German physicist Rudolf L Mössbauer for the work he carried out at the Max Planck Institute, Heidelberg in 1957. In short, it can be defined|1| as recoilless gamma resonance fluorescence (emission, absorption and scattering), i.e. no part of the energy is expended in recoil of the nucleus emitting or absorbing the gamma quanta. The consequences of this momentous discovery were so far reaching that research activity in Mössbauer effect sprang up in all the major laboratories throughout the world. In recognition of this contribution, he was awarded the Nobel prize in physics for 1961.

1.2 RESONANCE- The phenomena of resonance with visible and ultraviolet light (atomic resonance) has been known for a long time. Thus when a beam of white light from a mercury lamp is made to pass through a glass vessel containing mercury vapour, strong resonance absorption occurs which is due to the transition of an atom from ground state to the excited state. Since atomic resonance depends essentially on the existence of quantised levels and these levels also occur in nuclei, the possibility of observing nuclear resonance was obviously anticipated. A number of attempts to observe resonant absorption

with gamma radiation were made-but without success.

A natural question arises why it is relatively easy to observe resonance fluorescence with visible light but not with gamma radiation.

1.3 FACTORS RESPONSIBLE FOR RESONANCE- In order to see the factors responsible for observation of any type of resonance, consider a free atomic or nuclear system of mass M with two states A and B separated by an energy E_0 . When this atom or nucleus emits a photon, the system must recoil to conserve momentum. The recoiling system takes a share R of the available energy E_0 . Thus if E_γ is the energy of the emitted photon ($E_\gamma < E_0$) then because of momentum conservation,

$$\begin{aligned} p &= \text{momentum of the recoiling system} \\ &= E_\gamma/c, \text{ momentum of the emitted photon} \quad \dots (1.1) \end{aligned}$$

where c is the velocity of photon. Therefore, in the non-relativistic-approximation the recoiling system receives an energy $R = \frac{p^2}{2M} = \frac{E_\gamma^2}{2Mc^2}$. Furthermore according to energy conservation

$$\begin{aligned} E_0 &= E_\gamma + R \\ \text{or} \quad R &= E_0 - E_\gamma = \frac{E_\gamma^2}{2Mc^2} = \frac{E_0^2}{2Mc^2} \quad \dots (1.2) \end{aligned}$$

which gives the loss in the energy of emitted photon due to recoil of the system.

On the other hand a detailed examination employing

perturbation theory shows that any excited level (here decaying state B) can not be characterised by one well defined excitation energy E_0 only; but that the energy E of the state is distributed about the centre energy E_0 as shown in Fig.(1.1a) so that it is characterised also by its natural width Γ . This width Γ (also called half maximum width) is related to the mean life time τ of the excited state B by the Heisenberg uncertainty relation

$$\Gamma \tau = \hbar \quad \dots (1.3)$$

Thus the photon emitted in the transition from B to A shows a distribution in energy centred around $E_0 - R$ and displays a natural shape of width Γ (Fig.(1.1b)).

Furthermore to have resonance absorption, the energy of the incident gamma quantum from emitter must be (including loss of part of the energy due to the recoil of the absorber) greater than the resonance energy E_0 by same amount R as shown in Fig.(1.1c) i.e. it should possess energy $E_0 + R$. Thus only the overlap portion of the Fig.(1.1b) and (1.1c) as shown in Fig.(1.1d) is responsible for resonance fluorescence. Since the resonance maxima for emitter and absorber are separated by $2R$, the condition for overlap and hence for resonance becomes

$$2R \leq \Gamma \quad \dots (1.4)$$

Now let us see whether this condition of resonance is

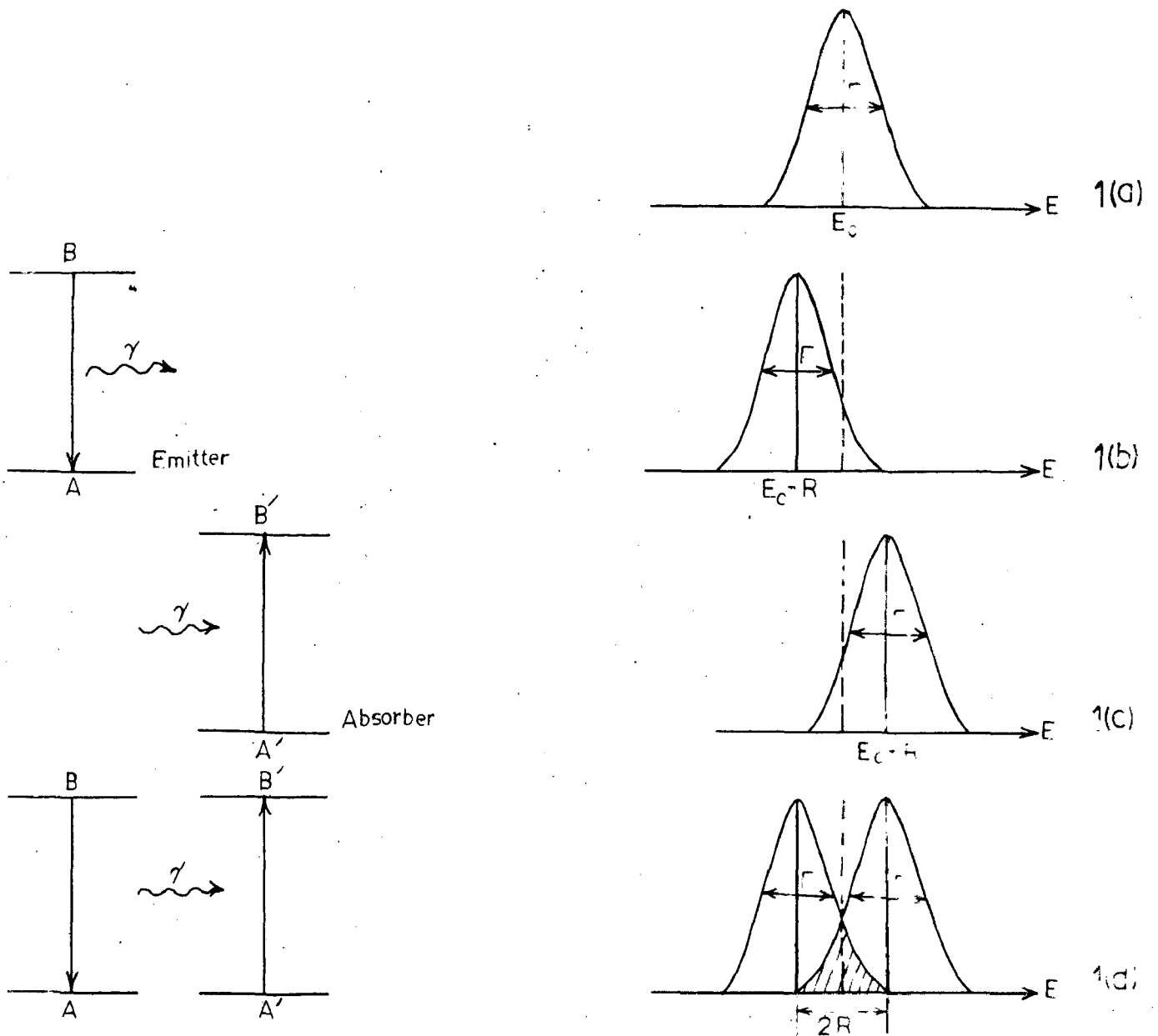


FIG.1.1- Energy distribution involved in resonance fluorescence:

- (a)- energy distribution of any excited state with excitation energy E_0 .
- (b)- energy distribution of photons emitted in transition $B \rightarrow A$ (emitter)
- (c)- energy spectrum required to excite the state A' and to provide the recoil energy R (absorber).
- (d)- Overlap of (b) and (c) viz. shaded area gives the probability of resonance.

satisfied in the atomic and nuclear cases.

(i) Atomic system - Take the case of mercury line for which $E_0 \sim 5$ eV, $M \sim 200$ amu therefore $R \sim 10^{-10}$ eV. τ , mean life of the excited state $\sim 10^{-8}$ sec, thus $\Gamma = \hbar/\tau \sim 10^{-8}$ eV

$\therefore 2R \ll \Gamma$ implying thereby that atomic resonance is easily observed.

(ii) Nuclear system- Take a typical case of γ -ray with energy $E_0 \sim 100$ keV, $M \sim 100$ amu, therefore $R \sim 10^{-2}$ eV. Since $\tau \sim 10^{-10}$ sec. therefore $\Gamma \sim 10^{-6}$ eV and thus $2R \gg \Gamma$ i.e. the gamma ray energy E_0 is well off the centre of the resonant line and hence no observable resonance effect is found under ordinary conditions.

1.4 EARLIER METHODS TO OBSERVE GAMMA RESONANCE

Prior to Mössbauer's discovery various methods were used to compensate for the recoil loss and thus to bring emission and absorption lines back into coincidence.

(i) Centrifuge- In order to observe resonance absorption or scattering with gamma rays the energy

shift $2\Delta E = \frac{E_0^2}{Mc^2}$ must be restored in some way. This can

be done if the gamma ray of interest is radiated by a

nucleus which is approaching the absorber with velocity

$U = \frac{E_0}{Mc}$, then the Doppler shift is $\frac{UE_0}{c} = \frac{E_0^2}{Mc^2}$ and the

resonance condition is easily satisfied. Such a type of

experiment was performed by Moon |2| in 1951 for the isotope Au^{198} . He was able to bring about resonance absorption by placing a radioactive source on a rapidly spinning wheel and the velocity required to compensate for the recoil energy losses in both emission and absorption was of the order of 8×10^4 cms/sec, which is close to the maximum realizable velocity with an ultra-centrifuge.

(ii) Heat - The second method makes use of the fact that the emitting and absorbing atoms are in constant thermal motion which introduces an additional widening of the emission and absorption lines. This broadening, commonly known as Doppler broadening D , increases with temperature as $D = 2\sqrt{RkT}$. Malmfors |3| in 1953 has successfully demonstrated the resonance scattering of γ -rays using a stationary source (Au^{198}) and absorber with the source heated to 1063°C . The large increase in the Doppler broadening of the gamma line energy is sufficient to restore the resonance condition for some of the emitted γ -rays.

(iii) Previous recoil- In this method utilized by Metzger |4| the recoil due to the previous emission of γ -quantum or β - is used to compensate for the recoil in the subsequent γ -emission.

One can see that all these methods of compensating for recoil, are, by their very nature, not very efficient

and require a good deal of ingenuity and skill. Their most serious drawback is that they cannot restore the natural width of the lines from their recoil broadened state and thus can not be used in investigating small changes in the energy levels. A remarkable new method for producing nuclear gamma resonance was reported by Mossbauer^[1] in 1958, who instead of compensating the nuclear recoil, tried to eliminate it.

1.5 MÖSSBAUER DISCOVERY AND ITS INTERPRETATION-

Rudolf L Mössbauer working in Heidelberg in 1957 demonstrated dramatically and yet accidentally the feasibility of observing γ -ray resonance by embedding the emitting and absorbing nuclei in well bound crystal lattices. He was investigating the nuclear resonance scattering of the 129 keV gamma ray from Ir^{191} , through a crystalline natural iridium (38.5% Ir^{191}). For this transition, R is 0.05 eV, whereas Doppler broadening D at room temperature is about 0.1 eV and thus there is an overlap of absorption and emission lines without employing any of the methods mentioned already to supply the missing energy. He also observed that this resonance absorption effect increased with decrease of temperature contrary to expectations. Furthermore by imparting modest velocities of the order of few cm/sec., he obtained an absorption line of width at half maximum Γ of nearly 2 cms/sec. which is double the natural line width. This is in agreement

with the picture of recoilless emission and absorption. The factor of two arises because the observed spectrum is the result of folding an emission and absorption line each with a width Γ . Mössbauer thus in single experiment achieved the compensation of recoil and also eliminated the Doppler broadening.

The essential mechanism underlying Mössbauer discovery and explanation of recoilless emission and absorption of γ -rays was well known in the theories of X-ray crystallography|5| and neutron scattering|6|. It was in fact Lamb's paper |6| on 'Capture of Neutrons by Atoms in a Crystal' which led Mössbauer to the interpretation of his unexpected and remarkable result. The detailed theoretical papers giving classical and quantum mechanical interpretation of the mechanism have been put forward by the discoverer |1,7,8| and others|9-12|. We would not reproduce the whole theory but will simply mention the salient features of the phenomena of recoilless emission and absorption of γ -rays.

Let the nucleus of one of the atoms of the crystalline lattice decay by γ -emission with energy $E=h\nu$ and momentum $p = \frac{h\nu}{c}$. Furthermore we examine as to how the emitting system takes the recoil momentum and the recoil energy. Since the atom, whose nucleus decays, is a part of the crystal lattice, we consider the following possibilities for accounting the conservation of momentum.

(i) the atom alone may recoil and get displaced from its equilibrium position in the lattice,

(ii) the crystal lattice as a whole recoils so that every atom in the lattice moves and the lattice structure is still preserved,

(iii) the lattice vibrations or any other collective oscillations of the lattice may take up the recoil momentum.

It is well known that the energy required to displace an atom from its equilibrium in a well bound crystalline lattice is of the order of 10 eV whereas the recoil energy is same 10^{-2} eV. Thus it looks improbable that the individual atom will take the recoil and get displaced from its equilibrium position. Lattice vibrations similarly cannot take up the momentum as to each wave with its momentum pointing in one direction there will be corresponding one, pointing in the opposite direction. Thus it appears that as a consequence of the γ -emission, the entire crystal recoils. In fact the momentum p is transferred to a single nucleus in a time short compared to the period of lattice vibrations and then distributed throughout the whole crystal with the velocity of sound via the binding forces. The mass of the recoiling system is therefore the mass of the crystal which is same 10^{21} times or more (assuming the crystal has a size of 1 cc) greater than the mass of a single atom and hence the energy taken up during this recoil is insignificant. Thus,

although the entire crystal takes the momentum the energy transfer is negligibly small, making recoilless emission possible.

Now let us consider the energy conservation. We again have to consider the above three possibilities, viz.,

- (i) the individual atom may take the energy,
- (ii) the entire crystal may take the energy or,
- (iii) the energy may be dissipated in creating lattice vibrations.

We have seen already that the first possibility is ruled out. The crystal does not take much energy even though it takes the momentum. It therefore appears that the recoil energy R must be dissipated to the lattice by increasing the vibrational energy of the crystal. An essential feature of the picture is that the energy states of the lattice being quantized; only certain energy increments are allowed and unless the recoil energy corresponds closely with one of the allowed increments, it cannot be transferred to the lattice, thus ensuring that the whole crystal recoils leading to negligible recoil energy.

To understand the possibility of the occurrence of the Mössbauer effect and the conditions under which it will occur, we take the case of a real crystal where all the atoms are vibrating with different frequencies ranging from zero to ν_{\max} . Let us denote the

initial state of the lattice of a particular crystal, before the nucleus in question has emitted a gamma ray by n_i and let n_f be the quantum number which describes one of the possible final states, after the nucleus has radiated the gamma ray. There are in general many possible final states for a given initial state. The initial state itself may be one of the possible final states. Let $E(n_i)$ and $E(n_f)$ be the corresponding lattice energies and $P(n_f, n_i)$ stand for the probability (normalised to unity) that the lattice goes from initial state n_i to the particular final state n_f . Then Lipkin's sum rule states|9|,

$$\sum_{n_f} [E(n_f) - E(n_i)] P(n_f, n_i) = R \quad \dots (1.5)$$

Stated in words, it implies that if many emission processes are considered, the average energy transferred per event to the lattice is exactly the free atom recoil energy R . Further those transitions in which no energy is transferred to the lattice i.e., the Mössbauer transitions, contribute nothing to the sum. Thus the sum rule allows an appreciable probability for no energy transfer to the lattice, if there is an appreciable probability for an energy transfer which is greater than that which a freely recoiling nucleus would receive. The true situation is, of course, not so simple. In fact we will tend to get an increased Mössbauer effect when there are many high frequency modes available to which the nuclei can transfer

energy, i.e., in a crystal with a high Debye temperature. Further at a low temperature close to absolute zero, the atomic vibrations within the crystal lattice are reduced to practically zero, so that during emission and absorption the atoms have little or no motion. Under these conditions the Doppler broadening is reduced practically to zero and the observed line reveals its natural line width.

The Mössbauer effect has been detected in about 88 γ -ray transitions in 72 isotopes of 42 different elements [13,14] e.g., 14.4 keV Fe⁵⁷, 23.9 keV Sn¹¹⁹ and 57.6 keV ¹²⁷I etc. 14.4 keV γ -ray of Fe⁵⁷ has been extensively used because of high recoilless fraction ($\sim 70\%$) even at room temperature, the relatively long half-life of the state (0.1 μ sec.) with the result that the natural line width is quite narrow ($\sim 4.6 \times 10^{-9}$ eV). Further large total cross-section at resonance (1.5×10^{-18} cm²) renders experiments feasible with absorbers of natural iron, even though the natural abundance of Fe⁵⁷ is only 2.17% .

1.6 MÖSSBAUER SPECTRUM- Mössbauer spectrum consists of a plot of transmission (or scattered) gamma beam intensity versus the Doppler velocity. To obtain the hyperfine (hf) spectrum, one proceeds as follows. The radioactive material which constitutes the source is incorporated into a non-magnetic cubic host, where its nuclear levels remain unsplit. The source is then mounted on the 'velocity modulator', i.e., on the

mechanical device which provides the motion for the Doppler shift. A stationary absorber containing the same material is now placed between the source and the detector. If the nuclear levels in the absorber are split by hf interaction, there will be a number of different energies at which absorption takes place. The counting rate at the detector will drop wherever the Doppler velocity applied to the source brings the emitted gamma ray into coincidence with an absorption energy in the absorber.

1.7 THE IMPORTANCE OF THE MÖSSBAUER EFFECT- The Mossbauer effect primarily derives its importance from the fact that it makes feasible the observation of the electronic perturbations of nuclear energy levels and thus making available the tool of highest energy resolution. Taking the case of Fe^{57} for which the life time of the excited state is 1.4×10^{-7} sec. and thus the natural width $\Gamma = 4.6 \times 10^{-9}$ eV and the fractional line width Q (which gives the sharpness of the line) is

$$Q = \Gamma/E_{\gamma} = 4.6 \times 10^{-9} / 14.4 \times 10^3 \approx 10^{-13}.$$

This is equivalent to the statement that so sharp is the resonance that any effect which changes the energy of emitting (or absorbing) nucleus by even so little as one part in 10^{13} will cause detectable shift from the resonance. Indeed in an extreme case a shift of one part in 10^{16} has been detected [15] with 93.0 keV transition in Zn^{67} . Here it may be pointed out that the

electromagnetic radiation with comparable stability, purity and line width has not yet been obtained by any other means even with the gas laser, where $Q \sim 10^{12}$. Thus the Mössbauer line is the most accurately defined electromagnetic radiation available for the physical experiments. Mössbauer effect has ingenious applications not only in nuclear physics, relativity and solid state physics but also in chemistry, biophysics, metallurgy and mineralogy etc. [14,16]. In certain cases it has come out as a unique tool, e.g., in the interpretation of clock paradox, a test of equivalence principle for rotating systems, in determination of the gravitational red shift, in study of the motion of the drum of the inner ear and the electron density at the nucleus in a direct and straightforward manner, etc.

1.8 PARAMETERS OF GAMMA-RESONANCE SPECTRA- The parameters of γ -resonance spectra can be classified arbitrarily into following two groups:-

(a) Dynamical parameters- These parameters depend on the dynamics of the motion of the emitting and absorbing nuclei in solids, e.g., probability of the Mossbauer effect and the temperature shift of the spectral lines etc.

As our work is related to the study of these parameters, their discussion is deferred to Chapter II, where these will be described in detail.

(b) Electromagnetic parameters- These parameters depend on the interaction, of the electric charge of the nucleus (Ze), of the electric quadrupole (Q) and of the magnetic dipole moment (μ) of the nuclei with intracrystalline and intramolecular electric (E) and magnetic (H) fields. Since these parameters have been a subject of profuse discussion in so many excellent books and review articles [13,14], these are touched here only briefly.

Depending upon the interaction, we can classify these into three types.

(i) Isomer shift or chemical shift- If the gamma radiation from ${}_{27}\text{Co}^{57}$ (which decays to ${}_{26}\text{Fe}^{57}$) source falls on an absorber where the iron nuclei are in an environment identical with that of the iron source atoms, then the resonant absorption of the gamma rays will occur at zero velocity. However, if the iron nuclei in absorber are in different environment than in the source, no absorption occurs and the radiation is simply transmitted. In order to obtain resonance absorption it is then necessary to impart a Doppler velocity to the source relative to the absorber. This velocity is known as the Isomer shift (I.S.), δ Fig.(1.2(a)). The dependence of δ on chemical environment can be derived on the basis that I.S. (similar to the isotopic shift in optical spectroscopy) is due to the difference in size of the nucleus between the ground and isomeric excited level which

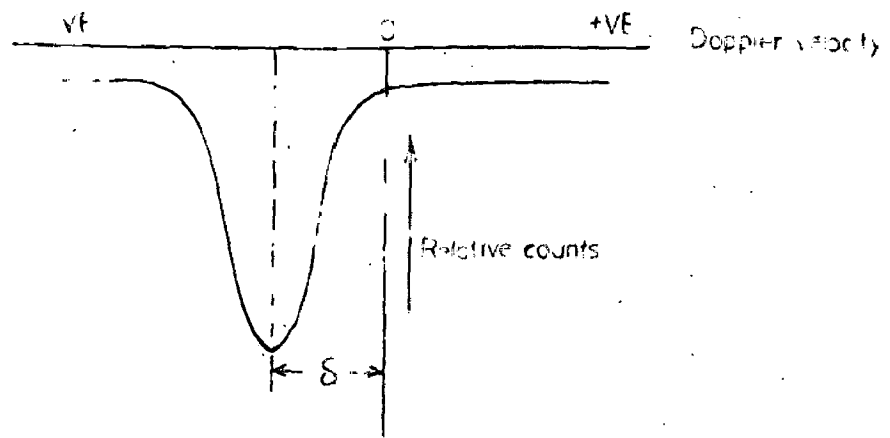


FIG. 1. (a) Theoretical Mössbauer spectrum showing the Isomer shift δ .

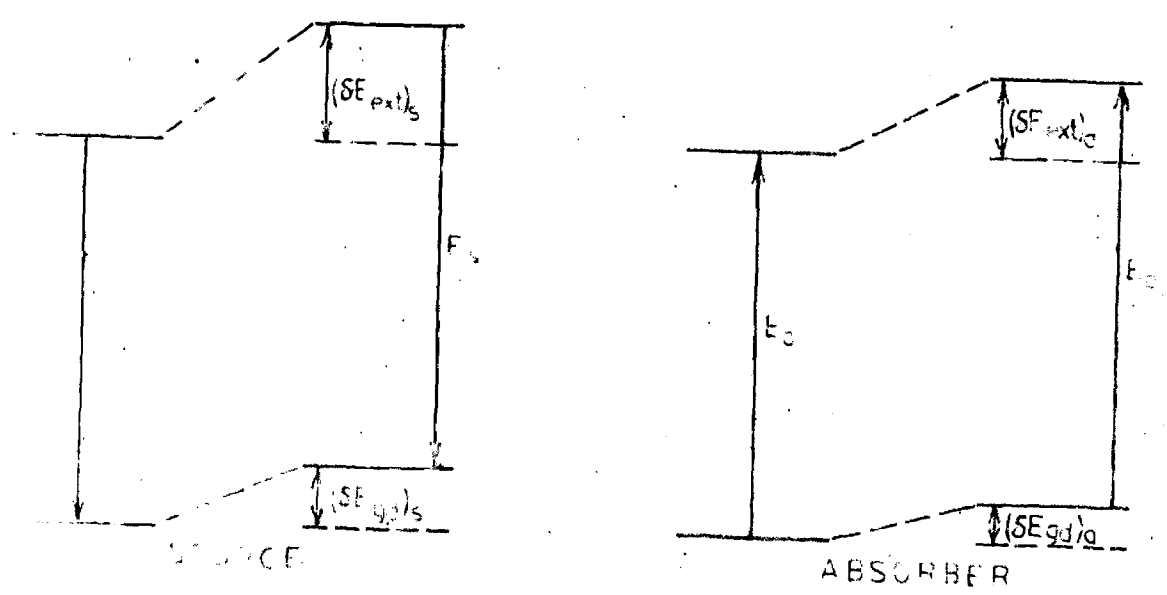


FIG. 1. (b) Shift of the nuclear levels due to the Coulombic interaction between the nuclear and electrostatic charges inside the nucleus. ($\langle R_{ext}^2 \rangle > R_{gd}^2$, $|\Psi(0)|_a^2 < |\Psi(0)|_s^2$, $\delta = E_a - E_s < 0$).

gives rise to difference in Coloumb interaction between the nucleus and the surrounding electrons. If the electron density at the nucleus is different between emitter and absorber for some reason or other, then such a difference will result in a shift of energy levels as shown in Fig. (1.2b). It can be shown that the electrostatic shift of the nuclear levels is given by [13,14],

$$\delta E_1 = \frac{2\pi}{5} Ze^2 |\Psi(0)|^2 R^2 \quad \dots (1.6)$$

Here R is the radius of the nucleus of charge Ze and $-e|\Psi(0)|^2$ represents the electronic charge density at the nucleus.

Thus for emitter, the total energy is

$$\begin{aligned} E_s &= E_0 + (\delta E_{\text{ext}})_s - (\delta E_{\text{gd}})_s \\ &= E_0 + \frac{2\pi}{5} Ze^2 |\Psi(0)|_s^2 [R_{\text{ext}}^2 - R_{\text{gd}}^2] \end{aligned}$$

and for absorber

$$E_a = E_0 + \frac{2\pi}{5} Ze^2 |\Psi(0)|_a^2 [R_{\text{ext}}^2 - R_{\text{gd}}^2]$$

Therefore $\delta = E_a - E_s$

$$= \frac{2\pi}{5} Ze^2 \left[|\Psi(0)|_a^2 - |\Psi(0)|_s^2 \right] R^2 \frac{\delta R}{R} \quad \dots (1.7)$$

where we have used $(R_{\text{ext}} - R_{\text{gd}}) \approx \delta R$ and $R_{\text{ext}} + R_{\text{gd}} \approx 2R$.

Equation (1.7) shows that I.S. depends on the

nuclear ($\delta R/R$) as well as the atomic parameters (electron density at the nucleus) and so one of these has to be calculated independently, if one is to determine the other. Walker et al. [17] were the first to carry out an analysis of the I.S. in different compounds of iron. Assuming that in completely ionized salts of divalent iron the configuration of valence shell is $3d^6$ while in similar salts of trivalent iron, it is $3d^5$, they computed the total s-electron density at the nucleus from the Watson's [18] free ion wavefunction. Comparing this with the measured isomer shift [19], the authors [17] have shown δR to be negative which implies that the excited state is smaller than the ground state. This also shows that if the isomer shift is positive then the s-electron density at the nucleus will decrease in going from source to absorber and vice-versa. There are two main effects which influence the electron density at the iron nucleus-

- (i) contribution from the s-orbitals and
- (ii) contribution from the d-orbitals

The effect of 4s-orbitals which may be obtained from Fermi-Segre-Goudsmit formula [20] follows directly. Adding s-electrons increases the electronic charge density and this will lead to a decrease in the isomer shift. On the other hand the effect of 3d electrons which can be calculated from Hartree-Fock calculations [18], is

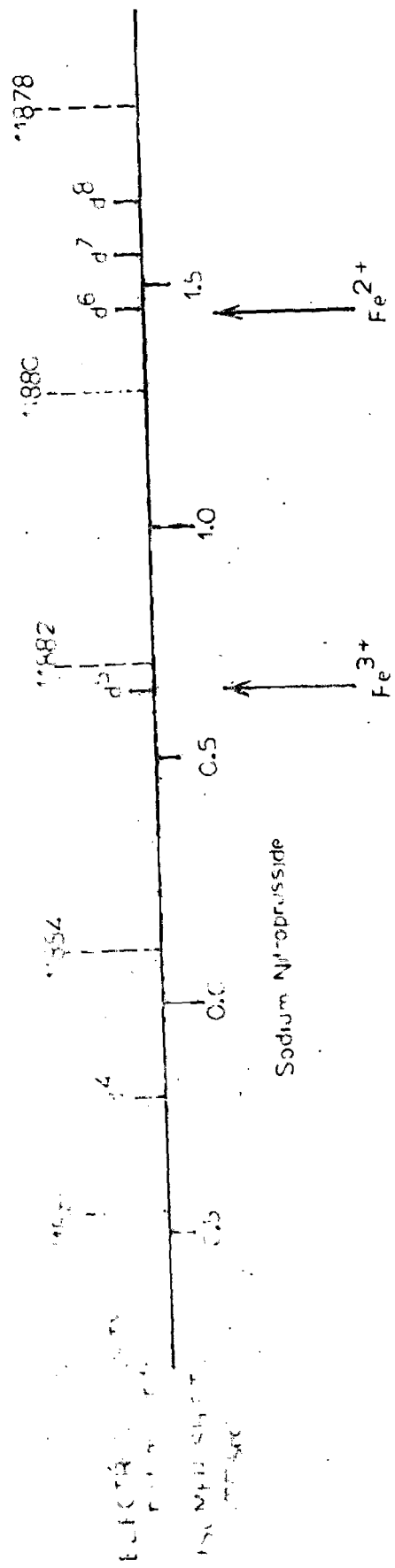
opposite to that of adding s-electrons due to the shielding of the s-electrons. In non-relativistic approximation the contribution due to p-electrons is negligible.

Figure (1.3) shows the relative electron density at the iron nucleus and the corresponding I.S. for various iron ions, with respect to sodium nitroprusside|21|. The I.S. values have thus been used to determine electron configuration in metals and alloys, to study the ordering mechanisms in alloys, to measure covalences and to study phase transitions etc. It may be remarked that the experimental shifts are actually not the true I.S. values rather it is a composite sum of the I.S. and S.O.D.|22,23|. This will be discussed in detail in Chapter II.

(b) Quadrupole Splitting- If the nucleus is non-spherical and the electric charge density at the nucleus is non-uniform then there will be splitting of the levels instead of shifting and one will get two absorption lines as shown in Fig.(1.4). The separation between the two absorption peaks is called the quadrupole splitting (Q.S.) denoted by ΔE_Q . More precisely the quadrupole splitting is due to the interaction of the nuclear quadrupole moment Q with the gradient of the electric field $\nabla \bar{E}$ at the nucleus due to other charges.

Mathematically this interaction can be represented by the Hamiltonian|24|

$$H = \frac{eq Q}{4I(2I-1)} \left[3I_z^2 - I(I+1) + \frac{\eta}{2}(I_+^2 + I_-^2) \right] \dots (1.8)$$



13
 FIG. 2 The relationship between the relative electron densities at the iron nucleus and the I. S. scale.

where $\eta = (V_{xx} - V_{yy})/V_{zz}$ is called the asymmetry parameter, and $0 \leq \eta \leq 1$ and $V_{xx} (= \partial^2 V / \partial x^2)$, V_{yy} and V_{zz} are the three components of the electric field gradient along x-, y- and z-direction respectively. I is the nuclear spin quantum number, I_+ and I_- are the raising and lowering operators. This equation has eigen values given by

$$E_Q = \frac{eq Q}{4I(2I-1)} \left[3m_I^2 - I(I+1) \right] \left(1 + \frac{\eta^2}{3} \right)^{1/2} \quad \dots (1.9)$$

$$m_I = I, I-1, \dots, -I$$

It is evident that the excited level of Fe^{57} ($I=3/2$) will split into two levels whereas the ground state ($I=1/2$) will remain degenerate. The observed spectrum will thus consist of two absorption lines corresponding to transitions $A \rightarrow B$ and $A \rightarrow C$ and the separation is given by (from Eq.(1.9)),

$$\begin{aligned} \Delta E_Q &= E_Q(3/2) - E_Q(1/2) \\ &= \frac{e^2 q Q}{2} \left[1 + \frac{\eta^2}{3} \right]^{1/2} \quad \dots (1.10) \end{aligned}$$

It may be emphasized that in the case of Fe^{57} , Mössbauer effect measures the quadrupole interaction of the excited state and thus presents unique information about the nuclear quadrupole interaction, because the conventional methods fail since there are no suitable isotopes of iron with a ground state spin $I_g > 1/2$.

Like I.S. values, the ΔE_Q values are also characteristics of ferrous and ferric compounds with further differentiation of low spin and high spin|25|.

(c) Magnetic hyperfine splitting- The third important hyperfine interaction is the nuclear zeeman splitting. This will occur if there is a strong interaction between the nuclear magnetic dipole moment μ with a magnetic field H. The magnetic field H can originate either from the internal magnetic field or as a result of placing the compound in an externally applied magnetic field. Due to such hyperfine interaction, the Mössbauer spectrum reveals resonance minima as shown in Fig.(1.5).

The Hamiltonian H_m of the interaction between μ and H can be written as |26|

$$H_m = -\vec{\mu} \cdot \vec{H} = -g\mu_n \vec{I} \cdot \vec{H} \quad \dots \quad (1.11)$$

and therefore the energy levels are given by |26|

$$E_m(m_I) = \frac{-\mu H m_I}{I} = -g H m_I \mu_n \quad \dots \quad (1.12)$$

where $\mu = g\mu_n I$, μ_n the nuclear magneton and g, is the nuclear g factor. It is obvious from Eq.(1.12), for Fe^{57} , that

- (i) ground state splits into two levels corresponding to $m_I = \pm 1/2$,
- (ii) excited state splits into four levels corresponding to $m_I = +3/2$ and $\pm 1/2$. Then according to

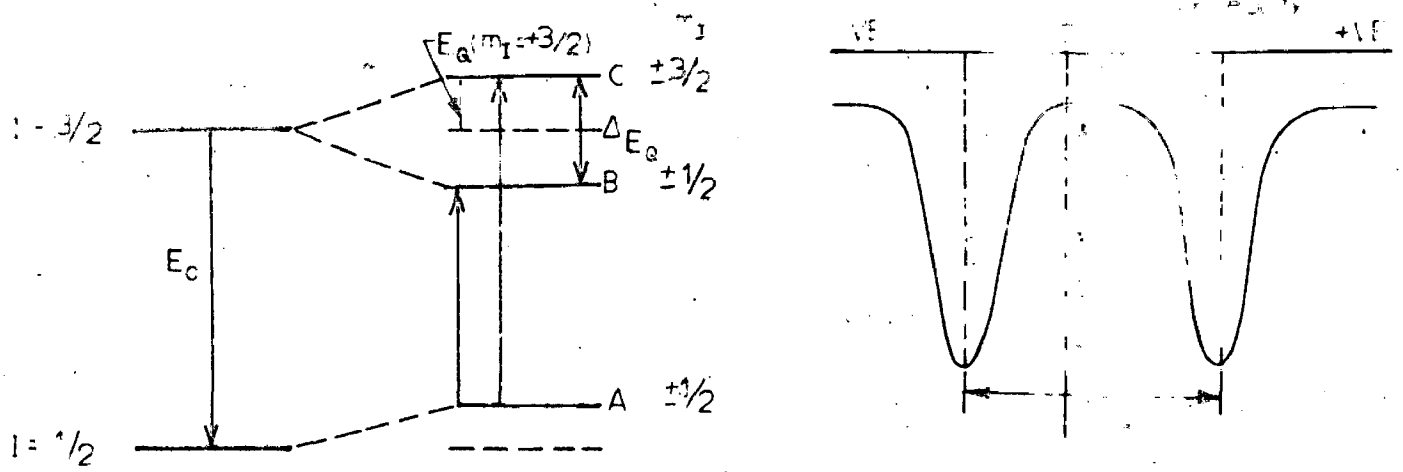


FIG.14- Energy levels and theoretical spectrum of Fe^{57} due to quadrupole interaction: $(\Delta E_Q = E_Q(3/2) - E_Q(1/2))$.

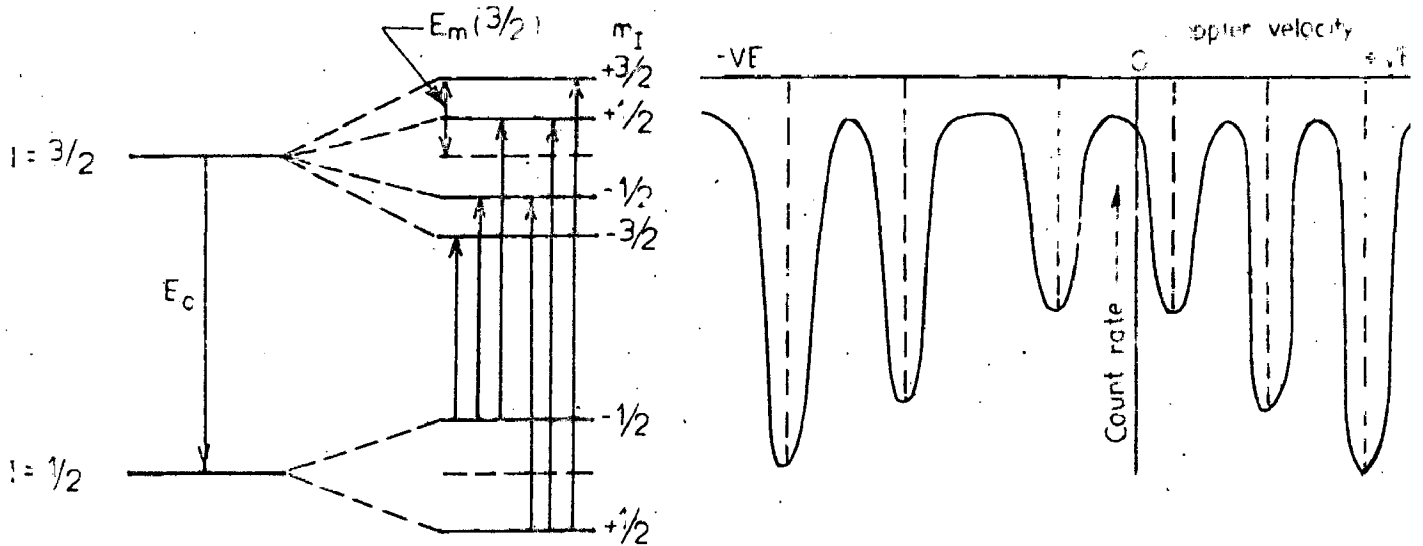


FIG.15- Energy levels and theoretical spectrum of Fe^{57} due to magnetic interaction.

CHAPTER-II

LATTICE DYNAMICAL PARAMETERS OF γ -RESONANCE
SPECTRA

2.1 INTRODUCTORY REMARKS- The two parameters which depends on the dynamics of the motion of the emitting and absorbing nuclei in a solid are the probability of the Mössbauer effect or recoilless fraction (f) and the temperature shift of the spectral lines, also called the second order Doppler shift (S.O.D.) δE_2 . First of all we will like to give the theoretical background for the quantitative estimation of these parameters and later on their relation to the properties of the solids.

2.2 PROBABILITY OF THE MOSSBAUER EFFECT - We have seen in Chapter I, when an emitting and absorbing atom is embedded in a solid, there is a definite probability that the emitted γ -ray has the full transition energy E_0 and the lattice remains in its initial state, that is, there is no excitation of the lattice vibrations (phonons) and thus the process is also called zero phonon process. This probability for the zero phonon process, defined as the Mössbauer fraction f , is zero for a free atom and increases with the increase of lattice rigidity, becoming unity for a perfectly rigid lattice.

Let e be the initial state of the nucleus prior to the emission and g be the final state of the nucleus

after emission; n_i and n_f are the initial and final vibrational states of the lattice. Then the fraction of the gamma rays emitted or absorbed by a nucleus bound in a crystal, without any change in the quantum state of the lattice (in quantum mechanical calculation) $f_{\text{c}}^{\text{g}}(n_i, n_i) \equiv f$ is given by [10, 20],

$$f = \left[\langle n_i | e^{i\vec{k} \cdot \vec{x}} | n_i \rangle \right]^2 \quad \dots (2.1)$$

a thermal average over the initial lattice states $\langle n_i |$, where \vec{k} is the wavevector of the emitted gamma ray ($|\vec{k}| = k = \frac{2\pi}{\lambda} = \lambda^{-1}$; λ is the gamma ray wavelength) and \vec{x} is the position vector of the radiating nucleus. This equation is very general and is valid for many crystals which contain an arbitrary number of atoms in a unit cell but which have a strictly regular structure. In order to get a more specific expression let us assume for simplicity that the solid can be represented as a one-dimensional harmonic oscillator with oscillation frequency ω . The nucleus of mass M is then bound in this harmonic potential. The Hamiltonian of the system H is [29],

$$\begin{aligned} H &= \text{kinetic energy} + \text{potential energy,} \\ &= \frac{p^2}{2M} + \frac{M\omega^2 x^2}{2} \end{aligned} \quad \dots (2.2)$$

with eigen values

$$E_n = \hbar\omega \left(n + \frac{1}{2} \right) \quad \dots (2.3)$$

and eigen functions [29]

$$\Psi_n(x) = N_n H_n(\alpha x) e^{-\frac{1}{2}\alpha^2 x^2} \quad \dots (2.4)$$

where,

$$\alpha = \left(\frac{MK'}{\hbar^2}\right)^{1/4}, \quad K' = \text{force constant} = M\omega^2$$

$$N_n = \left(\frac{\alpha}{\pi^{1/2} 2^n n!}\right)^{1/2}$$

and $H_n(\alpha x)$ is the Hermite polynomials. The first few of these polynomials are: $H_0(y) = 1$, $H_1(y) = 2y$, $H_2(y) = 4y^2 - 2$. Substituting $n=0$ in Eq.(2.4) and making slight algebraic manipulation, ground state wavefunction of Harmonic oscillator will be

$$\Psi_0(x) = \left(\frac{M\omega}{\pi\hbar}\right)^{1/4} e^{-\frac{M\omega}{2\hbar}x^2} \quad \dots (2.5)$$

and the corresponding f from Eq.(2.1) becomes

$$f = \langle \Psi_0 | e^{-iKx} | \Psi_0 \rangle \langle \Psi_0 | e^{iKx} | \Psi_0 \rangle$$

($\bar{K} \cdot \bar{x} = Kx$ since we are dealing with one dimensional oscillator)

$$\begin{aligned} &= \int_{-\infty}^{+\infty} \Psi_0^* e^{-iKx} \Psi_0 dx \int_{-\infty}^{+\infty} \Psi_0^* e^{iKx'} \Psi_0 dx' \\ &= 4 \left(\frac{M\omega}{\pi\hbar}\right) \int_0^{\infty} e^{-\frac{M\omega}{\hbar}x^2} e^{-iKx} dx \int_0^{\infty} e^{-\frac{M\omega}{\hbar}x'^2} e^{iKx'} dx' \\ &= 4 \left(\frac{M\omega}{\pi\hbar}\right) \int_0^{\infty} e^{-(tx^2 + t'x)} dx \int_0^{\infty} e^{-(tx'^2 - t'x')} dx' \end{aligned}$$

$$(t = \frac{M\omega}{\hbar}, \quad t' = iK)$$

$$= 4 \left(\frac{M\omega}{\pi\hbar}\right) e^{t'^2/2t} \int_0^{\infty} e^{-t(x + \frac{t'}{2t})^2} dx \int_0^{\infty} e^{-t(x' - \frac{t'}{2t})^2} dx' \dots (2.6)$$

Let $t(x' + \frac{t'}{2t}) = y$ so that $dx' = \frac{y^{-1/2} dy}{2t^{1/2}}$

and

$t(x' - \frac{t'}{2t}) = z$ so that $dx' = \frac{z^{-1/2} dz}{2t^{1/2}}$

Eq.(2.6) then reduces to

$$\begin{aligned}
 f &= 4 \left(\frac{M\omega}{\pi\hbar} \right) e^{t'^2/2t} \frac{1}{4t} \int_0^\infty e^{-y} y^{-1/2} dy \int_0^\infty e^{-z} z^{-1/2} dz \\
 &= 4 \left(\frac{M\omega}{\pi\hbar} \right) e^{-\frac{K^2\hbar}{2M\omega}} \frac{\hbar}{4M\omega} \pi \\
 &= e^{-\frac{K^2\hbar}{2M\omega}} \dots (2.7)
 \end{aligned}$$

Since for an harmonic oscillator the average potential energy is half of the total energy i.e.,

$$\frac{1}{2} M \omega^2 \langle x^2 \rangle = \frac{1}{2} \frac{\hbar\omega}{2}$$

Therefore, $\langle x^2 \rangle = \frac{\hbar}{2M\omega}$

Rewriting Eq.(2.7), one gets

$$f = \exp(-K^2 \langle x^2 \rangle) = \exp(-\langle x^2 \rangle / \lambda^2) = \exp(-2w) \dots (2.8)$$

where $\langle x^2 \rangle$ is the component of the mean square vibrational amplitude of the emitting atom in the direction of incident gamma ray due to its zero point and thermal vibrations. This is to be averaged over all possible modes of vibration that are occupied at a certain temperature.

The exponent $2W$ is the well known Debye Waller factor, which also determines the intensity of X-ray diffraction lines. Eq.(2.8) shows that f increases exponentially with decrease in $\langle x^2 \rangle$ which in turn depends on the firmness of binding and on the temperature. Further the displacement of the nucleus must be small compared to the wavelength λ of the γ -rays and thus the Mössbauer effect is not detectable in gases and non-viscous liquids.

For most experimentally reliable situation, Eq.(2.8) describes the zero phonon process to a high degree of accuracy, including the case where the emitting or absorbing atom is an impurity vibrating in a localized mode, and in the presence of anharmonic potential [30-33].

Now we would like to derive expression for $\langle x^2 \rangle$ using realistic model for interatomic forces for lattice vibrations. Let the crystal be represented by $3N$ oscillators of frequencies ω_j . ($j=1, 3N$). The average energy associated with each oscillator is

$$\bar{E}(\omega_j) = (\bar{n}_j + \frac{1}{2}) \hbar \omega_j \quad \dots (2.9)$$

where \bar{n}_j is given by the Planck distribution function

$$\bar{n}_j = \frac{1}{e^{\hbar \omega_j / kT} - 1}$$

If x_j is the root mean square displacement of the atoms due to the j th oscillator and assuming harmonic case, we

have the energy of the crystal attributable to the j th oscillator as

$$\frac{1}{2} M \omega_j^2 \langle x_j^2 \rangle = \frac{1}{2} \bar{E}(\omega_j) = \frac{1}{2} (\bar{n}_j + \frac{1}{2}) \hbar \omega_j \quad \therefore (2.10)$$

Summation over j gives

$$\langle x^2 \rangle = \frac{\hbar}{M} \sum_{j=1}^{3N} \frac{(n_j + \frac{1}{2})}{\omega_j} \quad \therefore (2.11)$$

Let $g(\omega)$ be the normalised lattice phonon frequency distribution function (p.f.d.f) i.e., number of phonons lying in the frequency interval ω and $\omega+d\omega$, then averaging Eq.(2.11) over the entire vibration spectrum, we have

$$\langle x^2 \rangle = \frac{\hbar}{M} \int_0^{\omega_{\max}} \left(\frac{1}{e^{\hbar\omega_j/kT} - 1} + \frac{1}{2} \right) \frac{g(\omega_j)}{\omega_j} d\omega_j \quad \therefore (2.12a)$$

$$= \frac{\hbar}{2M} \int_0^{\omega_{\max}} \coth\left(\frac{\hbar\omega_j}{2kT}\right) \frac{g(\omega_j)}{\omega_j} d\omega_j \quad \therefore (2.12b)$$

Hence from Eq.(2.8), one gets

$$\begin{aligned} f &= \exp \left[- \frac{\hbar}{2M\lambda^2} \int_0^{\omega_{\max}} \coth\left(\frac{\hbar\omega}{2kT}\right) \frac{g(\omega)}{\omega} d\omega \right] \\ &= \exp \left[- \frac{R}{\hbar} \int_0^{\omega_{\max}} \coth\left(\frac{\hbar\omega}{2kT}\right) \frac{g(\omega)}{\omega} d\omega \right] \quad \therefore (2.13) \end{aligned}$$

This is the general expression for calculating f when the actual p.f.d.f. is available either calculated theoretically or measured experimentally.

In the absence of availability of $g(\omega)$ one can as a first approximation use Debye model for the lattice which gives

$$g(\omega) = \frac{9N\omega^2}{\omega_{\max}^3} \quad \omega < \omega_{\max} \quad \dots (2.14)$$

$$= 0 \quad \omega > \omega_{\max}$$

subject to the normalization condition

$$\int_0^{\omega_{\max}} g(\omega) d\omega = 3N \quad \dots (2.15)$$

Thus from Eq.(2.13)

$$f = \exp \left[- \frac{2R}{\hbar} \int_0^{\omega_{\max}} \frac{g(\omega)}{\omega} \left(\frac{1}{2} + \frac{1}{e^{\hbar\omega/kT} - 1} \right) d\omega \right] / \int_0^{\omega_{\max}} g(\omega) d\omega$$

$$= \exp \left[- \frac{6R}{\hbar \omega_{\max}^3} \int_0^{\omega_{\max}} \left(\frac{1}{2} + \frac{1}{e^{\hbar\omega/kT} - 1} \right) \omega d\omega \right] \quad \dots (2.16)$$

Defining $\frac{\hbar\omega}{kT} = x$ with $\hbar\omega_{\max} = k\theta_D$ where θ_D is the Debye temperature of the lattice, Eq.(2.16) reduces to

$$f = \exp \left[- \frac{3R}{2k\theta_D} \left(1 + 4 \left(\frac{T}{\theta_D} \right)^2 \int_0^{\theta_D/T} \frac{x dx}{e^x - 1} \right) \right] \quad \dots (2.17)$$

Table for the evaluation of the Debye integral for different θ_D/T ratios is available [34].

2.3 SECOND ORDER DOPPLER EFFECT- The experimental fact that Mössbauer resonance very rarely occurs at zero velocity inspite of the identical environment of Mössbauer nucleus in source and absorber, is due to the S.O.D. shift which is purely a relativistic phenomena. The existence of S.O.D., also called thermal red shift, in

the Mossbauer spectra was almost simultaneously pointed out by Pound and Rebka|22| and Josephson|23|.

According to Pound and Rebka|22| approach, the emitting and absorbing nuclei are vibrating at random, at its lattice sites in the crystal, with fairly high speeds depending on the temperature of the solid. Therefore it might be expected that these vibrations would impart a Doppler shift to the gamma ray and consequently change the energy. The relativistic equation for Doppler effect on an emitted photon gives the observed frequency ν' for a closing velocity v as

$$\begin{aligned}\nu' &= \nu_{\text{obs.}} \left(1 - \frac{\bar{v} \cdot \bar{r}}{c}\right) / \left(1 - \frac{v^2}{c^2}\right)^{1/2} \\ &= \nu_{\text{obs}} \left(1 - \frac{\bar{v} \cdot \bar{r}}{c} + \frac{v^2}{2c^2}\right) \quad \dots (2.18)\end{aligned}$$

\bar{r} is the unit vector in the direction of propagation of gamma ray and ν_{obs} is the frequency for a stationary system. The velocity component of the vibrating atom changes its direction at frequencies characteristics of the lattice vibrations (10^{12} - 10^{13} sec⁻¹) and as the nuclear life time is of the order of 10^{-7} sec. (i.e. the average time over which a gamma is emitted), therefore as many as 10^5 - 10^6 oscillations take place within the life time of the nuclear levels useful in Mössbauer experiments. Since the positive and negative velocities

occur with equal probability, the first order term $(\bar{v} \cdot \bar{r})/c$ vanishes giving rise to unshifted Mossbauer line. However, the second order term will not average to zero as it is a term in v^2 and is therefore independent of direction and will cause a shift in the energy of the emitted or absorbed gamma ray. As a result Equation (2.18) reduces to

$$\nu' = \nu \left(1 + \frac{v^2}{2c^2}\right) \quad \dots (2.19)$$

and accordingly the shift in the Mossbauer line is given by

$$\frac{\delta E_2}{E_\gamma} = \frac{\delta \nu}{\nu} = \frac{\langle v^2 \rangle}{2c^2} \quad \dots (2.20)$$

where $\langle v^2 \rangle$ is the mean square velocity of the resonant atom in the solid.

Considering a change in the mass of the nucleus, when it emits or absorbs a gamma ray photon, the same expression (Eq.(2.20)) was derived independently by Josephson^[23]. As was done in the case of f, we now consider the description of δE_2 in terms of the lattice dynamics of the solid. If $\bar{E}(\omega_j)$ represents the average energy associated with each oscillator (Eq.(2.9)) then from the property of harmonic oscillator the square of the total velocity satisfies the relation

$$\frac{1}{2}M \langle v^2 \rangle = 3 \left(\frac{1}{2} \bar{E}(\omega_j)\right) \quad \dots (2.21)$$

$$\therefore \langle v^2 \rangle = \frac{3}{M} \bar{E}(\omega_j) \quad \dots (2.22)$$

Summing over all the possible modes of vibration ω_j the fractional energy change due to S.O.D. shift becomes

$$\begin{aligned} \frac{\delta E_\gamma}{E_\gamma} &= \frac{\langle v^2 \rangle}{2c^2} \\ &= \frac{3}{2Mc^2} \int_0^{\omega_{\max}} \bar{E}(\omega_j) g(\omega_j) d\omega_j \\ &= \frac{3\hbar}{2Mc^2} \int_0^{\omega_{\max}} \omega \left(\frac{1}{2} + \frac{1}{e^{\hbar\omega/kT} - 1} \right) g(\omega) d\omega \quad \dots (2.23(a)) \\ &= \frac{3\hbar}{4Mc^2} \int_0^{\omega_{\max}} \omega \coth\left(\frac{\hbar\omega}{2kT}\right) g(\omega) d\omega. \quad \dots (2.23(b)) \end{aligned}$$

In the special case if we take the Debye model for the lattice spectrum (Eq.(2.14)) then Eq.(2.23) reduces to

$$\begin{aligned} \frac{\delta E_\gamma}{E_\gamma} &= \frac{3\hbar}{2Mc^2} \int_0^{\omega_{\max}} d\omega \left(\frac{1}{2} + \frac{1}{e^{\hbar\omega/kT} - 1} \right) \frac{9N\omega^2}{\omega_{\max}^3} \int_0^{\omega_{\max}} g(\omega) d\omega \\ &= \frac{9\hbar}{2Mc^2} \frac{1}{\omega_{\max}^3} \int_0^{\omega_{\max}} \omega^3 \left(\frac{1}{2} + \frac{1}{e^{\hbar\omega/kT} - 1} \right) d\omega \\ &= \frac{9}{2Mc^2} \left[\frac{\hbar}{8} \omega_{\max} + \frac{\hbar}{\omega_{\max}^3} \int_0^{\omega_{\max}} \frac{\omega^3 d\omega}{e^{\hbar\omega/kT} - 1} \right] \quad \dots (2.24) \end{aligned}$$

Substituting $\frac{\hbar\omega}{kT} = x$ and $\hbar\omega_{\max} = k\theta_D$, the above equation becomes

$$\frac{\delta E_\gamma}{E_\gamma} = \frac{9kT}{2Mc^2} \left[\frac{1}{8} \left(\frac{\theta_D}{T} \right) + \left(\frac{T}{\theta_D} \right)^3 \int_0^{\theta_D/T} \frac{x^3 dx}{e^x - 1} \right] \quad \dots (2.25)$$

To evaluate the integral , we write

$$\frac{x}{e^x - 1} = (1 - \frac{x}{2} + \frac{x^2}{12} - \frac{x^4}{720} + \dots) \quad \dots (2.26)$$

and thus
$$\int_0^{\theta_D/T} \frac{x^3 dx}{e^x - 1} = \int_0^{\theta_D/T} x^2 (1 - \frac{x}{2} + \frac{x^2}{12} - \frac{x^4}{720} + \dots) dx$$

$$= \frac{1}{3} \left(\frac{\theta_D}{T}\right)^3 - \frac{1}{8} \left(\frac{\theta_D}{T}\right)^4 + \frac{1}{60} \left(\frac{\theta_D}{T}\right)^5 - \dots$$

... (2.27)

Therefore from Eq.(2.25)

$$\frac{\delta E_\gamma}{E_\gamma} = \frac{3kT}{2Mc^2} \left[1 + \frac{1}{12} \left(\frac{\theta_D}{T}\right)^2 - \frac{1}{1680} \left(\frac{\theta_D}{T}\right)^4 + \dots \right] \quad \dots (2.28)$$

$$= \frac{3kT}{2Mc^2} \left[1 + \frac{1}{12} \left(\frac{\theta_D}{T}\right)^2 \right] \quad \dots (2.29)$$

Before giving various lattice dynamical aspects which can be derived from f and S.O.D., we will discuss in brief the experimental methods of measuring f.

2.4 EXPERIMENTAL DETERMINATION OF MÖSSBAUER FRACTION

By measuring either of dip, line width or the area under the absorption curve, one can get the Mössbauer fraction of the absorber, f_a . In all the three methods, these quantities are measured using a given source with a several combinations of absorbers of various thickness t_a . In the dip method if $(C_R)_{exp}$ and $(C_N)_{exp}$ represents the resonant and nonresonant counting rates,

then assuming the source line width $\Gamma_s = \Gamma$, the natural line width (determined from the life time of the state), the maximum dip can be expressed as [35],

$$\text{dip}_{\text{max}} = 1 - \left(\frac{C_R}{C_N}\right)_{\text{max}} = f_s \left[1 - e^{-T_A/2} I_0\left(\frac{iT_A}{2}\right) \right] \quad \dots (2.30)$$

where f_s is the recoilless fraction in the source, $T_A = f_a t_a \sigma_0 n_a$ with t_a the physical thickness of the absorber in centimeters, n_a the number of Mössbauer nuclei per cm^3 , σ_0 the Mössbauer cross-section. $I_0\left(\frac{iT_A}{2}\right)$ is a zero order Bessel functions of the imaginary argument. Plot of $(\text{dip})_{\text{max}}$ versus t_a can give f_a provided f_s is known from other measurements.

O'Conner [35] has shown that for absorber with $T_A \ll 5$ the measured line width Γ_m is given by

$$\Gamma_m = \Gamma_a + \Gamma_s + 0.27 \Gamma f_a t_a \sigma_0 n_a \quad \dots (2.31)$$

Γ_a is the absorber line width. Plot of Γ_m versus t_a gives f_a (from the slope) and $\Gamma_a + \Gamma_s$ (from the intercepts).

The third and the most exact method of determining f_a and f_s consists in the measurement of the area under the peak of resonance absorption obtained in a velocity spectrum. It has been shown that the background corrected absorption area A is related to the absorption thickness t_a by the formula [36]

$$A = \frac{1}{2}\pi \left[f_s T_A e^{-T_A/2} \left[I_0\left(i \frac{T_A}{2}\right) + I_1\left(i \frac{T_A}{2}\right) \right] \right] \quad \dots (2.32)$$

where I_0 and I_1 are zero and first order Bessel function of imaginary arguments. Eq.(2.32) can be alternatively expressed as

$$A = \frac{1}{2}\pi \left[f_s T_A \left(1 - \frac{1}{4} T_A + \frac{1}{16} T_A^2 - \frac{5}{384} T_A^3 + \dots \right) \right] \quad \dots (2.33)$$

Using Eq.(2.32) or (2.33) the variation of A versus T_A for various values of f_s and f_a have been plotted [13]. Comparison of the experimental data of $A = \phi(T_A)$ with the most suitable curve of this series can give the desired value of f_a and f_s .

Housley et.al [37] have discussed the more accurate method commonly known as 'black absorber' method to determine the absolute recoilless fraction of source f_s for isotope Fe^{57} . The observed resonance strength F is given by

$$F = \frac{C_N - C_R}{C_N} = f_s f_{b\lambda} \quad \dots (2.34)$$

with $f_{b\lambda}$ is the fractional absorption of recoil free γ -rays, by the absorber (called the 'blackness'). In order to measure absolute f values, an absorber with known $f_{b\lambda}$ is required. They used an absorber consisting of a mixture of enriched Fe^{57} ammonium-lithium fluoroferrate (referred to as $Li-NH_4$ absorber) because of its special properties. The ammonium ferric fluoride has a pair of

broad lines for its absorption pattern; the lithium ferric fluoride has a single broad line pattern, which falls between the pair of lines of ammonium salts. Combined in the proper proportion the mixed salts have a broad, flat-topped absorption spectrum which has a full width of 1.36 mm/sec. ($\sim 15 \mu$) at the bottom of the well and a width of 1.64 mm/sec. at half height. Because the Li-NH₄ absorbers are very thick, they absorb essentially all of the Mössbauer γ -rays lying between ± 15 source line widths of the centre. This encompasses all of the source Mössbauer γ -rays, except 2.5% lying in the wings of the Lorentzian, hence making the absorbers 97.5% black and thus $f_b \lambda = 0.97$. Hence f_s can be calculated from relation $f_s = F/f_b \lambda$.

Using this technique Steyart and Taylor|38| have measured the absolute values of f of the 14.4 keV γ -rays of Fe⁵⁷ in Au, Cu, Ir, Pd, Pt, Rh and Ti. It should be noted that a normal black absorber as mentioned above can only be used for single line source or sources with small quadrupole splitting, since for larger quadrupole splittings one of the components falls outside the absorption region. Recently Kolk and Harwig|39| have shown that the effective width of the absorption region of a black absorber can be trippled by using an absorber system with the moving black absorbers with opposite velocities and keeping the third one stationary. With this triple absorber system, sources with a large quadrupole splitting can also be investigated.

2.5 APPLICATIONS OF MÖSSBAUER EFFECT TO THE STUDY OF SOLID STATE PHYSICS

Even though the Mössbauer effect is fundamentally concerned only with processes in which the quantum state of the lattice remain unchanged, it does not mean that the information concerning the motion of the lattice atoms is not obtained in an experiment where only recoil-free gamma rays are observed. The different lattice-dynamical aspects which can be profitably studied from f and S.O.D. include: the evidence of the force constant change q'/q of the impurity-host to host-host coupling [38,40-43], anharmonicity of the motion of the vibrating atom [30,44-47], anisotropy of the atomic binding forces [48-53], surface studies [54-57], molecular crystals [58-62], thin films [63], zero point root mean square velocity [64-67] and determination of the phonon spectra [11,68] etc. We will describe some of these, that too in brief.

(a) Determination of the mean square displacement $\langle x^2 \rangle$ (MSD) and mean square velocity $\langle v^2 \rangle$ (MSV) - can be done directly by measuring f and thermal energy shift values, through Eqs. (2.8) and (2.20).

(b) Evidence of force constant change and existence of localised modes for an impurity atom - The study of crystals containing defects constitutes one of the frontiers of modern physics and problems connected with defects

have aroused a good deal of interest in recent years. There does not seem to be any other way at the present time of measuring the mean square amplitude and velocity of an impurity atom in a crystal [38,40]. From such determination it is possible to obtain some information about the force constant of the interactions between the impurity and the host crystal [41-43]. This is discussed in detail in Chapter VIII.

(c) Anharmonicity- For some materials, measurements of $f(T)$ showed such an unusually weak temperature dependence that they could not be explained by the harmonic model and one has to include anharmonic effects. By anharmonicity we mean that the vibrating atom sits in a potential well which is not quite harmonic. This is easy to imagine if we place an emitting atom between two neighbours both of which produce identical attractions Fig.(2.1). Thus, in cases where the Mössbauer nucleus is in a large cage of atoms the binding is expected to be anharmonic. This results in anomalously large mean square displacements (and low f factors) especially at low temperatures [44]. A square well atomic potential was suggested for the binding of Mössbauer atom to explain the dynamics of a small noble gas atoms in a clathrate [45]. Recently to explain the low temperature dependence of f for divalent Fe^{57} impurities in ThO_2 Shechter et al. [46], have proposed the 'wine bottle' potential. Detailed discussion of

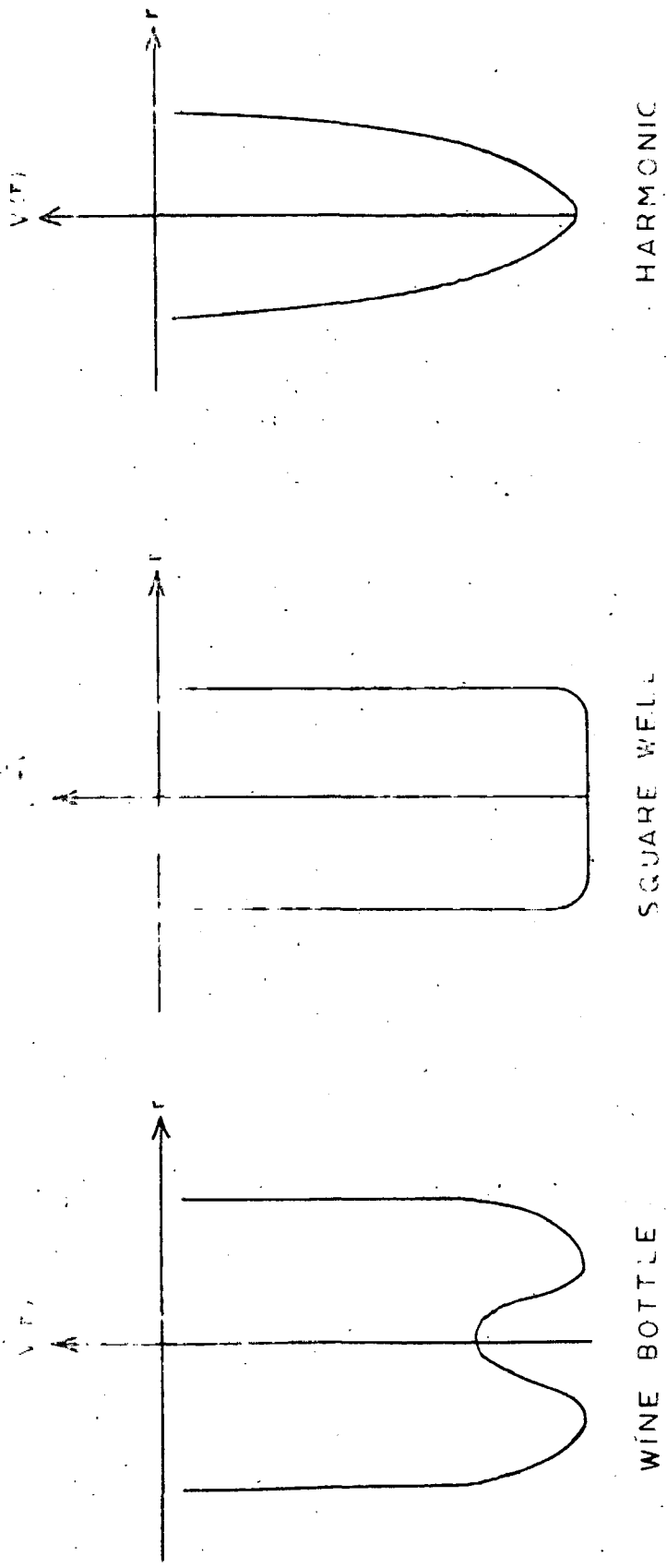


FIG.2.1.- Dependence of a potential well upon near neighbour distance .

anharmonicity follows in Chapter IV.

(d) Anisotropy- Another application of the Mössbauer fraction measurements is the investigation of the spatial anisotropy of atomic vibration. Consider, for example, a lattice in which the binding of the Mössbauer atom is strongly anisotropic. It is clear that since an average energy of kT is associated with motion along each of the coordinate axes, the amplitude of the motion will be greatest in the direction of weakest binding. It then follows that the recoil-free fraction will be smallest in the direction of weakest binding forces.

The asymmetric binding forces at the atomic-sites will give rise to anisotropic f values both in single crystals|48-50| as well as in polycrystalline samples|50-53|. Meecham and Muir|49| using single-crystal ^{tin} the absorbers, have observed the Mössbauer effect in Sn^{119} as a function of crystallographic orientation of the absorber. The resonance absorption (raw dip) ratio, (001) to (100), was found to be 0.67 ± 0.09 at room temperature and increased with decreasing temperature to 0.92 ± 0.03 at 100°K . Anisotropy of zinc have been studied from zinc crystal as well as from polycrystalline zinc and it is found that the M.S.D. in the direction of c-axis is nearly three times that of in a perpendicular direction|50|.

(e) Surface Physics- The Mössbauer effect because of its sensitivity to strength and angular distribution of binding,

to magnetic and electrical fields, the density of s-electrons at the nucleus, can be used as a tool to study surfaces [54-57]. Experiments on surfaces present great difficulties but they promise to yield information not obtainable by other methods and to complement the results of low-energy electron diffraction. Flinn et.al [55] have measured the relative probability of recoilless absorption in different directions in a specially prepared sample of Al_2O_3 of very high specific surface area in which some of the Al ions in surface sites were replaced by trivalent ions of Fe^{57} . They find an anisotropy in the f when the resonant nuclei are in the surface of Al_2O_3 sample, which, however, is absent when the nuclei are in the interior of the sample. Burton et.al. [54] using Fe^{57} on the surface of polycrystalline and single crystal tungsten, deduced the M.S.D. ratios, $[\langle x^2 \rangle_{\parallel} / \langle x^2 \rangle_{\perp}]_{\text{surface}} = 1.9 \pm 0.4$; $[\langle x^2 \rangle_{\perp} / \langle x^2 \rangle_{\text{bulk}}] = 1.3 \pm 0.2$ and $[\langle x^2 \rangle_{\parallel} / \langle x^2 \rangle_{\text{bulk}}] = 2.5 \pm 0.5$. It may be remarked that \parallel and \perp represents directions parallel and perpendicular to surface.

(f) Molecular Crystals- The earlier treatment given for the Debye Waller factor is strictly applicable only to an atom in a monatomic lattice of identical atoms where only the acoustical modes of lattice were considered. In more complicated solids e.g., molecular crystals, the presence of optical as well as acoustical modes

complicates the matter considerably. For such crystals the vibrational properties of the molecule which may be observed both in solution and in the solid by using infra-red absorption or the Raman effect, are retained in the solid due to the intermolecular (motion of the molecular units with respect to each other) binding which is relatively weak compared to the intramolecular (or interatomic motion of the atoms within a molecule) force. The former binding gives rise to the acoustical modes of vibration extending from zero to maximum frequency whereas the latter resulting in optical modes of vibrations (high frequency modes). For a molecule consisting of N atoms ($3N$ degrees of freedom), 3 degrees of freedom go over to the acoustic modes and the rest $3(N-1)$ modes of vibration, are tied up in the optical modes. The characteristic property of the optical modes is that their energy is independent of crystal momentum and thus can be approximated by one or a number of single-frequency Einstein oscillators. Regarding the probability of Mössbauer effect f , for such crystals, it can be expressed as a first approximation, as [58],

$$f = f_0 f_a \quad \dots (2.35)$$

where f_0 is the probability that the intramolecular vibration will not be excited and f_a is the probability that the intermolecular vibrations are not excited. The effect on f provided by an acoustic mode (f_a) which can be represented by Debye model is given in Eq.(2.17) with

R the recoil energy of the whole molecule whereas one provided by an optical modes (f_o) can be calculated from Eq.(2.13) by introducing the normalised $g(\omega)$ for a single frequency oscillator as a delta function|26|.

$$g(\omega) = 3N\delta(\omega - \omega_E) \quad \dots (2.36)$$

where N is the number of degrees of freedom contributing to the single frequency mode with $\hbar\omega_E = k\theta_E$, θ_E is the characteristic temperature for this oscillator. It can be shown that Eq.(2.36) when substituted in Eq.(2.13) yields

$$\begin{aligned} f_o &= \exp\left[-\frac{R}{\hbar\omega_E} \coth\left(\frac{\hbar\omega_E}{2kT}\right)\right] \\ &= \exp\left[-\frac{R}{k\theta_E} \coth\left(\frac{\theta_E}{2T}\right)\right] \quad \dots (2.37) \end{aligned}$$

with R the recoil energy of the Mössbauer atom.

By measuring the temperature dependence of f in molecular crystals, solid state information like normal mode vibrations etc. have been obtained by various investigators|59-62|.

(g) Zero point root mean square velocity- Kitchens et al|64| have shown that by intercomparing f and δE - both directly determined from the Mössbauer experiments, one can calculate zero-point mean square velocity. This quantity is valuable in permitting tests of theoretical models of impurities in crystal lattice, and of molecular crystals etc.|61|. They|64| have presented the results for a number of systems involving both the Fe⁵⁷ and Sn¹¹⁹

resonance, like Sn^{119} in SnTe , Nb_3Sn and Fe^{57} in Fe , Ir , Rh , Pt , Pd , Au , Cu etc. Suganthy et al|65| have calculated $\langle v^2 \rangle_0$ to be 3.9×10^8 and $6 \times 10^8 \text{ cm}^2/\text{sec}^2$ for Fe^{57} in FeF_2 and V respectively. This quantity (ZP velocity) in addition to zero point root mean square displacement (ZP displacement) which can be obtained from f factor at zero temperature, is a useful parameter in the study of superconductivity|66| as the recent work by McMillan|67| on the mechanisms controlling the critical temperature in superconductivity shows that a parameter likely to be of great importance is related to the ratio of the expectation of the mean square velocity to the mean square displacement within the lattice near zero temperature i.e., $\left[\frac{\langle \omega \rangle}{\langle \omega^{-1} \rangle} \right]_{\text{ZP}}$.

Finally it may be pointed out that glasses|69|, ferroelectric materials|70|, microcrystals|71|, disordered materials |72| and frozen liquids|73|, have also been studied both theoretically and experimentally, by various investigators, with Mössbauer spectroscopy to get the dynamical information.

CHAPTER-III

ANALYSIS OF MÖSSBAUER FRACTION IN THE
HARMONIC APPROXIMATION

3.1 INTRODUCTION

We have seen in Chapter I that for a nucleus bound in a crystal, the recoil energy is dissipated by the transfer of integral multiples n of the phonon energy $\hbar\omega$ to the lattice. Under certain conditions n is zero and the quantum state of the lattice remains unchanged. The emitted gamma-ray then has the full transition energy. The probability f , for this zero-phonon process for a cubic monatomic lattice, that is, harmonically bound, is given by (Eqs.(2.8) and (2.13)),

$$f = \exp(-2W) = \exp\left[-\frac{\langle x^2 \rangle}{\lambda^2}\right]$$
$$= \exp\left[-\frac{R}{\hbar} \int_0^{\max} \frac{g(\omega)}{\omega} \coth\left(\frac{\hbar\omega}{2kT}\right) d\omega\right] \quad \dots (3.1)$$

$2W$ is the Debye Waller factor, λ is the rationalised wavelength of the gamma ray and $\langle x^2 \rangle$ is the component of the mean square displacement of the emitting nucleus in the direction of gamma-rays. It is this particular quantity which needs the lattice dynamics of the host material and comparing the experimental measured f with the theoretical prediction, one can check how far the dynamical model,

used for calculation of lattice dynamics of the system under study is reliable. Information regarding anharmonic lattice forces etc. can also be obtained, as has been done by various workers, e.g., Varshni and Blanchard|74| in Ge^{73} , Jaswal|75| in alkali iodides, Deo|76| and Puri|76| in Ni^{61} , W^{182} , W^{183} and Schuster and Bostock|77| in $\text{Nb}_3\text{Sn}^{119}$. For detailed information, reference may be made to a recent review article by Bara|78|.

We have analysed the measured $f(T)$ variation for

- (i) 9.3 keV transition of Kr^{83} in solid Krypton|79|
 - (ii) 14.4 keV transition of Fe^{57} in natural Iron|80|
 - (iii) 77.3 keV transition of Au^{197} in Gold metal|81|
 - (iv) 26.8 keV transition of I^{129} in Cesium Iodide|82| and
 - (v) 81.0 keV transition of Cs^{133} in Cesium metal|82|.
- These will be discussed in turn.

3.2 9.3 keV Transition of Kr^{83} in Solid Krypton- Gilbert and Violet. (GV)|83| measured the f in solid krypton

between 5-85°K using the nuclear gamma-ray resonance of 9.3 keV transition of Kr^{83m} ($\frac{7}{2}^+ \rightarrow \frac{9}{2}^+$) isomer (1.9h) used as source produced by irradiating the Kr gas in a thermal neutron flux of 1.9×10^{13} neutrons/cm²sec. The source and absorbers were obtained by flowing the Kr gas into the source and absorber cells, both placed within the same cryostat. Later on Kolk|84| re-evaluated the recoilless fraction using a nuclear resonance cross section σ_0 derived by them from a remeasurement of the conversion

coefficient α of the 9.3 keV transition, which was found to be 40% lower than the value used by ⁷GV|83|. Krypton has a f.c.c. lattice. We have done the calculations using $g(\omega)$ at 0°K derived from the (m-6) Lennard-Jones potential|85|. This was obtained from the measurements of the phonon dispersion relations for the symmetric $[100]$, $[110]$ and $[111]$ branches in krypton by triple axes neutron spectrometry|86|. The input frequencies were corrected for mass change according to the relation $\omega(83) = \omega(83.8) \left(\frac{83.8}{83.0}\right)^{1/2}$ which was considered necessary since the $g(\omega)$ curve is for natural krypton (average atomic weight 83.8), whereas we require for Kr⁸³. Free atom recoil energy R for Kr⁸³ is 5.57×10^{-4} eV. The results of calculation of f versus temperature in the harmonic theory, using the frequency distribution of Brown and Horton|85|, are displayed in Fig.(3.1a), along with the experimental results of Kolk|84| showing the disagreement between the experiment and harmonic theory. To understand the cause of discrepancy, we decided to use p.f.d.f. at 0°K derived by Buckingham (exp-6) potential calculated by Gupta and Gupta|87| since as pointed out by Walkley|88| and Finegold and Philips|89| the (m-6) potentials are inadequate to account in detail for the thermodynamic properties of solidified raregases. Further the (exp-6) potential functions are theoretically more sound than the (m-6) potentials in the sense that both the attractive and repulsive terms have quantum mechanical foundation.

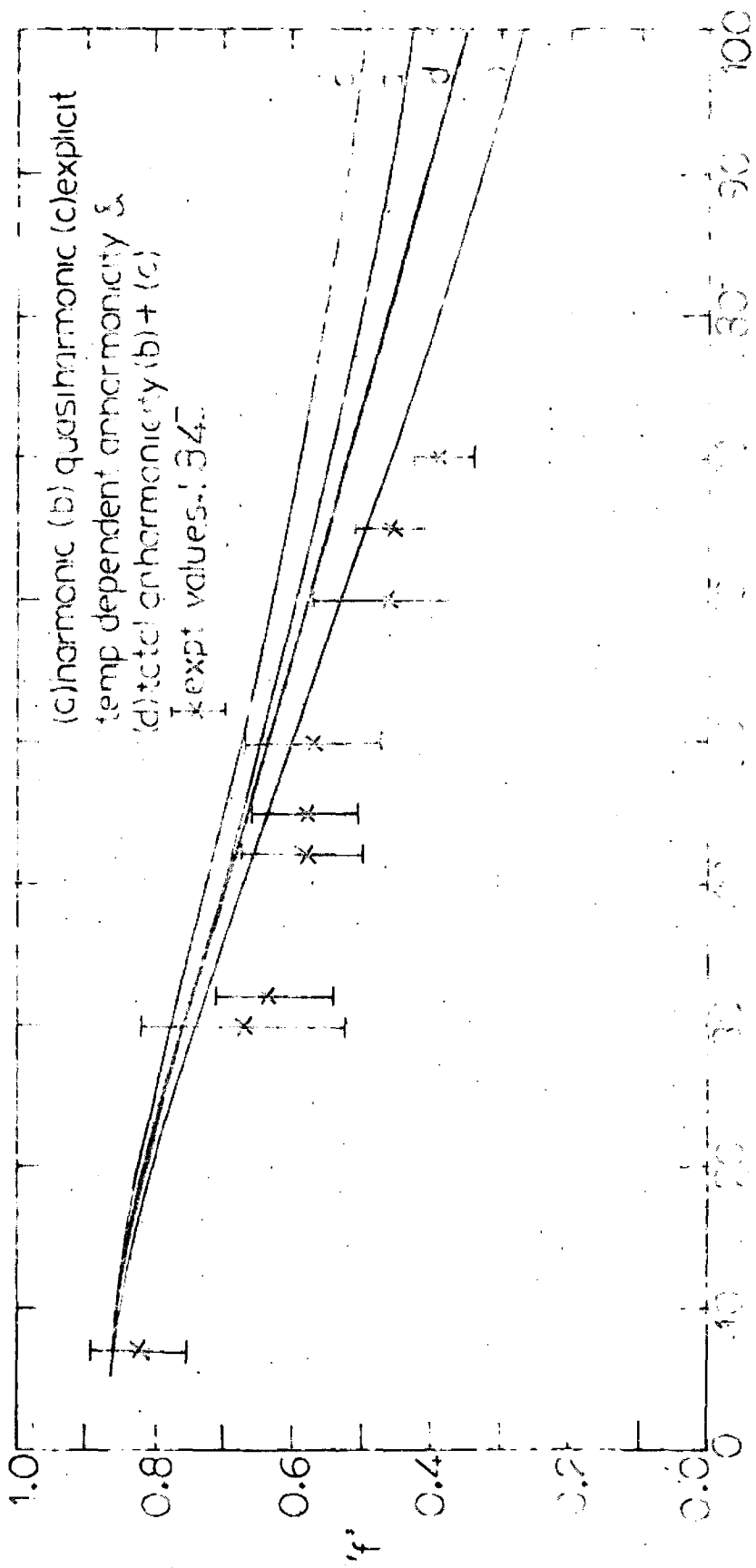


FIG. 2. Temperature dependence of the anharmonicity parameter f for solid Krypton, $\alpha = 0.1$ (m-6)

constant $\alpha = 0.1$ (m-6) (see text for definition of α). The curves are based on anharmonic

exponents $m = 1.34$ (see text for definition of m). The curves are based on anharmonic

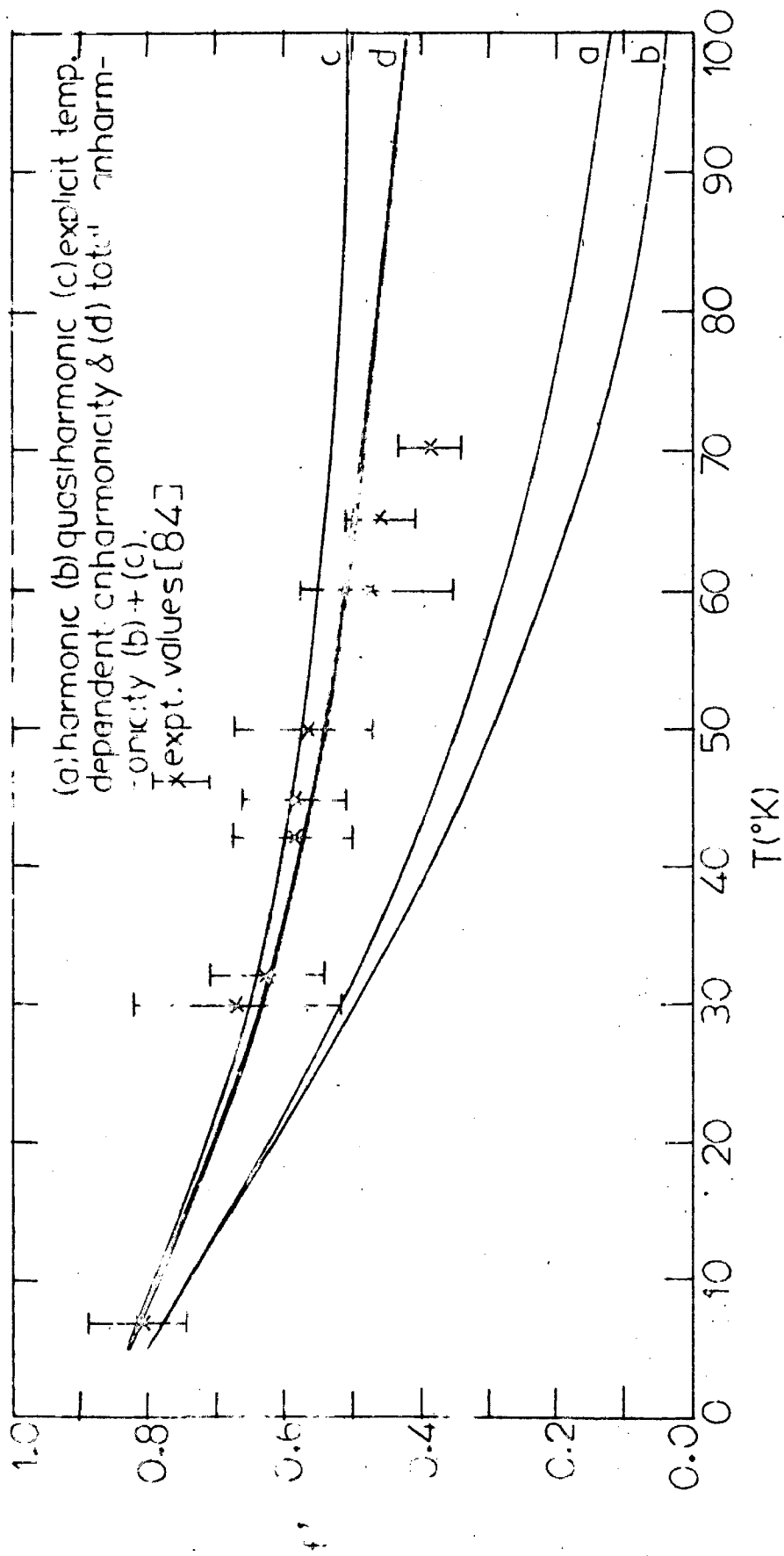


FIG.3.2- A Plot of 'f' versus temperature for Kr^{83} in solid Krypton, using (exp - 6) Buckingham potential, distribution function [87] in harmonic (a) and anharmonic approximation (b-d) along with the experimental values [84].

Figure (3.2a) shows the calculated $f(T)$ along with the experimental results|84|. From Figs.(3.1a) and (3.2a) it is evident that under harmonic approximation there appears disagreement with the experiment. Subsequent to our work, Gupta|90| have calculated f versus T using the distribution function derived from (exp-6)|91| and (exp-6) Buckingham potential|87|. Their results are in agreement with the values calculated by us(Fig.3.2a). Mahesh and Sharma |92| also calculated $f(T)$ variation using distribution function derived by Gupta|91| and results again agree with curve (3.2a). Vashishta and Pathak|93| using the Debye approximation with Debye temperature $\theta_D = 50^\circ\text{K}$, have found $f(T)$ dependence to be in agreement with the previous measurement of GV|83| but in disagreement with the recent measurement of Kolk|84|.

Thus it is obvious that no potential gives the satisfactory agreement with the experiment and it was therefore decided to calculate $f(T)$ in the anharmonic approximation. This will be discussed in detail in the next chapter.

3.3 14.4 keV TRANSITION OF Fe⁵⁷ IN NATURAL IRON -

Kovats and Walker |94| reported the intensity measurements of Mössbauer absorption of 14.4 keV γ -rays of Fe⁵⁷ in metallic iron over a temperature range 22-1400°C and obtained the recoilless fraction from the area analysis of the absorption curves. Furthermore, Owen and Evans|95|

studied the temperature variation of atomic vibrational amplitude in iron from the fall in intensity of X-ray reflection over the temperature range 50-900^oK.

Upto 1044^oK, iron is ferromagnetic and has b.c.c. phase (α). Free atom recoil energy R for the transition under study is 1.9567×10^{-3} eV. The p.f.d.f. of α -iron has been calculated theoretically [96-98] from phenomenological models of deLauany[96], Krebs[97] and modified angular force model [98] and derived experimentally from inelastic neutron scattering[99-102]. We employed the experimental phonon spectrum measured by Minkiewicz et al.[102] which is representative of reported experimental measurements.[99-102]. Minkiewicz et.al.[102] measured the room temperature phonon dispersion relation in principal symmetry directions of α -Fe using neutron inelastic scattering technique. A Born-Von-Karman fifth-neighbour general force constant central model was used to analyse the data and phonon distribution function was obtained. Using this distribution function, f at various temperatures varying from 150-1000^oK has been evaluated[80] on the basis of Eq.(3.1); after necessary modification of the vibrational frequencies for mass change according to the relation $\omega(57) = \omega(55.85) \left(\frac{55.85}{57.0}\right)^{1/2}$. The results, displayed in Fig.(3.3a), when compared with the experimental results show the disagreement. To account for the discrepancy we used the anharmonic effects. This will be discussed in Chapter IV.

3.4 77.3 keV TRANSITION OF Au¹⁹⁷ IN GOLD METAL - Recently Erickson et.al. [103] by fitting an appropriate theoretical line shape to the measured thick absorber spectra, have deduced f at temperatures ranging from 4.2-100°K for 77.3 keV γ -ray transition of Au¹⁹⁷ in gold metal. Gold has a f.c.c. lattice. Free atom recoil energy R is 1.629×10^{-2} eV. Since no experimental determination of dispersion relation for gold is available, we have to use the theoretical p.f.d.f. calculated at $T=0^\circ\text{K}$ recently by Christensen and Seraphin [104]. Employing this we calculated [81] $f(T)$ for gold in the temperature range $4.2 < T < 100^\circ\text{K}$ and the results are displayed in Fig. (3.4a) along with the experimental results [103]. Again, as in the earlier cases we have to include the anharmonic effects to seek comparison with the precise measurements of Erickson et al. [103]. This is accomplished in Chapter IV.

3.5 26.8 keV TRANSITION OF I¹²⁹ IN CsI LATTICE AND 81.0 keV TRANSITION OF Cs¹³³ IN CESIUM METAL

Some times back Hafemeister et al. [105] reported the solid state and nuclear results from Mössbauer studies performed with 26.8 keV, $\frac{5^+}{2} \rightarrow \frac{7^+}{2}$ transition of I¹²⁹ in CsI along with other alkali iodides using the ZnTe¹²⁹ as source at 80°K. By studying the dependence of the line width on the absorber thickness, they computed the recoilless fraction f of CsI¹²⁹ to be 0.24 ± 0.05 . On the other hand Boyle and Perlow [106] from the study of

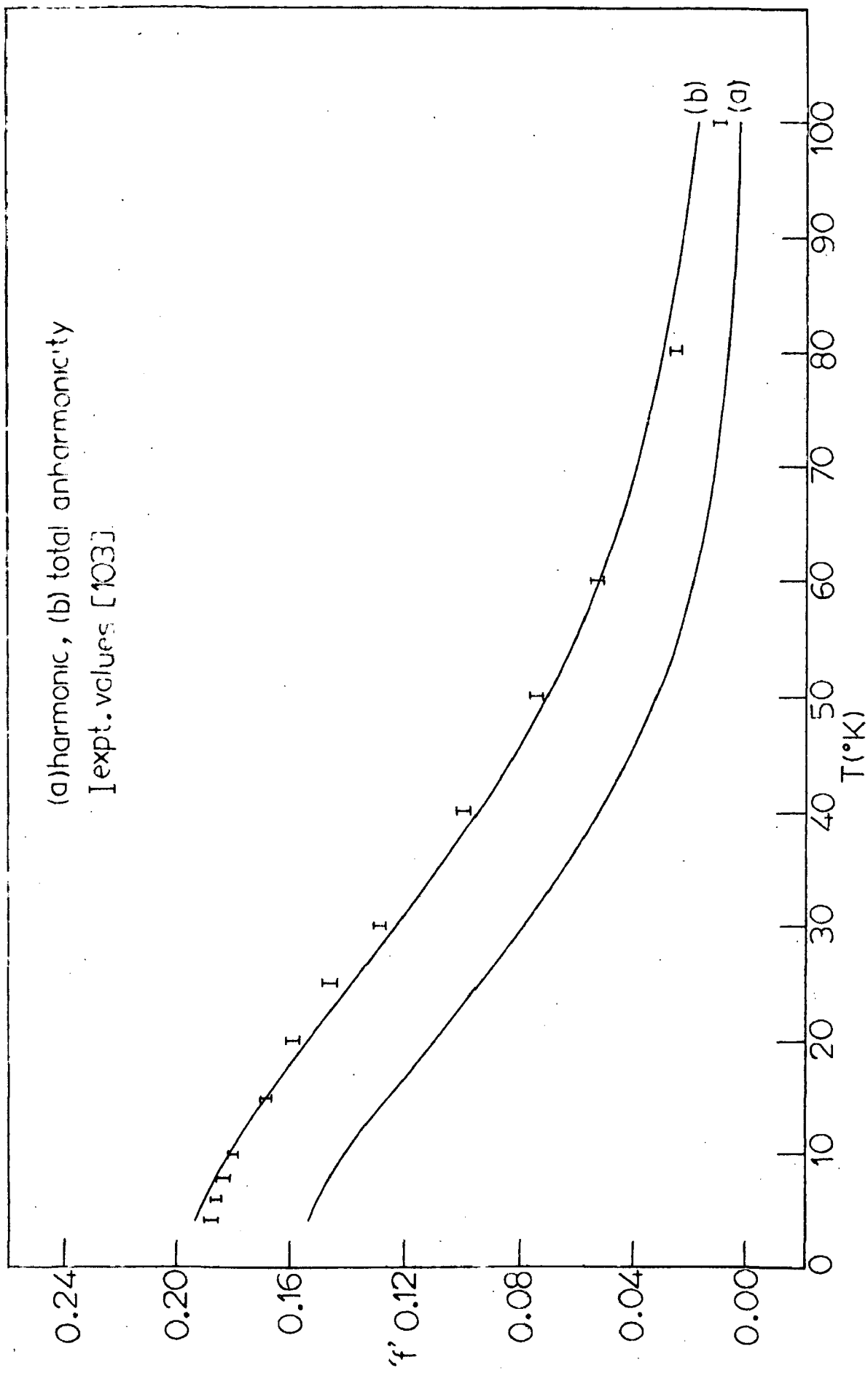


FIG.3.4- A Plot of f versus temperature for Au^{197} in gold metal in harmonic (a) and anharmonic approximation (b) along with the experimental results [103].

81.0 keV transition, $\frac{7^+}{2} \rightarrow \frac{5^+}{2}$ of Cs^{133} in CsI at 4.2°K , computed $f = (0.94 \pm 0.08) \times 10^{-2}$ by measuring the dependence of absorber thickness on the line width. From this one can easily deduce (through Eq.(3.1)) the corresponding f for I^{129} -26.8 keV transition at 4.2°K to be (0.590 ± 0.006) . Because of the importance of this parameter various workers [105,107-109] have tried to explain these values with different theoretical lattice dynamical models for p.f.d.f. and the results are collected in Table (3.1), given on page 49. Hafemeister et.al [105] have compared their experimental values with those calculated from Kagan and Maslov [110] theory derived for NaCl lattice based on nearest neighbour short-ranged interactions. This gives $f(80^\circ\text{K}) = 0.06$ as compared to the experimental value of 0.24 ± 0.05 . Assuming CsI to be monatomic lattice, Kamal et.al [107] using the theoretical $g(\omega)$ calculated from the classical Kellerman's [111] method, assuming spherical and nondeformable ions in the harmonic approximation and nearest neighbour interactions have derived f to be 0.601 and 0.145 at 4.2 and 80°K respectively. The disagreement at 80°K has been attributed to the presence of anharmonic forces and the deformation and polarisation of the ions. Mahesh and Sharma [108], using the Debye model of the phonon spectrum with the Debye temperature θ_D after modifying due to lattice thermal expansion as derived by them, have calculated f to be 0.660 and 0.308 at 4.2 and 80°K respectively. Haridasan

Table (3.1): Calculated Mössbauer fraction 'f' for 26.8 keV transition in CSI as reported by various workers along with the experimental results.

T (°K)	Expt. values	Calculated values				
		Our	[105]	[107]	[108]	[109]
4.2	0.590±0.006 106	0.600	-	0.601	0.660	0.603
80	0.24±0.05 105	0.216	0.06	0.145	0.308	0.210

and Nandini|109| taking CsI to be diatomic lattice, have calculated the same quantity with the theoretical calculated eigenfrequencies and corresponding eigen vectors based on shell model developed by Woods et.al|112| and found $f(4.2) = 0.603$ and $f(80) = 0.21$, in agreement with the experimental results|105,106|.

Inspite of the difficulties involved in obtaining the experimental dispersion curves for cesium halides, by neutron scattering experiments due to the small scattering cross section of cesium ion and its heavy mass, Bührer and Halg|113| recently have measured the frequencies of the normal modes of vibration of CsI at room temperature by means of the slow neutron inelastic scattering which were fitted with 14-parameter model to compute the frequency distribution function. In view of the availability of this experimental phonon spectra we decided to recalculate f for I^{129} and Cs^{133} in CsI lattice. Although CsI is diatomic lattice but as masses of the cesium (133) and iodine (129) are nearly equal, it can be treated as a monatomic lattice and accordingly one can use Eq.(3.1). The approximation of the monoatomicity of the CsI lattice seems acceptable due to the absence of any band gap in the phonon spectra |113| unlike the cases of LiI|114|, NaI|115| and KI|116| lattices where discernible band gap has been shown. For 26.8 keV transition of I^{129} , R is 3.205×10^{-3} eV. Employing the p.f.d.f.

107786

determined by Büher and Halg|113| with the measured frequencies modified again due to the mass correction as $\omega(129) = \omega(126.9) \left(\frac{126.9}{129.0}\right)^{1/2}$, $f(T)$ upto 300°K was calculated|82| from Eq.(3.1) and the results are presented in Fig.(3.5a) along with the experimental results |105,106|. The nice agreement with the experiment shows that either the anharmonic contribution to f is negligible or that the anharmonicity due to the lattice thermal expansion is more or less offset, by explicit temperature dependent anharmonicity|79| (See Chapter IV). Absence of anharmonicity seems acceptable because of the strong ionic binding, heaviness of the ions and the large cohesive energy of cesium iodide lattice. Fig.(3.5b) shows the plot of $f(T)$ for Cs^{133} -81.0 keV transition ($R=2.648 \times 10^{-2}$ eV) in CsI which gives $f(4.2^\circ\text{K})=1.12 \times 10^{-2}$ as compared to the experimental value |106| of $(0.94 \pm 0.08) \times 10^{-2}$. Further the temperature dependence of f for Cs^{133} is stronger as compared to that for I^{129} , in CsI. In addition, $f(T)$ was also calculated |82| for Cs^{133} -81.0 keV transition in cesium metal, between 2 - 10°K using the theoretical $g(\omega)$, recently calculated by Satya Pal|117| and the results are tabulated in Table (3.2). The experimental measured f at 4.2°K from the analysis of the absorption line using a source $\text{Ba}^{133}\text{Al}_4$ is 5.50×10^{-5} |118| as compared to the calculated value|82| of 0.062×10^{-5} . In view of the smallness of the measured effect, it is difficult

A plot of $\ln(I/I_0) - \frac{eV}{kT}$ versus V for ^{133}Cs ($105, 106$ eV) and ^{137}Cs ($105, 106$ eV) for ^{133}Cs ($105, 106$) and ^{137}Cs ($105, 106$) eV. I_0 and I denotes the experimental values for ^{133}Cs ($105, 106$) and ^{137}Cs ($105, 106$) eV. It should be noted that the ordinate is in the units of 10^{-2} , 10^{-1} and 10^0 in the case of ^{133}Cs , ^{137}Cs and ^{133}Cs respectively.

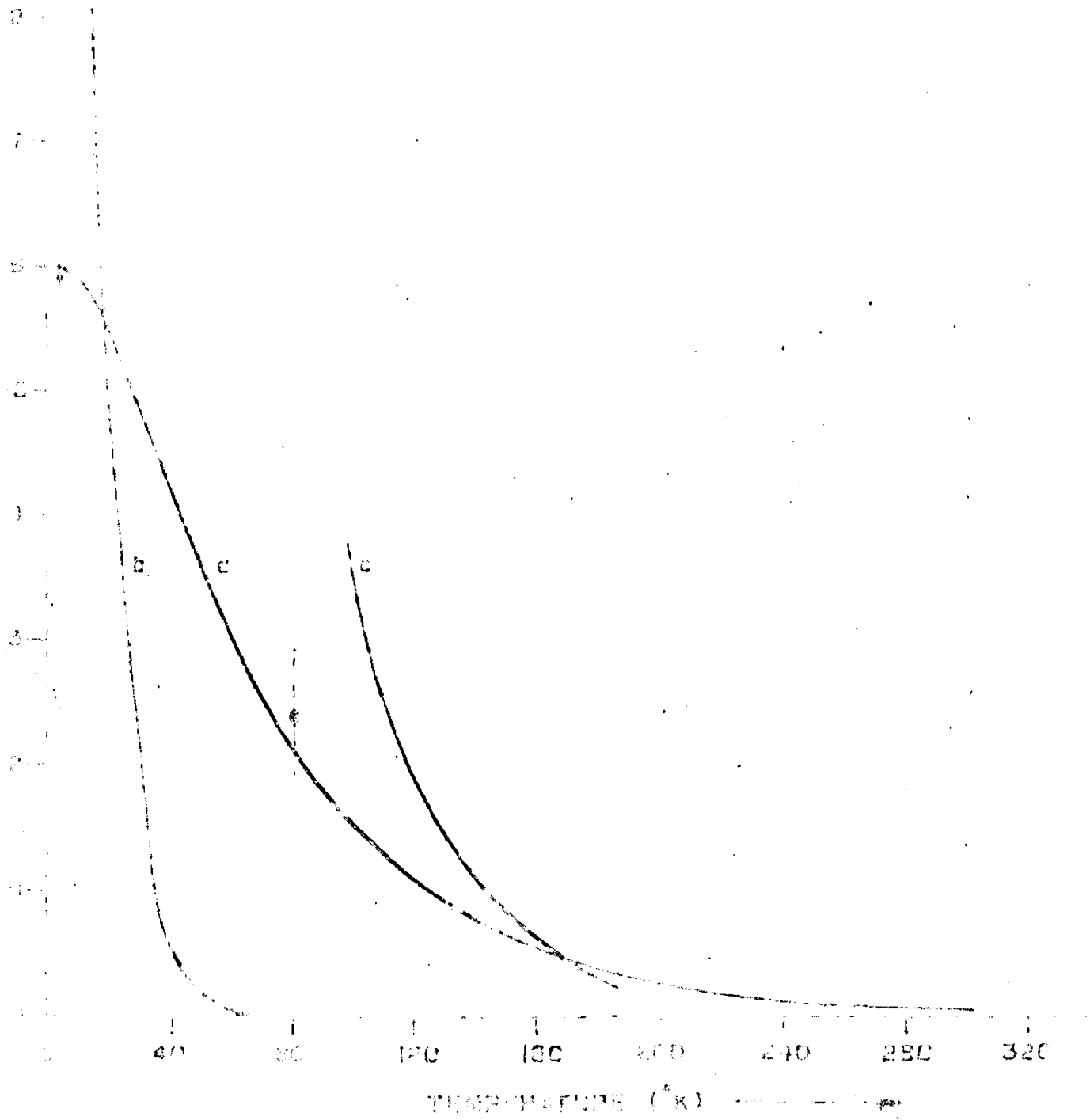


Table 3.2- Calculated Mössbauer fraction for 81.0 keV-Cs¹³³ transition in Cs metal [E-x=10^{-x}]

T (°K)	2.0	4.2	6.0	8.0	10.0
f	0.296	0.623	0.109	0.111	0.882
	E-5	E-6	E-6	E-7	E-9

CHAPTER-IV

ANALYSIS OF MÖSSBAUER FRACTION IN THE
ANHARMONIC APPROXIMATION

4.1 INTRODUCTION- In Chapter III we saw that even using the frequency distribution derived from the experimental phonon dispersion relation, the agreement of f factor with experimental was not obtained. The reason is simple because the treatment was based on harmonic approximation and no account was taken of anharmonicity but adequate analysis must include the latter effects|44,47,121,122| (Section 2.4c) which persists even at absolute zero because of the zero point vibrations. The anharmonic theory has been systematically developed during the last decade by Leibfried and Ludwig|121|, Maradudin and Flinn|122|, Cowley|123|, Pathak|124|, Koehler|125| and others.

The effects of anharmonicity are observable in neutron scattering measurements as frequency shifts and frequency widths of phonons with temperature|126-129| viz., anharmonic frequency is shifted from the harmonic value according to|130|

$$\omega(T) = \omega(0) + \Delta\omega(\bar{K}, j) + i\Gamma(\bar{K}, j) \quad \dots (4.1)$$

at each point \bar{K} , j denotes the branch. The imaginary part simply gives the change in phonon width and not the phonon shift. The widths are assumed to have the effect

of 'fuzziness' $\Delta g(\omega)$ versus ω curve where $\Delta g(\omega, T) = g(\omega, T) - g_h(\omega)$; $g(\omega, T)$ being the anharmonic and $g_h(\omega)$ the harmonic frequency distribution function. The average thermodynamic properties remain unaffected by the width and hence one has to consider only the frequency shifts with temperature.

Normally the temperature dependence of the frequencies of the normal modes of an anharmonic crystal are accounted for either in quasiharmonic approximation [92,93,131] (where lattice modes are assumed to be temperature dependent through volume expansion only) or explicit temperature dependent anharmonicity [131,132] where the frequencies depend explicitly on temperature and will be present even if the crystal is held at constant volume. This arises directly from terms in the potential energy expansion of higher order than quadratic in powers of displacements of the atoms from their mean positions. But it has been shown by Leadbetter [133] and Losee and Simmons [134] that the total anharmonic shifts in ω with temperature calculated from, the volume dependence through Grüneisen constant γ plus the explicit temperature dependence of entropy change $\Delta \omega^{\text{anh}}$; are in excellent agreement with the frequency shifts observed in inelastic neutron scattering [126]. Therefore it is argued that a proper calculation of temperature-dependent properties should include both the change in

volume due to thermal expansion as well as the explicit anharmonic effects; and not just the either as has been done by some earlier workers [92,93,131].

According to Barron [129,135,136], the anharmonic shift in the frequency at temperature T can be approximated from its value at $T=0$ by the expression

$$\omega(T) = \omega(0) \left[1 - \gamma \frac{\Delta V}{V} + \tau \langle E_{\text{vib}} \rangle \right] \quad \dots (4.2)$$

where $\Delta V = V(T) - V(0)$. The second term describes the volume dependence while the parameter τ describes the explicit anharmonic temperature dependence through average vibration energy per normal mode $\langle E_{\text{vib}} \rangle$, including the zero point energy. The sign of τ may be negative or positive depending on whether the cubic or quartic anharmonic terms is dominant in the expansion of lattice potential energy [137] and this account at least qualitatively why an integral property like heat capacity, even of strongly anharmonic solids; may not show any marked anomalous behaviour [135,138].

So far we have done the qualitative aspect of anharmonicity; regarding quantitative study, the most useful experimental quantity in the quasiharmonic approximation is Grüneisen constant γ , giving dependence of frequencies with volume, is defined by [139]

$$\gamma(V, \bar{k}, j) = \frac{d \ln \omega_{\bar{k}, j}}{d \ln V} \quad \dots (4.3)$$

$\omega_{\bar{k},j}$ and V being the eigen frequencies and volume respectively.

Assuming that a change in volume gives rise to the same relative change of frequency of every mode, from Eq.(4.3) it can be shown that

$$\omega_{\bar{k},j}(T) = \omega_{\bar{k},j}(0) \exp\left[-3 \int_0^T \alpha(T') \gamma(T') dT'\right] \quad \dots (4.4)$$

where 3α is the volume expansion and $\omega_{\bar{k},j}(0)$ is the eigen frequency at $T=0^\circ\text{K}$. In all our calculation γ is assumed to be independent of mode (\bar{k},j) .

On the other hand according to Barron^[135] and Overton^[140] the explicit anharmonic effects can be taken into account by a relative shift in the frequency of each lattice mode proportional to lattice energy ^[85,128, 141], i.e.,

$$\frac{\Delta\omega(\bar{k},j)}{\omega(\bar{k},j)} = \frac{AE_{\text{vib}}}{3Nk} \quad \dots (4.5)$$

with

$$E_{\text{vib}} = kT \sum_{\bar{k},j} \left[\frac{x}{2} + \frac{x}{e^x - 1} \right] ; x = \frac{\hbar\omega(\bar{k},j)}{kT}$$

Here, as pointed out by Barron¹³⁵, it should be noted that different shifts $\Delta\omega$ are needed for different thermodynamic properties like entropy, heat capacity etc. Leadbetter^[133], Barron^[135] and Overton^[140] have shown that the shift $\Delta\omega^S$ corresponding to the

entropy are identical to the shifts derived by Maradudin and Fein|126| for inelastic neutron scattering. The shift $\Delta\omega$ in Eq.(4.5) as assumed by Barron|135| corresponds to that of the entropy shift. The parameter A in Eq.(4.5) is different for different substances and is dependent on mode (\bar{K}, j) , volume |131|, particular model chosen|141| and the thermodynamic function being considered|141|. In the reasonable first approximation one can ignore the dependence of A on (\bar{K}, j) |85| and on volume for the study of explicit anharmonic contribution. Further we will consider A corresponding to entropy frequency shift. To estimate A for a given model, Feldman et.al.|142| have shown in the limit of low temperatures that

$$\theta_0^a = \theta_0^h \left(1 + \frac{3}{8} A \theta_0^h\right) \quad \dots (4.6)$$

where θ_0^a is the anharmonic (experimental) Debye temperature at low temperatures while θ_0^h and θ_∞^h refers to the harmonic Debye temperature obtained from a particular model (of phonon distribution function) at low and high temperatures respectively. To calculate Debye temperature, one has to first calculate from given p.f.d.f., the specific heat at constant volume $C_v(T)$ through the standard relation |143|

$$C_v(T) = k \int_0^\infty \left(\frac{\hbar\omega}{kT}\right)^2 \frac{e^{\hbar\omega/kT}}{(e^{\hbar\omega/kT} - 1)^2} g(\omega) d\omega \quad \dots (4.7)$$

Comparing this $C_V(T)$ with specific heat, obtained from Debye theory [143]

$$C_V(T) = 3k \left(\frac{T}{\theta_D} \right)^3 \int_0^{\theta_D/T} \frac{x^4 e^x}{(e^x - 1)^2} dx \quad \dots (4.8)$$

for various θ_D/T ratios, one can calculate θ_D at any temperature. Taking into account both the quasi-harmonic (Eq.(4.4)) and explicit temperature dependent anharmonicity (Eq.(4.5)), the modified frequency for individual mode becomes

$$\omega^a(\bar{k}, j) = \omega(\bar{k}, j) + \Delta\omega^{qh}(\bar{k}, j) + \Delta\omega^{a'}(\bar{k}, j) \quad \dots (4.9)$$

with

$$\frac{\Delta\omega^{qh}}{\omega} = e^{-B} - 1; \quad B = 3 \int_0^T \alpha(T') \gamma(T') dT' \quad \dots (4.10)$$

and

$$\frac{\Delta\omega^{a'}}{\omega} = \frac{AE_{vib}}{3Nk} \quad \dots (4.11)$$

This leads to the final expression

$$\omega^a = \omega^0 \left(e^{-B} + \frac{AE_{vib}}{3Nk} \right) \quad \dots (4.12)$$

Gilat and Nicklow [129] have measured the phonon dispersion curves of aluminium at 80 and 300°K and have calculated the p.f.d.f. at these temperatures. A comparison of their spectrum reveals a rather uniform shift in frequencies (~3%) accompanied by a slight change (~10%) in the relative heights of peaks in $g(\omega)$. The overall shape of the distribution function does not change

appreciably. Furthermore any change in $g(\omega)$ consequent upon the change in ω is unimportant as it is a normalised function.

Employing the formalism outlined above, we have recalculated variation of Mössbauer fraction with temperature for

- (i) Kr^{83} in solid Krypton|79|
- (ii) Fe^{57} in natural Iron|80| and
- (iii) Au^{197} in Gold metal|81| .

These cases are discussed in turn.

4.2 9.3 keV transition of Kr^{83} in Solid Krypton

The anharmonicity plays an important role in all rare gas solids because of small binding energies of these crystals|144|. Beaumont et al|145| have shown from the shape of experimental θ_D versus temperature curve that anharmonic contribution to the vibrational properties of solid krypton are appreciable, particularly in the range $T \gg \theta_D/10$. Vashishta and Pathak|93| using Debye theory ($\theta_D = 50^\circ\text{K}$) have calculated $f(T)$ variation considering only the quasiharmonic approximation (Eq.(4.10)) i.e. allowing the Debye temperature to vary only with volume. The calculated values, when compared with the experiment|84|, get worsened than that obtained with the use of harmonic approximation. The lack of agreement is due to the use of (i) the Debye approximation and (ii) only one type of anharmonicity.

Here we will like to point out that for krypton the quartic anharmonic term dominates the cubic term at all temperatures|144| and thus τ (Eq.(4.2)) will be positive and will remain so. Thus as both the corrections have opposite effect on the frequency shift, therefore $\omega(T)$ will be determined by the resultant of these contributions.

We have calculated |79| $f(T)$ ranging from $T=5-100^{\circ}\text{K}$ using Eq.(2.13) after modifying the measured frequencies |85,87| (harmonic) according to Eqs.(4.10-4.12) for the quasiharmonic, explicit temperature dependent anharmonicity and total anharmonicity respectively. The input data of $\gamma(T)$ and $3\alpha(T)$ at various temperatures studied were taken from the experimental work of Losee and Simmons|134|. For (m-6) potential distribution function|85| the value of the anharmonic parameter $A = 1.0 \times 10^{-3}/^{\circ}\text{K}$, as calculated by Feldman and Harton|146|, was used. On the other hand for (exp-6) Buckingham potential distribution function|87|, A was evaluated from Eq.(4.6) with $\theta_0^h = 61.0$, $\theta_{\infty}^h = 57.5$ (calculated from Eqs.(4.7) and (4.8)) and $\theta_0^a = 70.9^{\circ}\text{K}$ |145,147| and turned out to be $7.53 \times 10^{-3}/^{\circ}\text{K}$. Figure (4.1) shows the variation of Debye temperature $\theta_D(V_0)$ with temperature, as calculated from (a), (m-6) potential, $g(\omega)$ and (b), (exp-6) potential $g(\omega)$; along with the Debye temperature derived from measurement of specific heat |145,147|.

The results for the calculation, for the quasi-harmonic, the explicit temperature dependent anharmonic and total anharmonic cases, are displayed in Fig.3.1(b,c,d) and Fig.3.2(b,c,d) respectively for the (m-6) and (exp-6) potentials, phonon distribution functions. The nice agreement with the experiment is observed especially for the distribution function derived from the (exp-6) potential|87|. An independent calculation of $f(T)$ dependence was made by Brown|148| who also included both kinds of anharmonicity in the same way as we did, and the results are in agreement with ours, (Fig.(3.1d)).

Finally, we would like to point out that the inadequacies in the existing model calculation may emanate from various causes; firstly the use of two body interatomic potential for the study of lattice dynamics of the rare gas solids may be questionable|141,149|. For example Losee and Simmons|150,151| measured the equilibrium vacancy concentration in solid krypton and concluded that upto 20% of the total potential energy might be contributed by many body forces. Some further indication that three body effects may be important in krypton comes from the non-agreement of the experimentally measured value of Poisson ratio|152| near $T=0$, with the calculations based on only central two body interactions|153|. Secondly the thermal formation of atomic vacancies|150,151| which have a significant effect on all the thermodynamic properties of solid krypton especially at high

temperatures [134,145] will reduce the binding and hence will make the observed f values small. Thirdly the discrepancy may be due to the breakdown of the perturbation approach when applied to inert gas solids, above $\sim 4/10$ of their melting temperature (i.e. for root mean square amplitudes greater than $\approx 6\%$) [149,154,155] and one should perform the calculation of f in the framework of self consistent phonon theory of Born [156-158]. Lastly the approximations used in the anharmonic model may also be partly responsible.

4.3 14.4 keV TRANSITION OF Fe^{57} IN NATURAL IRON- Using Eq.(2.13) with the necessary modification of vibrational frequencies for anharmonicity according to Eqs.(4.10 to 4.12), Lamb-Mössbauer factor has been calculated [80] at various temperatures ranging from 150-1000^oK with the phonon spectra measured by Minkiewicz et,al. [102]. Due to the non-availability of the temperature dependence of Grüneisen parameter $\gamma(T)$, it was evaluated from the expression

$$\gamma(T) = \frac{3\alpha(T)V_T}{K_T C_V(T)} \quad \dots (4.13)$$

where the isothermal compressibility

$$K_T = \frac{3}{C_{11}(T)+2C_{12}(T)} \quad \dots (4.14)$$

$\alpha(T)$, V_T and $C_V(T)$ are respectively the linear expansion;

molar volume and specific heat at constant volume. The various quantities used are taken from latest experimental measurements, viz., the elastic constant C_{11} and C_{12} from the work of Rayne and Chandersekhar|159|, Lord and Beshar|160| and Lees and Lord|161|; α and V_T from Ridley and Stuart|162| and C_V from Schweiss et al.|99|. The anharmonic parameter A determined from Eq.(4.6) with $\theta_0^a = 442.60$ |163|, $\theta_0^h = 437.03$ and $\theta_\infty^h = 422.0$ °K (Eqs.(4.7) and (4.8)), came out to be $0.0805 \times 10^{-3}/^\circ\text{K}$ as compared with $7.53 \times 10^{-3}/^\circ\text{K}$ for krypton lattice. Since the experimental measurement of p.f.d.f. pertained to 300°K ; the calculations of all the anharmonic frequency shifts at various temperatures were normalised with respect to 300°K . To quote typical values, it turns out that at $T = 1000^\circ\text{K}$, harmonic frequency is shifted by -3.72% in quasiharmonic, $+5.51\%$ due to explicit anharmonicity, leading to a total shift of $+1.79\%$. The corresponding f values are changed by -7.96% , $+11.32\%$ and $+3.76\%$ respectively as displayed in Fig.3.3(b-d) along with the experimental results |94,95|.

Thus inspite of using all the input quantities measured experimentally, agreement with the experiment is not much improved (Figs.4.1(a and d)) and shows some extra factor contributing to f. Further the fact, that the residual discrepancy in f from measurements, being large at low and relatively small at high temperature (near Curie temperature), indicate possible

contribution of magnetic ordering. This is in conformity with the experimental finding of Coey et.al. |164| observed in the case of thermal energy shift in HoFeO_3 system and theoretical prediction of Bashkirov and Selyutin |165|. It will be discussed in detail in Chapter V.

4.4 77.3 keV TRANSITION OF Au^{197} IN GOLD METAL

Employing the p.f.d.f. measured at 0°K by Christensen and Seraphin |104|, the recoilless fraction has been recalculated |81| over a temperature range $4.2-100^\circ\text{K}$ after incorporating the contribution due to anharmonicity as done in the above two cases. The experimental specific heat C_p measured by Gebelle and Giaque |166| after correcting for $C_p - C_v$ and C_e -electronic heat capacity, yields $\theta_0^a = 166.56^\circ\text{K}$ whereas θ_0^h and θ_∞^h calculated from Eqs.(4.7) and (4.8) gives $\theta_0^h = 142.96$ and $\theta_\infty^h = 200^\circ\text{K}$. Eq.(4.6) then gives the anharmonic parameter $A = 2.20 \times 10^{-3}/^\circ\text{K}$. The coefficient of linear thermal expansion $\alpha(T)$ was taken from the measurements of Fraser and Hollis Hallett |167| and Kos |168|. Further the Grüneisen coefficient $\gamma(T)$ was calculated from Eq.(4.13) with K_T taken from the measurements of Neighbour and Alers |169|. To quote specific value, the maximum frequency shifts at 100°K with respect to 0°K come out to be -0.64% , $+24.85\%$ and $+24.21\%$ for quasi-harmonic,

only anharmonic and combined anharmonicity respectively. The corresponding $f(T)$ change due to combined anharmonicity (Eq.(4.12)) is shown in Fig.(3.4b) and exhibits nice agreement with the experimental measurements^[103].

CHAPTER-V

ANALYSIS OF MÖSSBAUER FRACTION IN SPIN-ORDERED
SYSTEM

5.1 INTRODUCTION We have seen in Chapter IV that the Mössbauer fraction for Fe^{57} in natural iron, calculated from experimentally measured phonon frequencies even after modifying frequencies due to anharmonicity, was in disagreement with the measured $f(T)$ variation (Fig.3.3). The important feature of the plot in Fig.(3.3) is that the departure from the experimental values starts at the magnetic transition temperature (Curie temperature, T_c). This suggests that the observed effect is associated with some kind of magnetic ordering in the system and is not simply the consequence of the inadequacy of model used in describing the phonon spectrum or anharmonicity. Alekseev et.al.[170], have also observed such an anomaly in Yttrium iron Garnets from Mössbauer studies. Coey et.al.[164] studied the temperature dependence of Mössbauer spectrum shift for $\text{HoFe}^{57}_2\text{O}_3$ ($T_N = 642^\circ\text{K}$) in the temperature range $99-875^\circ\text{K}$ and Bashkirov et.al.[171] for $\alpha\text{-Fe}_2\text{O}_3$ ($T_N=956^\circ\text{K}$) in the temperature interval from 80 to 1080°K , and made the similar observations. Such type of anomaly has also been observed in various other properties like thermal

expansion|172|, specific heat |173| etc. Thus, it seems that the existence of magnetic ordering plays an important role in the origin of all these anomalies, in other words these quantities are influenced by the exchange interaction of magnetic ions. The reason is simple- the energy of exchange interaction of magnetic ions in the crystal depends on the distance between the interacting ions. Therefore, the presence of exchange forces can not have an influence upon the elastic constants of the lattice and consequently on the vibrational spectrum of the crystal. Since the intensity of the Mössbauer effect as well as the relative-shift **in the Mössbauer spectrum** depends on the parameters which characterize the vibrational spectrum of the crystal, therefore it becomes clear that exchange forces between spins of the electrons on neighbouring magnetic ions in a crystal lattice will influence (and contribute to) the magnitude of these quantities. Further the exchange interaction energy also depends on the relative orientation of the spins of the interacting ions, and hence f and S.O.D. should vary with a change in the degree of ordering of the spin system in the crystal.

Quantitative solution of the problem, formulated above has been made by Bashkirov and Selyutin for both the cases viz., intensities |174| and relative shift of Mossbauer spectrum|165|. We will describe in brief their

approach to the problem.

The Debye Waller factor and centre shift in the Mössbauer spectrum may be expressed as [175]

$$2W = \frac{4\pi^2\hbar}{2NM} \sum_{\bar{K}j, \bar{K}'j'} \frac{(\bar{g} \bar{e}(\bar{K}j))(\bar{g} \bar{e}(\bar{K}'j'))}{\sqrt{\omega(\bar{K}j)\omega(\bar{K}'j')}} \times \langle A_{\bar{K}j}^-(0) A_{\bar{K}'j'}^-(0) \rangle \quad \dots (5.1)$$

$$\frac{\delta E_\gamma}{E_\gamma} = \frac{M}{2(M')^2 c^2} \frac{\hbar}{2N} \sum_{\bar{K}j, \bar{K}'j'} \bar{e}(\bar{K}j) \bar{e}(\bar{K}'j') \sqrt{\omega(\bar{K}j)\omega(\bar{K}'j')} \times \langle B_{\bar{K}j}^-(0) B_{\bar{K}'j'}^-(0) \rangle \quad \dots (5.2)$$

where M' is the mass of the Mössbauer atom, \bar{g} is the wave vector of the gamma quantum, $\omega(\bar{K}j)$ and $\bar{e}(\bar{K}j)$ are the phonon frequency and polarisation vector. $A_{\bar{K}j}^- = a_{\bar{K}j}^- + a_{\bar{K}j}^+$ and $B_{\bar{K}j}^- = a_{\bar{K}j}^- - a_{\bar{K}j}^+$ with $a_{\bar{K}j}^-$ and $a_{\bar{K}j}^+$ are respectively the annihilation and creation operators for a phonon mode $\bar{K}j$. Thus the solution of the problem reduces to determination of the phonon correlation functions $\langle A_{\bar{K}j}^-(0) A_{\bar{K}'j'}^-(0) \rangle$ and $\langle B_{\bar{K}j}^-(0) B_{\bar{K}'j'}^-(0) \rangle$ taking account of the distortion (perturbation) of the phonon spectrum of the crystal introduced by the exchange interaction of the magnetic ions.

The operator which describes the exchange interaction of magnetic ions is

$$\hat{H}_{\text{exch.}} = \sum_{i > \lambda} I(\bar{x}_{i\lambda}) \hat{\bar{S}}_i \cdot \hat{\bar{S}}_\lambda \quad (5.3)$$

where \bar{S}_i is the spin operator of the i th atom, $\bar{x}_{i\lambda}$ characterizes the distance between the i th and λ th ion. One can arrange the above expression successively in the order of relative shifts $u_{i\lambda}^j$ of magnetic ions, retaining upto quadratic terms in $u_{i\lambda}^j$:

$$\begin{aligned} \hat{H}_0 &= \sum_{i > \lambda} I_0(\bar{x}_{i\lambda}) \hat{\bar{S}}_i \cdot \hat{\bar{S}}_\lambda \\ \hat{H}_1 &= \sum_{i > \lambda} \bar{S}_i \cdot \bar{S}_\lambda \sum_j \left(\frac{\partial I(\bar{x}_{i\lambda})}{\partial \bar{x}_{i\lambda}^j} \right) u_{i\lambda}^j \quad \dots (5.4) \\ \hat{H}_2 &= \sum_{i > \lambda} \bar{S}_i \cdot \bar{S}_\lambda \sum_{j,r} \frac{1}{2} \frac{\partial^2 I(\bar{x}_{i\lambda})}{\partial \bar{x}_{i\lambda}^j \partial \bar{x}_{i\lambda}^r} u_{i\lambda}^j u_{i\lambda}^r \end{aligned}$$

The Hamiltonian H_L which describes the vibrations of the crystal in the harmonic approximation is

$$\hat{H}_L = \sum_{\bar{k}j} \hbar \omega(\bar{k}, j) \left[a_{\bar{k}j}^+ a_{\bar{k}j} + \frac{1}{2} \right] \quad \dots (5.5)$$

Finally the Hamiltonian of the problem can be expressed as

$$\hat{H} = \hat{H}_L + \hat{H}_S + \hat{H}_{LS}$$

with

$$\hat{H}_{LS} = \hat{H}_0 + \hat{H}_1 + \hat{H}_2 \quad \dots (5.6)$$

\hat{H}_L and \hat{H}_S describe the state of the lattice oscillators and the spin system of the crystal respectively without taking into account the interaction between them, while

\hat{H}_{LS} represents the interaction of the two subsystems mentioned.

Using the standard Green function technique to calculate the correlation function, Bashkirov and Selyutin|165,174| have shown that in a crystal containing exchanged coupled magnetic ions, f and $\delta E_Y / E_Y$ can be calculated from Eqs.(2.13) and (2.23), with the phonon frequencies ω (in the absence of any exchange interaction) is changed to ω' as

$$\omega'(\bar{K}, j) = \omega(\bar{K}, j)(1+B)^{1/2} \quad \dots (5.7)$$

with B related to the correlation function $\langle \bar{S}_i \cdot \bar{S}_j \rangle$ as

$$B = -(8\pi^2 \langle \bar{S}_i \cdot \bar{S}_j \rangle \frac{a^2}{v^2 M}) J_e''(a) \quad \dots (5.8)$$

$a = x_i^0 - x_j^0$ is the distance between neighbouring magnetic ions, v , the velocity of sound in the lattice and $J_e''(a)$ is the second derivative of the exchange integral.

Using this formalism we will try to explain the discrepancy obtained in f for Fe^{57} in natural iron.

5.2 14.4 keV TRANSITION OF Fe^{57} IN NATURAL IRON

As has been done by other workers|164,176|, we have assumed molecular field model for exchange interaction where exchange parameter B can be written as

$$B = B_0 \mu^2 (T) \quad \dots (5.9)$$

where $\mu(T)$ is the reduced sublattice magnetisation and $B_0 \approx 1$ (for both ferromagnet and antiferromagnet). Treating B_0 as a variable parameter, Lamb-Mössbauer factor has been calculated [80] from Eq.(2.13) with the measured phonon frequencies [102] modified due to the presence of exchange interactions (Eqs.(5.7) and (5.9)) combined with the frequency shift due to the total anharmonicity (Eq.4.12). The reduced sublattice magnetisation $\mu(T)$ at various temperature was taken from Housley and Hess [177]. The corresponding curves of f for $B_0 = 0.2, 0.4$ and 0.6 are displayed in Fig.(5.1).

Thus we find that the Mössbauer intensity data is explained satisfactorily by the addition of a magnetisation dependent f , with magnetisation terms proportional to μ^2 and constant of proportionality $B_0 = 0.4 \pm 0.2$. This B_0 will be used in Chapter VII to analyse the measured energy shift for Fe^{57} in natural iron.

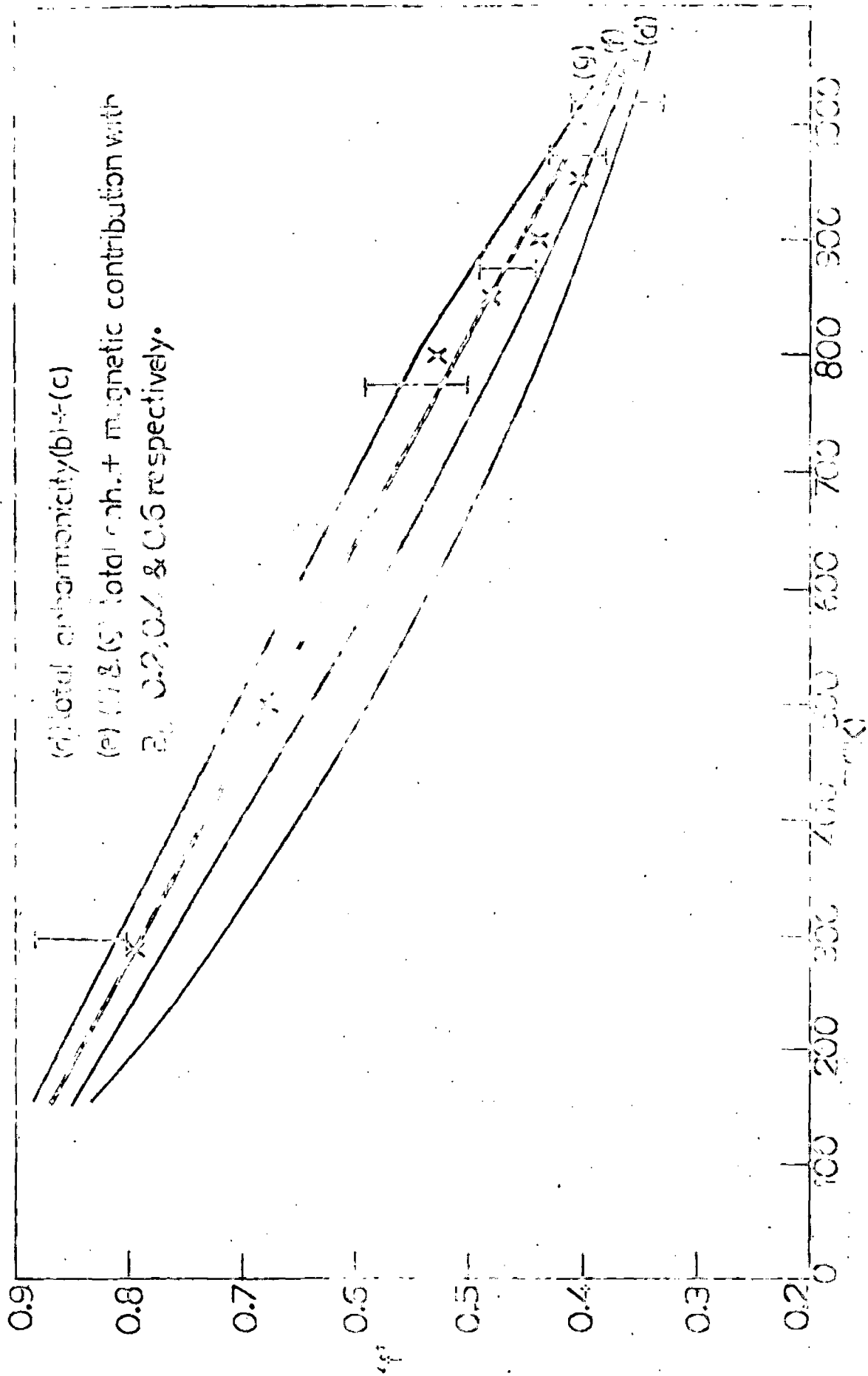


FIG. 5.1. A plot of f versus temperature T for iron, including anharmonicity (a) and magnetic contribution with various values of D_0 .

CHAPTER VI

THE INFLUENCE OF PRESSURE ON
MÖSSBAUER EFFECT

6.1 INTRODUCTION- Mossbauer effect because of the sharpness of the resonant line it emits, and of their sensitive dependence upon both the immediate environment of the nuclei and upon the lattice characteristics of the crystals in which they are located, has become major topic of research in several areas of physics. Unfortunately, at the present stage only a few elements can be studied with this technique because of the various restrictions (mentioned in Chapter I) in observing the Mossbauer effect. One such restriction is the tight binding of the host lattice. On the other hand if the pressure on the lattice, containing the nucleus, is increased, the lattice rigidity also increases. This as a result should bring about an enhancement in the amount of recoilless radiation. Thus the use of high pressure may allow the study of Mossbauer effect for materials where it is either marginal or non-existent at zero external pressure.

Quantitatively, one can incorporate the effect of pressure on Mössbauer parameters f and S.O.D., through either the Gruneisen relation [139,178]

$$\gamma = - \frac{d \langle n \omega \rangle}{d \langle n V \rangle} = - \frac{d \langle n \theta_D \rangle}{d \langle n V \rangle} \quad \dots (6.1)$$

or the Lindeman relation [179]

$$\theta_D = \frac{\text{Const.}}{3/\bar{V}} \sqrt{\frac{T_m}{M}} \quad \dots (6.2)$$

as both give the variation of lattice frequencies (hence Debye temperature) with volume. In the above equations γ is the Grüneisen constant; θ_D and T_m are the Debye temperature and melting point at the specific volume V .

Following Hanks [180] and Dlouha [181], we employ the Grüneisen relation. Assuming, in the first approximation that γ is independent of volume and all the frequencies shift equally by the application of pressure then from Eq.(6.1) the lattice frequency ω_P at pressure P becomes,

$$\omega_P = \omega_0 \left(\frac{V_P}{V_0}\right)^{-\gamma} \quad \dots (6.3)$$

ω_0 is the lattice frequency at zero pressure. Rewriting it in terms of Debye temperature θ as

$$\theta_P = \theta_0 \left(\frac{V_P}{V_0}\right)^{-\gamma} \quad \dots (6.4)$$

where θ_P and θ_0 are the Debye temperatures at the specific volumes V_P and V_0 respectively. V_P/V_0 can be known from the experimental measurement of equation of state.

However, in the absence of this, one can approximate

$(V_P/V_0)^{-\gamma}$ to

$$\left(\frac{V_P}{V_0}\right)^{-\gamma} = (1 + \gamma K_T \Delta P) \quad \dots (6.5)$$

where $\Delta P = P_2 - P_1$ and $K_T = \frac{1}{V_0} \frac{\Delta V}{\Delta P}$ the compressibility of

the host lattice. In the light of this formalism, we are interested in the two types of studies.

(a) Southwell et.al. |182| have measured the Mössbauer fraction for 14.4 keV transition of Fe^{57} in natural iron over the pressure range 0-85 Kbar and Panyushkin and Voronov |183| have measured f for Sn^{119} in white tin upto 110 Kbar. It is worthwhile to compare the measurement with the calculations in order to check the validity of the model used.

(b) Mössbauer fraction for Cs^{133} in cesium |118|, K^{40} in potassium |184| and Au^{197} in gold metal |103| is observed to be very small even at low temperatures. It will be interesting to see whether the effect of high pressure can obviate the necessity of low temperatures, which are normally required to study these elements and their compounds.

All these cases will be discussed below:

6.2 77.3 keV TRANSITION OF Au^{197} IN GOLD METAL

Variation of f with pressure has been calculated |81| from Eq.(2.13) with phonon frequencies, calculated by Christensen and Seraphin |104|, modified according to Eq.(6.3) for pressures ranging from 0-200 Kbar. Calculations were done at $T=4.2$ and 80°K . Gruneisen constant γ was taken as 2.40 and 3.02 at 4.2 and 80°K respectively (Sec.(4.4)) and V_P/V_0 at various pressures was taken from

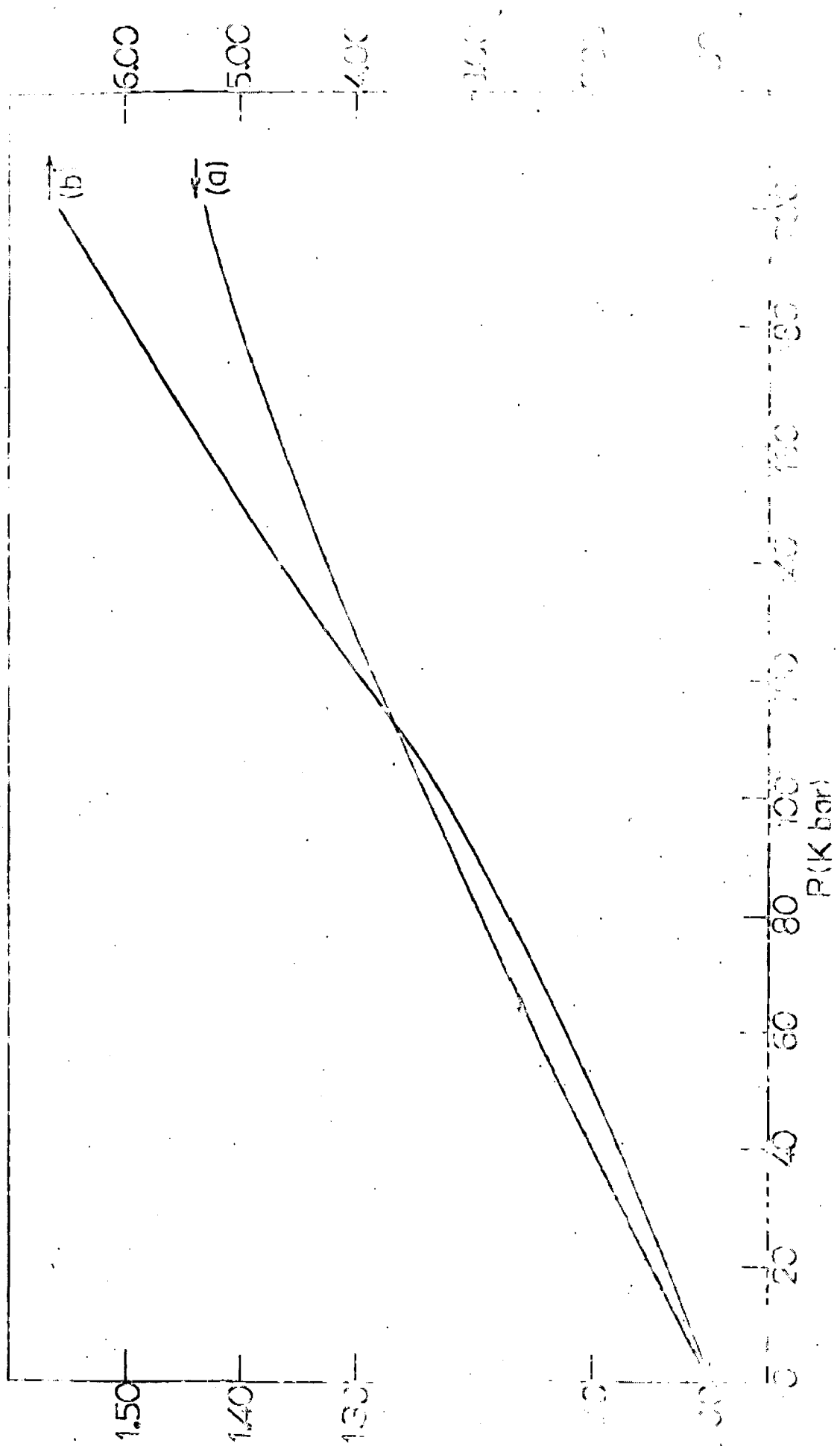


Fig. 9. Plots of (p/p_0) versus pressure for Au^{197} in Gold metal, at (a) $T = 4.2$ (soft or ductile) and (b) $T = 6.0$ (right ordinate).

the reported measurements of Vaidya and Kennedy|185| and McQueen and Marsh|186| and was taken to be independent of temperature. The results are displayed in Fig.(6.1). However, the prediction has to wait its verification till measurements are available. To quote specific value, at $P=200$ Kbar with $V_p/V_o = 0.917$ |186| we get $f_p/f_o = 1.431$ and 6.596 at 4.2 and 80°K respectively. It clearly shows that one can perform the experiments with Au^{197} even at relatively higher temperature say liquid nitrogen to get observable effect provided an impressed pressure of the order of 200 Kbar is applied.

6.3 26.8 keV TRANSITION OF I^{129} IN CESIUM IODIDE AND 81.0 keV TRANSITION OF Cs^{133} IN CESIUM IODIDE AND CESIUM METAL

We have seen in Chapter III that the probability of Mössbauer effect is rather very small in all these cases. Because of the high compressibility of these materials it is worthwhile to study the effect of pressure on these transitions. We have calculated f versus pressure |82| for Cs^{133}I ($T=4.2$ and 80°K), CsI^{129} ($T=80$ and 300°K) and Cs^{133} ($T=4.2^\circ\text{K}$) upto 100 Kbar pressure. Unperturbed phonon frequencies, taken from the work of Bührer and Halg|113| for CsI and Satya Pal |117| for Cs lattice, were modified through Eq.(6.3) at various pressures. Values of V_p/V_o at different pressures are taken from the work of Bridgman|187| for CsI and Bridgman|188| for cesium metal and assumed to

be independent of temperature. γ was taken as, 2.0 for CsI at all the three temperatures [189] and 1.29 for Cs at 4.2°K [190]. The resulting f versus pressure for CsI¹²⁹ is shown in Fig.(6.2) and for Cs¹³³I and Cs¹³³ are tabulated in Table 6.1. For Cs¹³³ in cesium the results are also plotted in Fig.(6.3) which shows the discontinuity in f between 40-50 Kbar. Similar type of discontinuity is also seen in the S.O.D. shift δE_2 versus pressure plot (Chapter VII). It may be pointed out that the transition in f and δE_2 is due to the discontinuity in volume V_P/V_0 which is of the order of 0.056 at 45 Kbar [188]. Although no experimental results are available for these but from Fig.(6.2) and Table (6.1), we observe much stronger effect in these cases especially in cesium metal as expected due to its high compressibility. Thus we conclude that by applying a pressure of the order of 100 Kbar, CsI¹²⁹ and Cs¹³³I can be studied even at 300 and 80°K respectively whereas Cs¹³³ metal can be investigated at liquid helium temperature with considerably higher accuracy.

6.4 23.9 keV TRANSITION OF Sn¹¹⁹ IN WHITE TIN(β)-Panyushkin

and Voronov [183] have studied the Mössbauer effect in metallic tin at pressures upto 110 Kbar and at $T=300^\circ\text{K}$. Comparing the areas of the resonance curves for different pressures with the area of the curve at atmospheric pressure and taking the absolute probability, of the

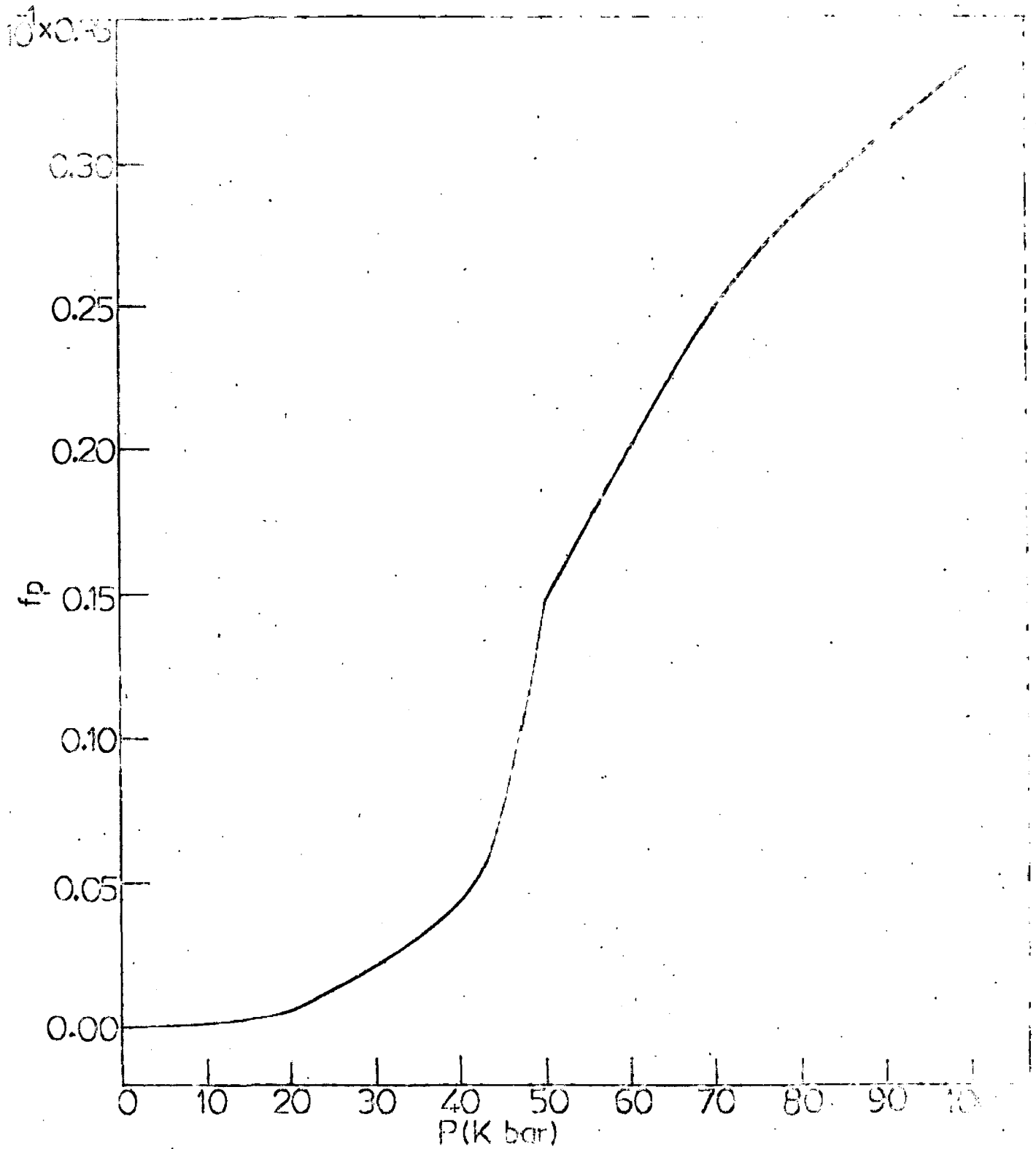


FIG.6.3-Variation of $f(P)$ for Cs^{133} -81.0 KeV transition in Cesium metal.

Table (6.1)-Calculated dependence of pressure on Mossbauer fraction for Cs^{133} -81.0 keV transition in CsI and Cs metal

(Note, $E-x=10^{-x}$)

Pressure (Kbar)	Cs^{133}	Cs^{133}I	
	T=4.2°K	T=4.2°K	T=80°K
0.0	0.623E-6	0.112E-1	0.154E-5
10.0	0.861E-4	0.199E-1	0.311E-4
20.0	0.534E-3	0.295E-1	0.199E-3
40.0	0.430E-2	0.502E-1	0.178E-2
60.0	0.199E-1	0.707E-1	0.611E-2
80.0	0.284E-1	0.902E-1	0.134E-1
100.0	0.333E-1	0.108E-0	0.230E-1

effect in β -tin, the value of 0.060 ± 0.006 , at zero external pressure|191|, they obtained the pressure dependence of f . Although they analysed their results the framework of Debye theory to get the Gruneisen constant but in view of the available phonon spectra of white tin|192|, it was decided to calculate variation of f with pressure.

Strictly speaking Eq.(2.13) is applicable only to a monatomic cubic lattice. However, as a first approximation likewise the earlier workers|193,194|, we will apply this equation to study white tin which has a tetragonal structure. Using Eq.(2.13) after modifying the phonon frequencies |192| with pressure P according to Eq.(6.3), dependence of f on pressure upto 110 Kbar ($T=300^\circ\text{K}$) is calculated |195|. Gruneisen γ is taken to be 1.71, calculated from Eq.(4.13) with the input quantities taken from the experimental measurements reported in the literature. V_P/V_0 at various pressures is taken from the work of Bridgman |196|, Vaidya and Kennedy|185| and McQueen and Marsh|186|.

The calculated values of $f(P)$ are shown in Fig.(6.4) along with the experimental results|183|. Evidently there is nice agreement with the measurement.

6.5 29.4 keV TRANSITION OF K^{40} IN POTASSIUM METAL- For this transition, f even at 4.0°K is 3.6%. |184|. Due to the large compressibility of alkali metals, it stands

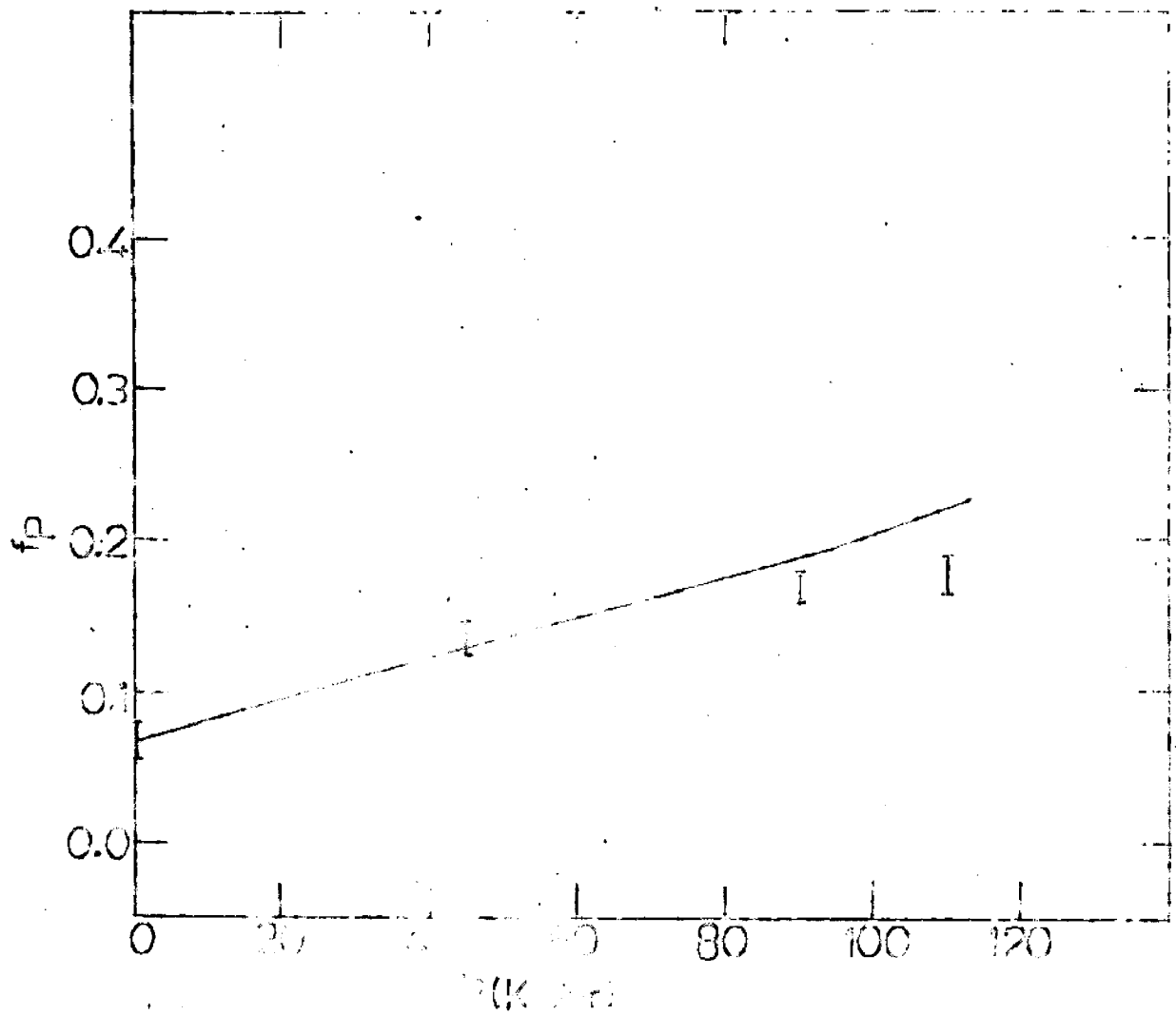


FIG. 6.4- Variation of $f(F)$ for S_{100} in white tin, at 300°K , along with the experimental measurements [183].

to reason to anticipate distinctly noticeable pressure effects. Taking the p.f.d.f. measured, from inelastic, neutron scattering, by Cowley et.al. |197|, $f(P)$ was calculated, at 4.0 and 80°K, for a pressure range 0-100 Kbar. The values of V_P/V_0 are taken from the experimental measurements of Bridgman |188| and Vaidya et.al. |198| and assumed to be independent of temperature. γ is taken as 1.45 and 1.41 at 4 and 80°K respectively |199|. The calculated f versus pressure is shown in Fig.(6.5) |200|. To quote typical values these are at 4°K; $f(0) = 0.0988$, $f(100)=0.439$ and at 80°K, $f(0)=0.439 \times 10^{-4}$ and $f(100)=0.195$. Although no contact of these predictions can be made with the experiment due to lack of measurements; it is, however, abundantly clear that at 80°K, a pressure of 100 Kbar will bring f to an observable value of 0.195. In other words the crystal binding is changed sufficiently, to increase f by four orders of magnitude. Thus it is concluded that 100 Kbar pressure renders feasible the measurement of f for 29.4 keV transition in potassium even at 80°K.

6.6 14.4 keV TRANSITION OF Fe⁵⁷ IN NATURAL IRON- Southwell et al. |182| reported the Mössbauer spectra for 14.4 keV transition of Fe⁵⁷ in natural iron-foil source over the pressure range 0-85 Kbar at room temperature. From the area of the absorption dips in the transmission curve, normalised to unity far off-resonance, with the assumption that absorption area is proportional to the source

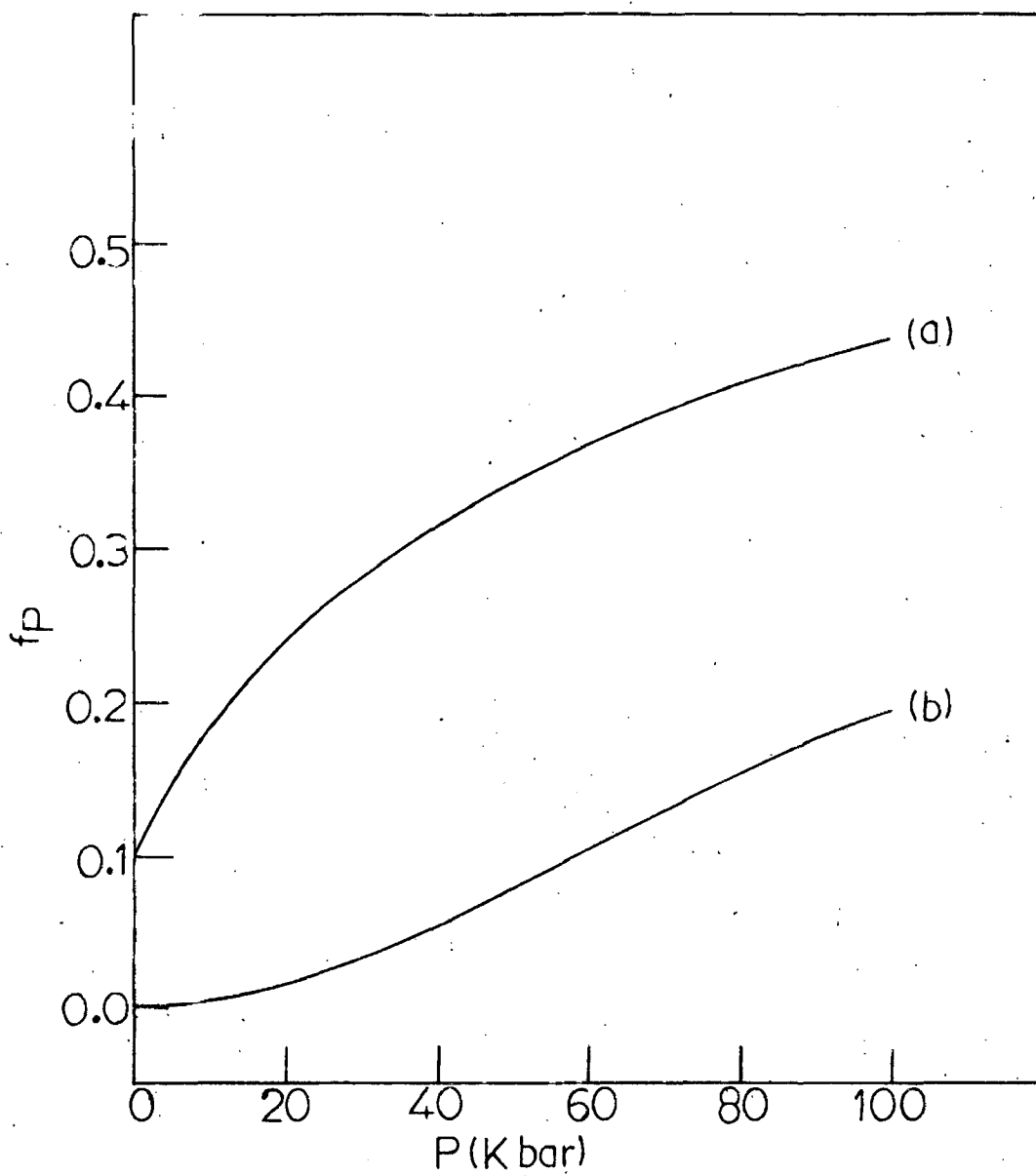


FIG.6.5- Variation of $f(P)$ for K^{40} in Potassium metal at (a) 40 and (b) 80°K.

recoilless fraction f_s (Eq.(2.32)); they obtained the value of $\frac{\partial}{\partial P} (f_p/f_o) = \frac{\partial}{\partial P} (A_p/A_o) = 0.0017 \text{ Kbar}^{-1}$; where f_p and A_p represent the Mössbauer fraction and area of the absorption curve respectively at pressure P and f_o and A_o the corresponding values at zero atmosphere. With atmospheric Debye temperature $\theta_D = 400^\circ\text{K}$ and $\gamma=1.6$, they calculated $\frac{\partial}{\partial P} (f_p/f_o) = 0.00038 \text{ Kbar}^{-1}$ |182| showing that measured f factor increases with pressure nearly three times as rapidly as the theoretical estimate. They attributed the discrepancy due to the polarisation of iron with pressure. It may be pointed out that it is appropriate to apply the experimental $g(\omega)$ before attempting the comparison of the calculation with the measurement. It was thus decided to recalculate $f(P)$ using phonon frequencies measured by Minkiewicz et.al. |102| from inelastic scattering of neutrons and look into the discrepancy. Using Eq.(2.13) with the phonon frequencies |102| modified according to Eq.(6.3); $f(P)$ was calculated at $T=300^\circ\text{K}$ for pressures upto 100 Kbar. V_P/V_o was replaced by Murnaghan equation |201|

$$\frac{V_P}{V_o} = \left(1 + \frac{P}{275}\right)^{-0.169} \quad \dots (6.6)$$

for b.c.c. iron. γ was taken as 1.6 |178|. No temperature anharmonicity was included since both the experimental f_p as well as p.f.d.f. were obtained at room temperature. Figure (6.6) shows the results of present calculation.

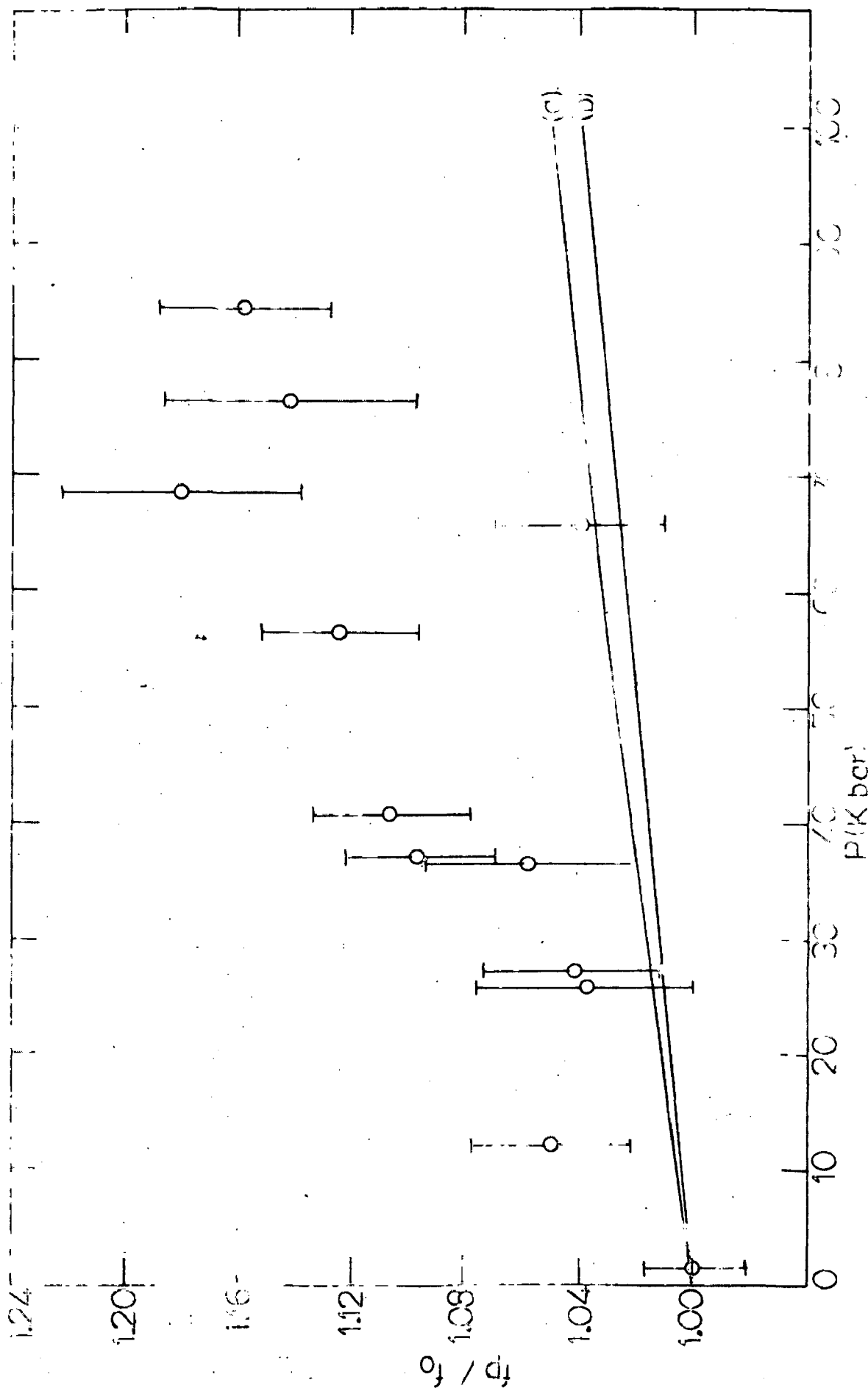


FIG.6.6 - Plot of f_p/f_0 versus pressure for Fe^{57} in natural iron using (a) actual phonon distribution function [102] (b) Debye phonon distribution function [182], along with the expt. values [182].

(a) Debye model calculation [182] along with the experimental results [182]. Thus inspite of refined calculation we find the same discrepancy as observed by Southwell et.al.[182] and one can state that the residual discrepancy may have its possible origin in the change of polarisation of iron lattice with pressure, resulting from pressure dependent changes in the anisotropy and magnetostriction constant [202]. The fact that polarisation of the iron foil changes with pressure can be seen from Fig.3 of Southwell et al. paper [182], which shows the variation of intensity, of lines 2 and 5 in the six finger pattern of Fe, with pressure. On the other hand Vanfleet and Decker[203] have shown that there is some evidence that the f-factor in iron is a function of polarisation. Thus it is concluded that the discrepancy between theory and experiment can be resolved if the experiment can be performed with more accuracy which is possible only if either the unpolarised or completely polarised foil is available or some quantitative estimation regarding polarisation dependent f is made.

CHAPTER-VII

ANALYSIS OF MÖSSBAUER GAMMA RAY
ENERGY SHIFT

7.1 INTRODUCTION- So far we have been dealing with Mössbauer intensity. In this chapter we will explore the second dynamical parameter of Mössbauer effect viz., Mössbauer gamma-ray energy shift. As seen in Chapter II this can also give fund of information. Because of extremely high resolution (about 1 part in 10^{15}) of Mössbauer resonance absorption, a number of relativistic effects|26| have been measured-most notable being the accurate measurement of the gravitational shift |204| and the thermal shift |22| etc. In any experiment the total spectrum shift (δE) which is actually measured is the sum of the isomeric shift (I.S.) of the absorber relative to the source (δE_1) and the difference between the second order Doppler shifts (S.O.D.) of the source and absorber (δE_2). These two arise in quite distinct ways. The I.S. of the energy levels of the absorber with respect to the source is a result of the different electrostatic interactions of these nuclei with the field of surrounding electrons and, in the non-relativistic approximation, is given by the relation (Eq.(1.7)),

$$\delta E_1 = \frac{2\pi}{5} Ze^2 (R_e^2 - R_g^2) [|\Psi(o)|_a^2 - |\Psi(o)|_s^2] \quad \dots (7.1)$$

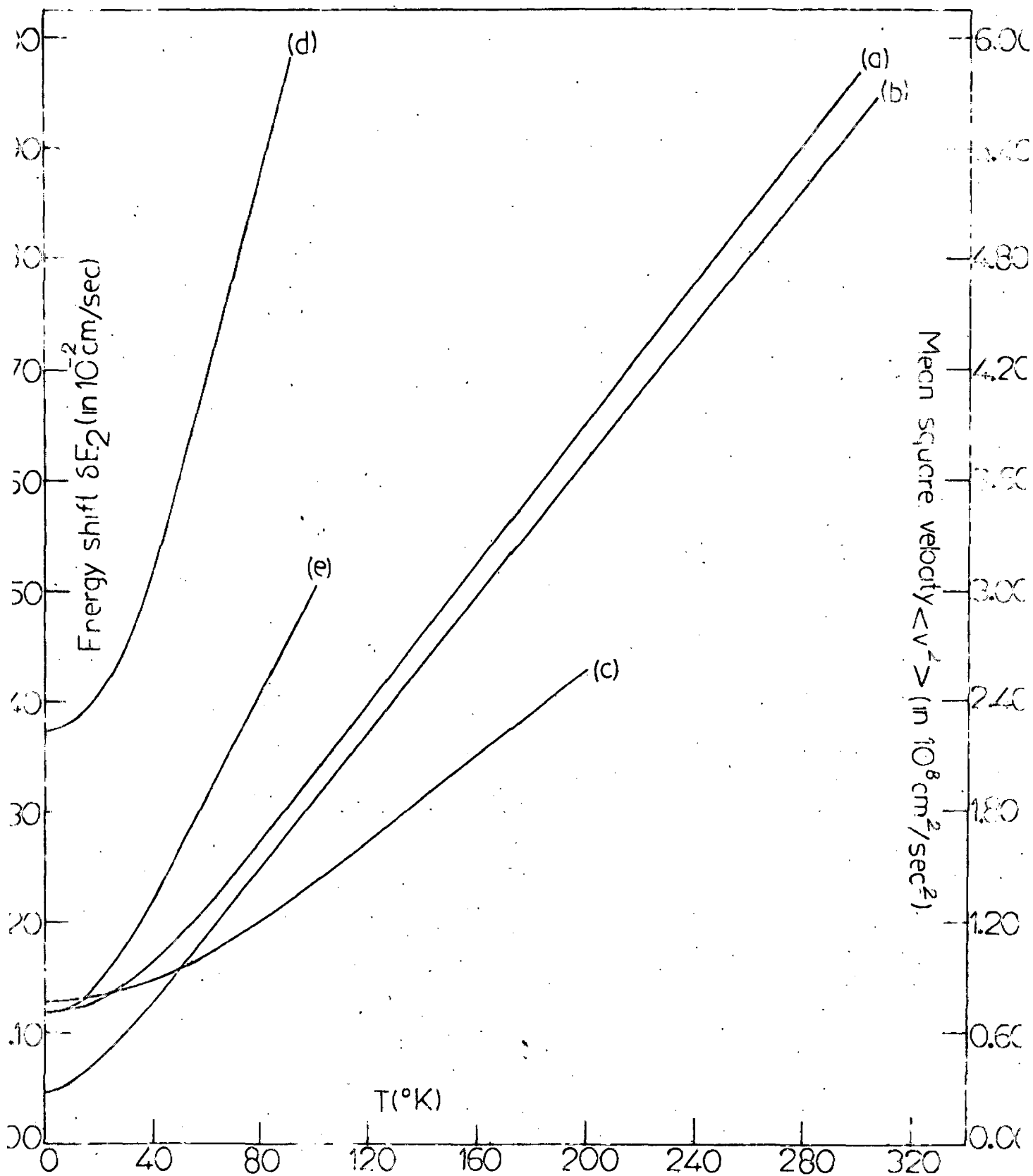
where R_e and R_g are the nuclear radii of the excited and ground state and $|\Psi(o)|_a^2$ and $|\Psi(o)|_s^2$ are the total s-electron densities at the absorber and emitting nuclei. On the other hand the energy shift due to S.O.D. in turn is given given by (Eq.(2.20))

$$\delta E_2 = \frac{\delta E_\gamma}{E_\gamma} = \frac{\langle v^2 \rangle}{2c^2} \quad \dots (7.2)$$

where $\langle v^2 \rangle$ is the mean square velocity of the emitting or absorbing nucleus and depends on the lattice properties. Using the phonon spectrum of the lattice one can calculate this contribution to the energy shift and subtracting it from the accurately measured energy shift δE , one can draw some important conclusions regarding I.S. or s-electron density at the nucleus, its variation with temperature and pressure.

7.2 ENERGY SHIFT DUE TO S.O.D. IN CsI, Cs, Au, K AND Kr LATTICE

Figure (7.1) shows the temperature variation of γ -ray energy shift due to S.O.D. effect and the corresponding mean square velocity of the resonant atom in CsI(a), Cs(b), Au(c), K(d) and Kr(e) lattice, in harmonic approximation, calculated from Eq.(2.23) with respective p.f.d.f. mentioned already in the f calculation. Figure (7.2) represents the pressure dependence of the same in CsI at $T=80(a_1)$ and $300^\circ\text{K}(a_2)$; Cs at $4.2^\circ\text{K}(b)$; Au at $80^\circ\text{K}(c_1)$ and $4.2^\circ\text{K}(c_2)$ and in K lattice at $4.0^\circ\text{K}(d_1)$ and $80^\circ\text{K}(d_2)$, calculated from Eq.(2.23) with the input frequencies modified due to pressure according to Eq.(6.3).



7.1 - Variation of S.O.D. shift (δE_2) in the energy of the gamma ray with temperature, in CsI (a), Cs (b), Au (c), K (d) and Kr (e) lattice. The right ordinate gives the corresponding mean square velocity of the resonant atom in these lattices.

state. All states lying below the Fermi level by more than kT remains occupied; however the states near the Fermi energy mix with the higher states. This changes the s-electron density at the nucleus and hence I.S. with temperature and pressure.

Analysis carried out by Housley and Hess|177| for thermal shift in iron, have given evidence of a non-negligible temperature dependence of I.S. Further, from the shape of I.S. $(=\delta E - \delta E_2)$ versus T curve, they |177| have shown that the temperature dependence cannot be accounted for by thermal expansion alone and have qualitatively attributed the discrepancy to be arising from magnetisation. It was decided to tackle the problem more carefully by calculating the S.O.D. of the absorber and source (including anharmonicity) from the experimentally determined p.f.d.f. |102|.

The total shift of the Mossbauer γ -ray energy is given by

$$\delta E = \delta E_1 + (\delta E_2)_s - (\delta E_2)_a \quad \dots (7.3)$$

In the experiment done by Preston et.al.|206| the source Fe^{57} doped in Cu lattice was maintained at constant temperature and thus S.O.D. of the source, $(\delta E_2)_s$, has no temperature dependence. Furthermore the S.O.D. for an impurity atom of mass M' in a host of mass M is given by |207|

$$(\delta E_2)_s = \frac{3kT}{2M'c} \left[1 + \frac{1}{2} \left(\frac{h\nu_{\max}}{kT} \right)^2 \frac{M}{M'} \frac{q'}{q} \right] \quad \dots (7.4)$$

where ν_{\max} is the cut-off frequency for the host lattice and q'/q is the binding force constant ratio of the impurity in the host lattice.

The shift of the nuclear levels due to the finite size of the nucleus can be written as from Eq.(7.1) as

|208|

$$\delta E_1 = \alpha |\Psi(0)|^2 + \text{constant}. \quad \dots (7.5)$$

where α is the scaling factor containing electronic and nuclear parameters and $|\Psi(0)|^2$ is the total s-electron density at the nucleus in the host under consideration. Since we are interested in the volume expansion of $|\Psi(0)|^2$, only the 4s- and 3s- electron contributions are considered. Thus the total electron density at the nucleus becomes

$$|\Psi(0)|^2 = |\Psi_{4s}(0)|^2 + |\Psi_{3s}(0)|^2 \quad \dots (7.6)$$

Starting from the free atom wavefunctions |18,209| for the configuration $3d^7 4s^1$ for b.c.c. metallic iron |19|, Ingalls |208| has performed a Stern's modified-tight-binding (MTB) calculation for the wavefunction in the real solid along various directions and for several volume. He has shown that the electron density for the 3s and 4s contribution is

$$|\Psi(0)|^2 = n_s |\Psi_{\uparrow}(0)|^2 + \beta \langle n U_{\max}^2 \rangle_{av} + \text{constant}. \quad \dots (7.7)$$

The dependence of I.S. with volume is

$$\frac{\partial(\delta E_1)}{\partial \ln V} = \alpha (-n_s \gamma_1 |\Psi_{\uparrow 1}(o)|^2 + \beta \frac{\partial \langle nU_{\max}^2 \rangle_{av}}{\partial \ln V} + |\Psi_{\uparrow 1}(o)|^2 \frac{\partial n_s}{\partial \ln V} + \beta \frac{\partial \langle nU_{\max}^2 \rangle_{av}}{\partial n_d} \frac{\partial n_d}{\partial \ln V}) \quad \dots (7.8)$$

where $n_s = \int_0^{E_F} N_s(E) dE$ is the number of s-electrons per iron atom, with $N_s(E)$ is the number of s-states in the 3d-4s conduction band; $|\Psi_{\uparrow 1}(o)|^2$ is the 4s wavefunction at $|\vec{k} \equiv 0$ and varies with volume as, $|\Psi_{\uparrow 1}(o)|^2 \propto$ constant $V^{-\gamma_1}$ with $\gamma_1 = 1.25$. Like n_s , $n_d = \int_0^{E_F} N_d(E) dE$ is the number of d-electrons per iron atom with $N_d(E)$ the d-like density of states per atom and the other symbols have been explained in Ingalls paper [208]. Stern [210] has shown that there is a decrease of $N_d(E)$ with respect to $N_s(E)$ with the decrease of volume, with the consequence that there is a transfer of electrons from s- to d-band. If we further assume that the number of electrons in the 3d-4s conduction band of iron is constant, we have

$$\frac{\partial n_s}{\partial \ln V} = - \frac{\partial n_d}{\partial \ln V} = X \quad \dots (7.9)$$

where X is then evidently the s \leftrightarrow d electron transfer parameter. Thus the volume dependence of the I.S. at some reference volume, say $V=V_1$, becomes

$$\frac{\partial (\delta E_1)}{\partial (nV)} \Big|_{V=V_1} = \alpha (-n_s \gamma_1 |\Psi_{\Gamma_1}(0)|^2 + \beta \frac{\partial \langle nU_{\max}^2 \rangle_{av}}{\partial (nV)})_{V=V_1} + \alpha X (|\Psi_{\Gamma_1}(0)|^2 - \beta \frac{\partial \langle nU_{\max}^2 \rangle_{av}}{\partial n_d})_{V=V_1} \dots (7.10)$$

On the right hand side, all the quantities except α and X are known [208] while the left hand side can be obtained from the experimental measurements of δE . Employing the experimental pressure study of Mössbauer γ -ray energy shift [182,211] corrected for S.O.D. from Eqs.(2.23) and (6.3), and using Eq.(7.10) the relation between α and X is established [212]. This relationship in turn is used in the study of temperature variation of I.S. In this manner it was possible to correlate the temperature and pressure studies of the Mössbauer γ -ray energy shift of Fe^{57} in natural iron [212].

Figure (7.3) shows the plot of S.O.D. variation with pressure and at $T=300^{\circ}K$ (a), calculated from Eq.(2.23) after modifying the frequencies for pressure, Eq.(6.3) along with the experimental results for energy shift δE [182,211]. No temperature anharmonicity was included as both the experimental measurement of the energy shift δE as well as the p.f.d.f. [102] was carried out at room temperature. Figure (7.4) shows the variation of I.S., $\delta E_1 (= \delta E - E_2)$ versus pressure and volume (Eq.(6.6)). A linear fit to the I.S. data according to the form

$$\partial(\delta E_1) = A \left(\frac{\delta V}{V} \right)$$

gives $A = \left. \frac{\partial \delta E_1}{\partial \lambda n V} \right|_{V=V_1} = 1.2 \pm 0.2 \text{ mm/sec.}$

where $V_1 (=80a_0^3)$ is the volume of the unit cell of iron lattice at room temperature and zero atmosphere. Using the present value of $\frac{\partial(\delta E_1)}{\partial \lambda n V}$ and the various quantities in Eq.(7.10) as given below |208|,

$$\left. \begin{aligned} \beta = -5.5 a_0^{-2}, \quad \gamma_1 = 1.25, \quad \frac{\partial \langle n U_{\max}^2 \rangle_{av}}{\partial \lambda n V} = 0.03 a_0^{-1} \\ \frac{\partial \langle n U_{\max}^2 \rangle_{av}}{\partial n_d} = 0.9 a_0^{-1}, \quad n_s = 0.53 \end{aligned} \right\} \dots (7.12)$$

and $|\Psi_{\uparrow 1}(0)|^2 = 7.1 a_0^{-3}$

where the the last two values are at room temperature ($V_1 = 80a_0^3$), one gets the relation

$$1.20 = -4.87\alpha + 12.05\alpha X \dots (7.13)$$

which any independent measurement of α and X must satisfy. This is plotted in Fig.(7.5). Since from Stern's |210| work one expects $X > 0$, so only the portion of the curve pertaining to $X > 0$ in Fig.(7.5) is pertinent for the study of temperature variation of the I.S.

To study the variation of the I.S. with temperature with respect to $T=0^\circ\text{K}$ (the volume |213| V_0 at $0^\circ\text{K} = 78.95 a_0^3$), we once again use the Eq.(7.10)

$$\begin{aligned} \frac{\partial(\delta E_1)}{\partial \langle nV \rangle} \Big|_{V=V_0} &= \alpha (-n_s \gamma_1 |\Psi_{\Gamma_1}(0)|^2 + \beta \frac{\partial \langle nU_{\max}^2 \rangle_{av}}{\partial \langle nV \rangle})_{V=V_0} \\ &+ \alpha X (|\Psi_{\Gamma_1}(0)|^2 - \beta \frac{\partial \langle nU_{\max}^2 \rangle_{av}}{\partial n_d})_{V=V_0} \end{aligned} \quad \dots (7.14)$$

From Fig.(4) of Ingalls paper [208], $|\Psi_{\Gamma_1}(0)|^2 = 7.2a_0^{-3}$ for $V = V_0 (=78.95 a_0^3)$ [214] and using $X = \frac{\partial n_s}{\partial \langle nV \rangle} = 0.205$ (arbitrarily* from Fig.(7.5)). We have the number of s-electron per iron atom at $T = 0^\circ K$, $n_s = 0.527$. The rest of the quantities on the right-hand side have the same value as used previously (Eq.(7.12)). Employing these values one gets

$$\frac{\partial(\delta E_1)}{\partial \langle nV \rangle} \Big|_{V=V_0} = \alpha [-4.91 + 12.15X] \quad \dots (7.15)$$

Taking α ranging from 0.246 (corresponding to $X=0$) to $-0.800 a_0^3$ mm/sec. (corresponding to $X = 0.279$) one obtains

$$\frac{\partial \delta E_1}{\partial V} = \frac{\partial \delta E_1}{\partial \langle nV \rangle} \cdot \frac{1}{78.95} = (0.153 \pm 0.001) \times 10^{-1} \text{ mm/sec.}$$

The corresponding δE_1 at $T = 1000^\circ K$ (where the volume $V = 82.52 a_0^3$ [213] with respect to $T = 0^\circ K$ will be $(0.548 \pm 0.003) \times 10^{-1}$ mm/sec. The uncertainty covers all the different combinations of α and X (of course for $X > 0$)

* The value of X was taken arbitrarily since it is found from Eq.(7.14) that by taking any combination of α and $X(X > 0)$ satisfying Eq.(7.13), and the corresponding n_s , the overall effect on the temperature variation of I.S., $\partial \delta E_1 / \partial T$, comes out to be very small $\sim (0.548 \pm 0.003) \times 10^{-4}$ mm sec⁻¹ °K⁻¹.

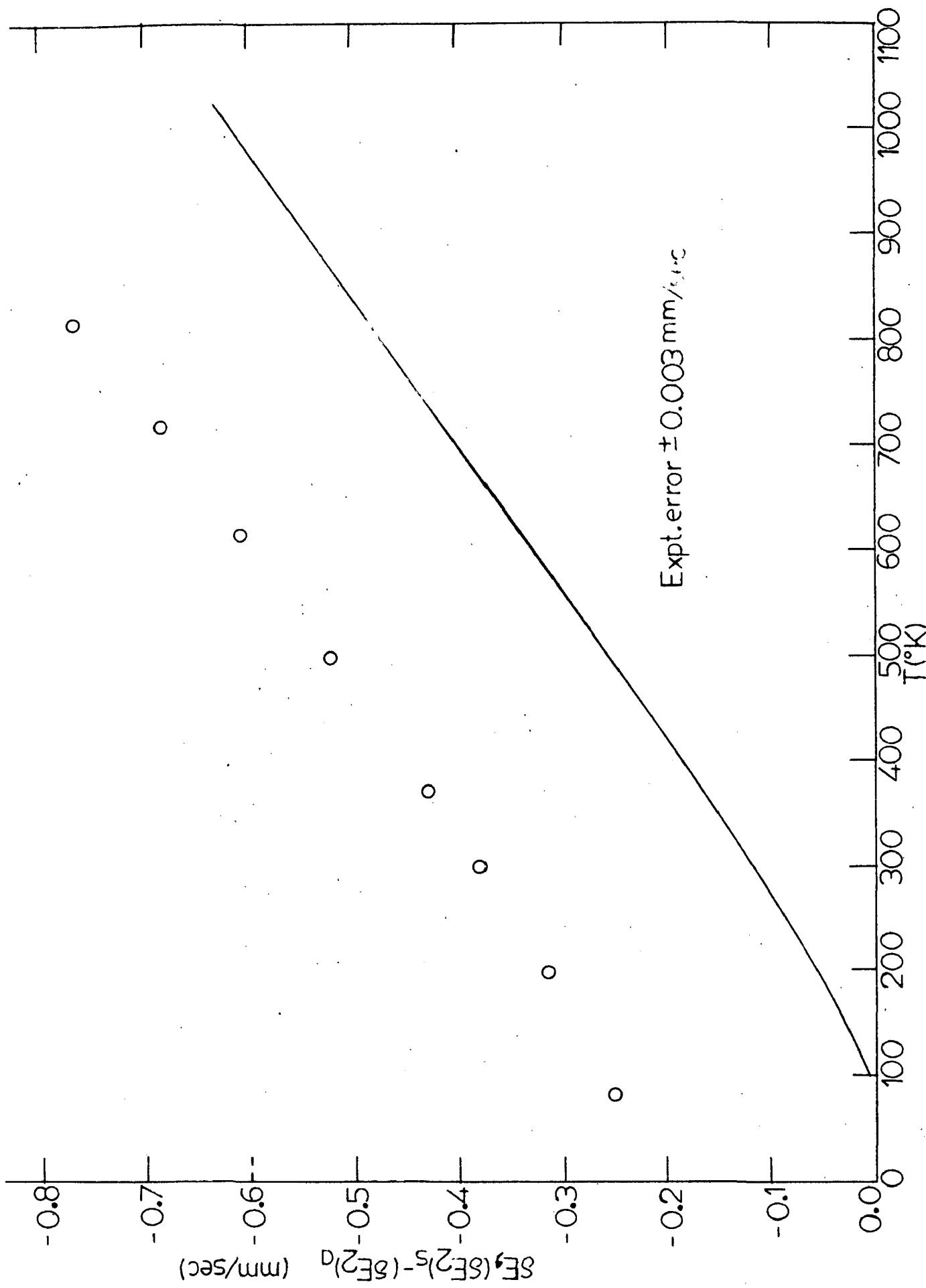


FIG.7.6_Variation of the calculated $[\delta E_2(s) - \delta E_2(d)]$ with temperature (solid line) along with the experimental

various temperature, along with the actual* experimental γ -ray energy shift δE [205], after correcting for the measured energy shift at constant pressure to constant volume by means of the thermodynamic relation [179],

$$\frac{1}{V} \left(\frac{\partial \nu}{\partial T} \right)_V = \frac{1}{V} \left(\frac{\partial \nu}{\partial T} \right)_P - \frac{1}{V} \left(\frac{\partial \nu}{\partial \ln V} \right)_T \left(\frac{\partial \ln V}{\partial T} \right)_P \quad \dots (7.16)$$

where the conversion term

$$\frac{1}{V} \left(\frac{\partial \nu}{\partial \ln V} \right)_T \left(\frac{\partial \ln V}{\partial T} \right)_P = 0.16 \times 10^{-15} / ^\circ K \text{ at room temperature}$$

and $0.18 \times 10^{-15} / ^\circ K$ at high temperature [205]. Figure (7.7) shows the temperature variation of the I.S., δE_1 $\left[= \delta E - ((\delta E_2)_s - (\delta E_2)_a) \right]$ between the source and absorber. This is after subtracting the solid line from the experimental points in Fig.(7.6). The shape of the curve suggests that the observed effect is associated with some kind of magnetic ordering in the system. This could arise from either of the following two possible causes:

- (a) the dependence of the I.S. (s-electron density at the nucleus) on the degree of magnetic order and /or
- (b) the dependence of the S.O.D. on the degree of magnetic order in the system.

*The relative value of S.O.D. were converted to the absolute values on the basis of its actual measurement (shown in Fig.4 of Ref. [205]) at $295^\circ K$ where $\delta E = -0.350$ mm/sec.

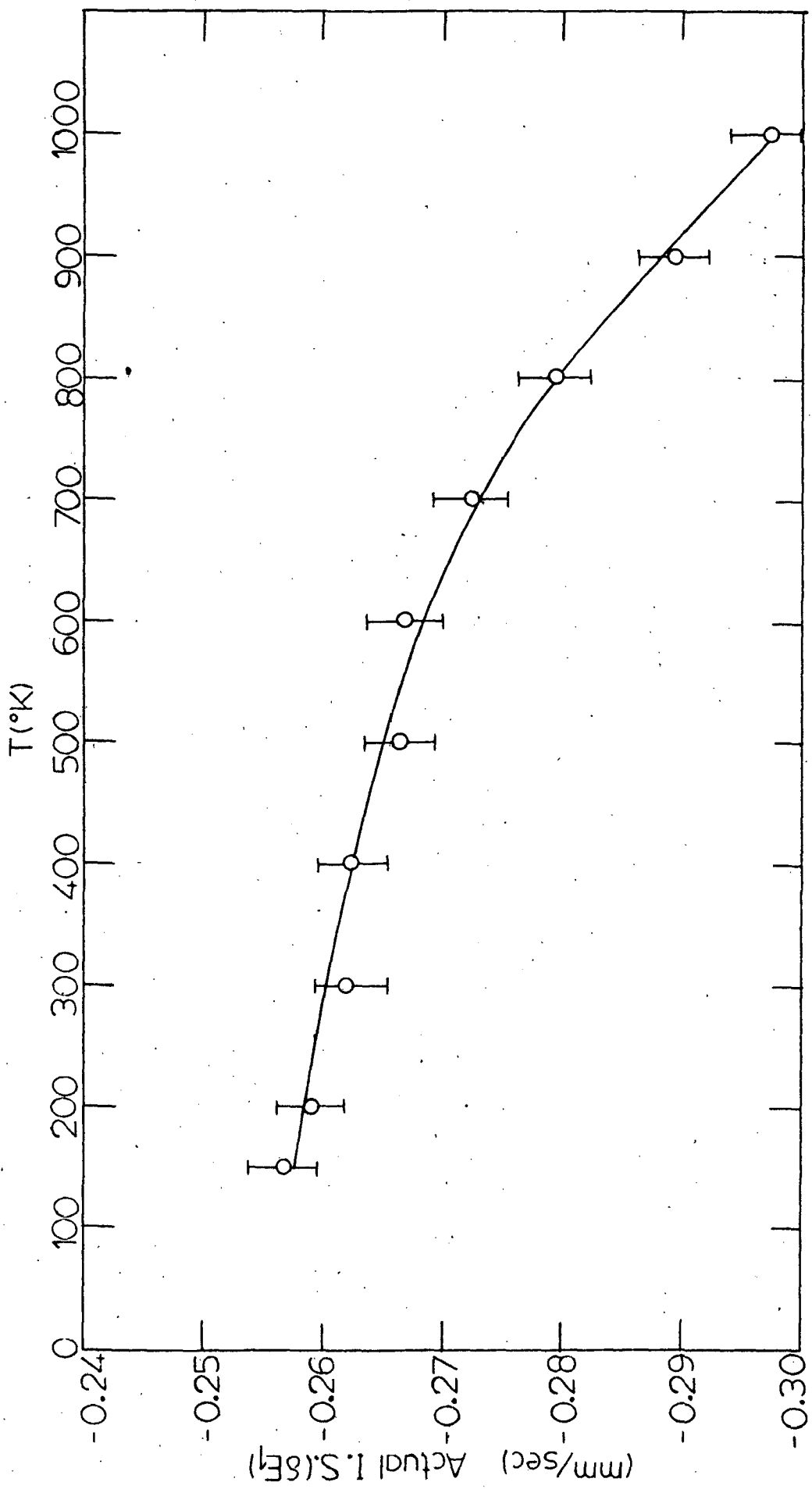


FIG.7.7- Variation of the actual I.S. (δE_1) (obtained without correction for the magnetic contribution to S.O.D. (δE_2)). The solid line is a visual fit to the I.S. data.

Both are to be expected theoretically from the band model of iron lattice as suggested by Alexander and Treves [216]. Regarding the first, the magnetic splitting of the 3d-band changes with temperature and this causes a shift in the absolute position of the Fermi level and through this, a change in the number of 4s-electrons; as a result the I.S. changes. Regarding the second conjecture, because of the phonon-magnon interactions, some of the atomic kinetic energy is contained in relatively high frequency modes which are essentially magnons. The change of magnon spectrum with temperature leads to a change in the S.O.D. Following Bashkirov and Selutin the phonon frequency shift due to magnetic ordering can be expressed as (Eq.(5.7)),

$$\nu' = \nu(1+B)^{1/2}$$

where the symbols are explained already. By assuming a molecular field model, B can be written as $B=B_0\mu^2(T)$ with $\mu(T)$ the reduced sublattice magnetisation. In our earlier work (Chapter V), the experimental data on f was fitted by assuming $B_0=0.4\pm 0.2$ [80]. Again using Eq.(2.13) with the phonon frequencies corrected for anharmonicity and magnetic ordering (Eqs.(4.12) and (5.7) with $A = 0.08052 \times 10^{-3}/^{\circ}\text{K}$ and $B_0=(0.4\pm 0.2)$, $(\delta E_2)_a$ is recalculated at all temperatures and the new values of corresponding I.S. are derived. Figure (7.8) shows in particular the I.S. plot corresponding to $B_0=0.4$. Within the experimental

error , the points lie on the straight line with slope (calculated from least square fit), $\frac{\partial}{\partial T}(\text{I.S.}) = (0.60 \pm 0.03) \times 10^{-4} \text{ mm/sec}^\circ\text{K}$ (\pm covers the range of B_0). This compares with $(0.55 \pm 0.09) \times 10^{-4} \text{ mm/sec}^\circ\text{K}$ which was obtained from the independent pressure studies. The corresponding value for $\frac{\partial(\text{I.S.})}{\partial T}$ obtained by Housley and Hess [177] by fitting the derived I.S. data with the functional form

$$\delta E_1 = A + sT + x\mu(T) \quad \dots (7.17)$$

is $1.0 \pm 0.3 \times 10^{-16} / ^\circ\text{K}$ or $0.30 \pm 0.09 \times 10^{-4} \text{ mm/sec}^\circ\text{K}$. From the shape dependence of I.S. versus temperature (Fig.(7.8)), it is difficult to comment on a possible contribution of the magnetic ordering to the I.S. It is small, if at all present as was already suggested by Housley and Hess [177].

It will be seen in Chapter IX that the combined effect of temperature and pressure on Mössbauer spectrum shift can give useful information regarding the isomer shift variation with temperature and pressure.

CHAPTER VIII

ANALYSIS OF MÖSSBAUER PARAMETERS FOR
AN IMPURITY ATOM

8.1 INTRODUCTION - In this chapter we will consider the information about atomic motion that can be obtained when the Mössbauer atom is an impurity in another lattice. Here the ability of the Mössbauer effect to pick out the motion of the impurity atom is particularly valuable and specific for a particular atom.

The study of crystal containing imperfections constitutes one of the frontiers of modern physics and problems connected with defects have aroused a great deal of interest in recent years. Many physical properties of solids are strongly dependent on defects present in them rather than on the host crystal itself. Quite striking changes in the vibrational properties are observed when defects are introduced into a crystal. There are alterations in the frequencies of the normal modes of vibrations of the crystal lattice, and in the pattern of the atomic displacements in the normal modes. Localised modes can appear when activated by a light impurity or by a defect coupled to its neighbouring atoms more strongly than a host-host atom. The frequencies of the localised or bound states lie in the ranges forbidden for the normal modes of the pure host crystal. Quasilocalised

or resonance modes may also appear for a heavy impurity or defect coupled weakly to its neighbours compared to the host atoms. The frequencies of the resonance modes lie in the ranges of the frequencies allowed to the normal modes of the pure host crystal. These modes are characterised by a large vibrational amplitude of the defect or of these atoms with which it directly interacts. An increase in the density of states near the resonance frequency is observed which gives rise to peaks in the frequency spectrum of the impure crystal. Further these modes have finite life-time because they can decay into the band modes.

Thus we see that when a Mössbauer atom of atomic mass M' is an impurity placed in a lattice composed of atoms with the atomic mass M , the lattice dynamics of the composite system is no longer that of the pure crystal. In particular the change in mass at defect site and change in the force constants in the vicinity of this site will influence the mean square displacement $\langle x^2 \rangle$ and the mean square velocity $\langle v^2 \rangle$ of the impurity atom. This, in turn, will influence f and δE_2 and its temperature |217| and pressure dependence |218|. Such measurements of f and δE_2 may yield rather unique information of the impurity-host to the host-host binding q'/q , in the sense that one studies directly the vibrations of impurity atoms themselves without recourse to the bulk properties. Much theoretical work has been devoted to

the study of the dynamics of an impurity atom in a variety of crystal models, including the effect on $\langle x^2 \rangle$ and $\langle v^2 \rangle$, of changes in the mass [31,219] and / or force constants [40,220] of the impurity.

Debye Waller factors for 14.4 keV, γ -rays of Fe⁵⁷ atoms as a dilute impurity have been measured at constant temperature for different crystal lattices [221,222] as well as for a definite crystal over a wide temperature range [38,137,223,224]. These measurements were considered to be consistent with the calculations of Visscher [219] and Maradudin and Flinn [31] and it was inferred [221] that the impurity - host coupling constant is about the same as the host-host coupling constant. On the other hand Lehman and DeWames [40] have used the matrix partitioning technique which in addition the mass change admits the change in the force constant as well as polarisation of phonons. Their analysis for Fe⁵⁷ impurity in Al, Cu and Pt lattices indicates that the impurity-host to host-host force constant ratio q'/q is appreciably different from unity. Nussbaum et.al [137] have measured very accurate values of f for Fe⁵⁷ impurity in Cu, Pt and Pd over the temperature range 4-760°K and have drawn similar conclusions. Recently Mannheim [220] has derived a closed form expression for $\langle x^2 \rangle$ and $\langle v^2 \rangle$ for the central force b.c.c. and f.c.c. crystal models in which there are changes in the nearest neighbour forces around the defect site. Mannheim and Simopolus [223] measured experimentally

the variation of $\langle x^2 \rangle$ and $\langle v^2 \rangle$ with temperature from 100-700°K for Fe⁵⁷ in vanadium and analysing the measurements, found the evidence for force constant change, $q'/q = 1.67-2.5$. Making use of the Mannheim expression |220| for $\langle x^2 \rangle$ and experimental $g(\omega)$ for Cu, Pt, Mo and W, Raj and Puri |42,225,226| have shown the evidence of q'/q for Fe⁵⁷ in these host matrices.

Recently pressure variation of f at room temperature has been measured by Moyzis et.al. |218| for Fe⁵⁷ impurity in Cu, V and Ti. By analysing this f data in Debye approximation, it was decided to seek evidence for q'/q due to impurity. In Debye approximation, the recoilless fraction f is given by Eq.(2.17). To account for the effect of impurity on host Debye temperature θ_D , there are two simple models which have been treated in the literature. Visscher |219|, assuming (i) a substitutional impurity in a harmonic simple cubic lattice with nearest neighbour interactions only and (ii) that shear spring constants are equal to compressive spring constants, has shown that in the limit of low temperatures, f is approximated quite well by Eq.(2.17) provided host Debye temperature θ_D is replaced by the effective Debye temperature θ_{eff} through the relation

$$\theta_{eff} = \theta_D \left(\frac{M}{M'} \frac{q'}{c} \right)^{1/2} \quad \dots (8.1)$$

Maradudin and Flinn have calculated the recoilless fraction

in the high temperature limit considering nearest neighbour interactions in a f.c.c. lattice. As with Visscher's theory it is possible to define θ_{eff} by the relation,

$$\theta_{\text{eff}} = \theta_D \left(\frac{M}{M'} \right)^{1/2} \left[1 + 0.60 \left(1 - \frac{q'}{q} \right) + 0.74 \left(1 - \frac{q'}{q} \right)^2 + \dots \right]^{-1/2} \dots (8.2)$$

For our calculations we will confine ourselves to Visscher's model.

On the other hand to account for the effect of pressure, it has been shown already Eq.(6.3), if θ_{eff} is the effective Debye temperature of the lattice at zero atmospheric pressure then at pressure ΔP , the $\theta'_{\text{eff}}(P)$ will be

$$\theta'_{\text{eff}}(P) = (V_P/V_0)^{-\gamma} \theta_{\text{eff}} \dots (8.3a)$$

$$= (1 + \gamma K_T \Delta P) \theta_{\text{eff}} \dots (8.3b)$$

Finally the recoilless fraction becomes

$$f(P) = \exp \left[- \frac{6R}{k\theta'_{\text{eff}}} \left(\frac{1}{4} + \frac{1}{Z^2} \int_0^Z \frac{x dx}{e^x - 1} \right) \right] \dots (8.4)$$

with $Z = (\theta'_{\text{eff}}/T)$.

We have calculated $f(P)$ for Fe⁵⁷ as a dilute impurity in Ti, V, Cu, Ni, Mo, W and Pd from 0-100 Kbar. These hosts are elements in which the atomic size is very close to the atomic size of the Fe-impurity; hence we can expect the assumptions made in Debye theory, and

the refinements there on by Visscher |219| to hold. Integral in Eq.(8.4) for different Z values can be known from Muir's table |34|. The values of K_T, γ, θ_D etc. have been taken from the latest literature. Regarding q'/q values, these have been taken from the work of various investigators |38,137,223-225|. The calculated plots of f_p/f_0 versus pressure for various force constant ratios are shown in Figs.(8.1) and (8.2)|41|. The values of slope obtained from Figs.(8.1) and (8.2), and experimental measurements, along with the input data are given in Table(8.1), given on page 102.

From Table (8.1) the following conclusions are drawn:

(i) For the fixed value of θ_{eff} , the pressure effect increases with increase of γK_T instead of K_T alone as was pointed out by Hanks |180|; who took the constant value of 2 for γ of all the hosts.

(ii) For fixed value of γK_T , the pressure effect depends on the effective Debye temperature and it increases with the decrease of θ_{eff} . This is physically plausible since if the binding is rigid, the effect of impressed pressure will be less as compared to when the binding is loose. The only available experimental results are for the systems Fe: Cu, F:V and Fe: Ti reported by Moyzis et.al.|218| we discuss these cases below.

Table 8.1.- Values of $\Delta f/(f(\Delta P))$ (10^{-4} Kbar $^{-1}$) for Fe⁵⁷ embedded in various hosts along with the input data used.

Sr. No.	Host	θ_D ($^{\circ}$ K)	q'/q	$\theta_{\text{eff.}}$ ($^{\circ}$ K)	K_T (10^{-12} cm 2 /dyn)	γ	γK_T (10^{-12} cm 2 /dyn)	$\Delta f/(f\Delta P)$	
								Calc.	expt. 218
1.	Ti	278 221	1.00	254.80	0.931 218	1.232 218	1.148	12.50	7.21+1.39
			1.30	290.51				10.19	
			1.50	312.06				8.55	
2.	V	273 221	1.00	258.10	0.645 218	1.257 218	0.810	8.70	7.81+0.56
			1.20	282.61				7.40	
			1.67 223	333.53				5.30	
3.	Ni	380*	1.50 137	472.33	0.540 190	1.880 190	1.014	3.33	-
4.	Cu	324 229	1.00	342.06	0.750 218	2.000 218	1.500	8.50	8.14+0.65
			1.19 137	373.14				7.38	-
5.	Mo	425 221	0.50 225	389.90	0.360 190	1.570 190	0.565	3.00	-
6.	Pd	275 221	0.80 137	336.10	0.540 190	2.230 190	1.2042	7.34	-
7.	W	379 221	0.50 225	481.40	0.300 190	2.620 190	0.486	1.50	-

* The value of θ_D for Ni taken from the heat capacity data (13 to 300 $^{\circ}$ K) of |227| as interpreted by |228|.

the refinements there on by Visscher [219] to hold. Integral in Eq.(8.4) for different Z values can be known from Muir's table [34]. The values of K_T, γ, θ_D etc. have been taken from the latest literature. Regarding q'/q values, these have been taken from the work of various investigators [38,137,223-225]. The calculated plots of f_p/f_0 versus pressure for various force constant ratios are shown in Figs.(8.1) and (8.2)[41]. The values of slope obtained from Figs.(8.1) and (8.2), and experimental measurements, along with the input data are given in Table(8.1), given on page 102.

From Table (8.1) the following conclusions are drawn:

(i) For the fixed value of θ_{eff} , the pressure effect increases with increase of γK_T instead of K_T alone as was pointed out by Hanks [180]; who took the constant value of 2 for γ of all the hosts.

(ii) For fixed value of γK_T , the pressure effect depends on the effective Debye temperature and it increases with the decrease of θ_{eff} . This is physically plausible since if the binding is rigid, the effect of impressed pressure will be less as compared to when the binding is loose. The only available experimental results are for the systems Fe: Cu, F:V and Fe: Ti reported by Moyzis et.al.[218] we discuss these cases below.

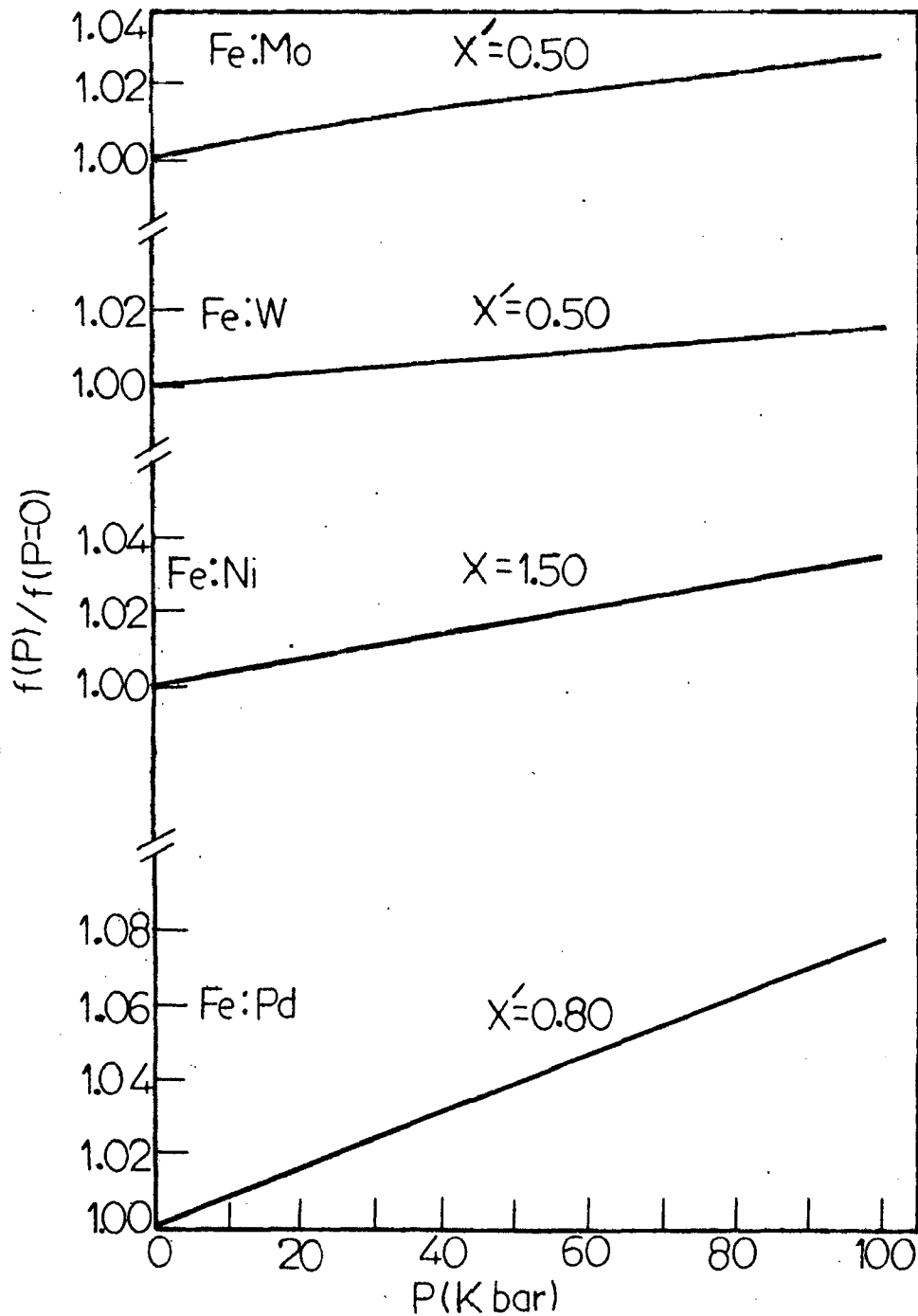


FIG.8.2-Calculated f_P/f_0 versus pressure for Fe^{57} as an impurity in Pd, Ni, W and Mo lattices for various X' ($=q'/q$) values.

Table 8.1. Values of $\Delta f/(f(\Delta P))$ (10^{-4} Kbar $^{-1}$) for Fe⁵⁷ embedded in various hosts along with the input data used.

Sr. No.	Host	θ_D ($^{\circ}$ K)	q'/q	$\theta_{\text{eff.}}$ ($^{\circ}$ K)	K_T (10^{-12} cm 2 /dyn)	γ	νK_T (10^{-12} cm 2 /dyn)	$\Delta f/(f\Delta P)$	
								Calc.	expt. 218
1.	Ti	278 221	1.00	254.80	0.931 218	1.232 218	1.148	12.50	7.21 + 1.39
			1.30	290.51				10.19	
			1.50	312.06				8.55	
2.	V	273 221	1.00	258.10	0.645 218	1.257 218	0.810	8.70	7.81 + 0.56
			1.20	282.61				7.40	
			1.67 223	333.53				5.30	
3.	Ni	380*	1.50 137	472.33	0.540 190	1.880 190	1.014	3.33	-
4.	Cu	324 229	1.00	342.06	0.750 218	2.000 218	1.500	8.50	8.14 + 0.65
			1.19 137	373.14				7.38	-
5.	Mo	425 221	0.50 225	389.90	0.360 190	1.570 190	0.565	3.00	-
6.	Pd	275 221	0.80 137	336.10	0.540 190	2.230 190	1.2042	7.34	-
7.	W	379 221	0.50 225	481.40	0.300 190	2.620 190	0.486	1.50	-

* The value of θ_D for Ni taken from the heat capacity data (13 to 300 $^{\circ}$ K) of [227] as interpreted by [228].

102

8.2 Fe⁵⁷ AS AN IMPURITY DIFFUSED IN Cu LATTICE

The calculated values of the slope: 8.5×10^{-4} for $q'/q = 1.00$ and $7.38 \times 10^{-4} \text{ Kbar}^{-1}$ for $q'/q = 1.19$, when compared with the experimental value, $(8.14 \pm 0.65) \times 10^{-4} \text{ Kbar}^{-1}$ yield the evidence of small force constant change, $1.0 < q'/q < 1.20$. Thus the pressure studies support qualitatively the q'/q value of 1.19 obtained by Nussbaum et.al. [137] from the variation of f with temperature and that of $q'/q = 1.20$ obtained by Steyart and Taylor [38].

8.3 Fe⁵⁷ AS AN IMPURITY DIFFUSED IN Ti LATTICE

In the case of Fe:Ti the calculated slope when compared with the experimental slope gives q'/q of the order of 1.5 i.e., Fe impurity in titanium is about 50% strongly bound than Ti in Ti.

Qaim [222] by analysing the measured f only at 300°K with similar theory, finds that the impurity-host force constant is much weaker than the host-host force constant. The discrepancy, we think is due to the difficulties of measuring accurately the $f(P)$ values, as pointed out by Moyzis et.al [218]. One can strive for a better comparison when more reliable value of either $f(T)$ or $f(P)$ is available.

8.4 Fe⁵⁷ AS AN IMPURITY IN V LATTICE - Here the slopes have been calculated for three different values of $q'/q = 1.00$, 1.20 and 1.67 and on comparison with the experimental

value $(7.81 \pm 0.56) \times 10^{-4}$ again yield unambiguously the evidence of small force constant change, $1.0 < q'/q < 1.20$. The force constant change $1.67 < q'/q < 2.50$ as inferred by Mannheim and Simopoulos |223| from the analysis of variation of f with temperature, is decisively higher than our value. This discrepancy is understandable in view of the higher value of f (≈ 0.78) at room temperature measured by Mannheim and Simopoulos |223|, in comparison with the value (0.55 ± 0.03) reported by Bara and Hryniewicz |221| and (0.547 ± 0.024) by Moyzis et al. |218|, at 50 Kbar. The latter authors have given the measured value only at 50 Kbar and as such the value f_0 at atmospheric pressure will be slightly lower. Further our value of q'/q is in agreement with the value obtained by Qaim |222|. Finally it may be remarked that pressure variation of f is sensitively dependent on θ'_{eff} (and hence on q'/q) value, and thus such an analysis can augment the much desired information on force constant change for impurity-host binding obtainable from variation of f with temperature.

CHAPTER IX

COMBINED EFFECT OF TEMPERATURE AND PRESSURE
ON MOSSBAUER PARAMETERS-ANALYSIS

9.1 INTRODUCTION- We will see in this chapter that the Mössbauer parameters especially spectrum shift, can give useful information regarding electron transfer parameter and isomer shift variation etc., when measured as a function of temperature for various fixed pressures and vice-versa.

9.2 14.4 keV TRANSITION OF Fe⁵⁷ IN PLATINUM LATTICE-

Recently reliable measurements of f versus pressure upto 100 Kbar at 23 and 600°C for Fe⁵⁷ doped in Pt lattice have been made available [230]. The values of $\frac{1}{f_0} \frac{\partial f}{\partial P} = (7.9 \pm 0.9) \times 10^{-4}$ at 23°C and $(22.54 \pm 2.00) \times 10^{-4}$ Kbar⁻¹ at 600°C have been used to estimate q'/q at both the temperatures [43] and to assess the extent to which it agrees with the independent evaluation of this ratio as reported by Raj and Puri [226] from the analysis of $f(T)$.

In the light of the procedure outlined already in Chapter VIII (Eq.(8.3)), $f(P)$ was calculated [43] upto 100 Kbar at $T=300$ and 873°K with q'/q as a variable parameter. The experimental measurement of specific heat of Pt after correcting for $C_p - C_v = 9\alpha^2 VT/K_T$, and

electronic specific heat $C_e (= \gamma_e T)$; were utilized to derive the value of θ_D at both the temperatures. Grüneisen constant γ is calculated from Eq.(4.13) and turns out to be 2.7 and 3.0 at 300 and 873°K respectively. The requisite values of C_p , α , K_T and γ were taken from the literature [231-233]. Furthermore the value of V_p/V_0 (assuming it to be independent of temperature) are taken from the reported measurements of Bridgman[196] and Walsh et al.[234]. The calculated f_p for a range of q'/q values are displayed in Fig.(9.1), along with the experimental values. The thick lines are the best fit straight lines as obtained by Stokes[230] through the measured f factors. It is obvious that the agreement is attained for q'/q lying around 0.40 at 300°K and 0.45 at 873°K. It is gratifying to note that the predicted range of q'/q (0.4-0.5) compares reasonably with $q'/q=0.5$ obtained Raj and Puri[226], and 0.33 reported by Patnaik and Mahanty[235] from the analysis of f versus T measurements. Value of q'/q being less than unity implies that iron atom is weakly bound in Pt host as compared to the Pt-Pt binding.

9.3 14.4 keV TRANSITION OF Fe⁵⁷ IN COPPER LATTICE-

Recently Williamson and Ingalls[236] measured the recoilless fraction and thermal energy shift for Fe⁵⁷ in dilute solution in Cu upto 130 Kbar at 94 and 298°K. Using Eq.(8.5) and the corresponding equation for S.O.D. δE_2 ,

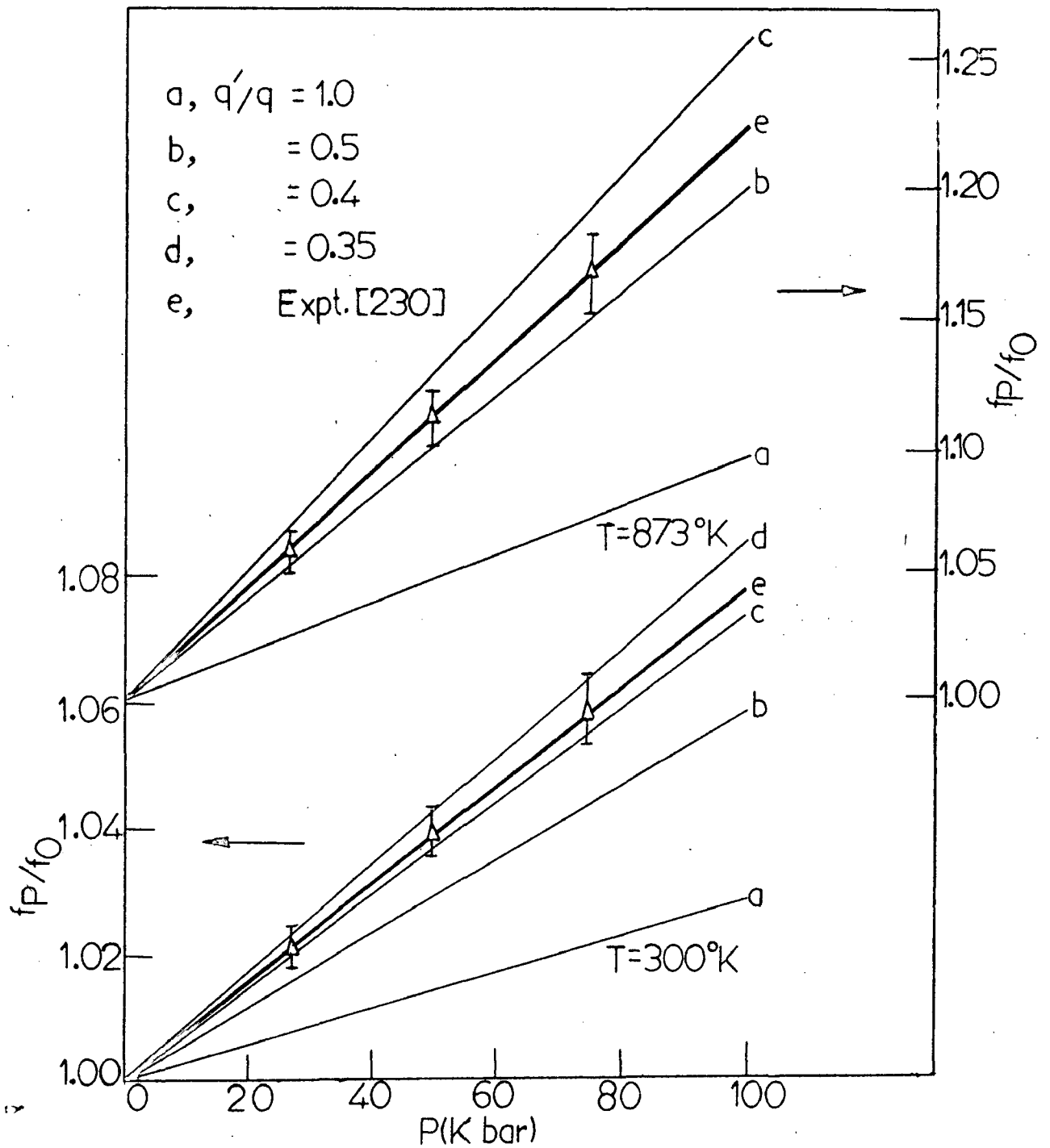
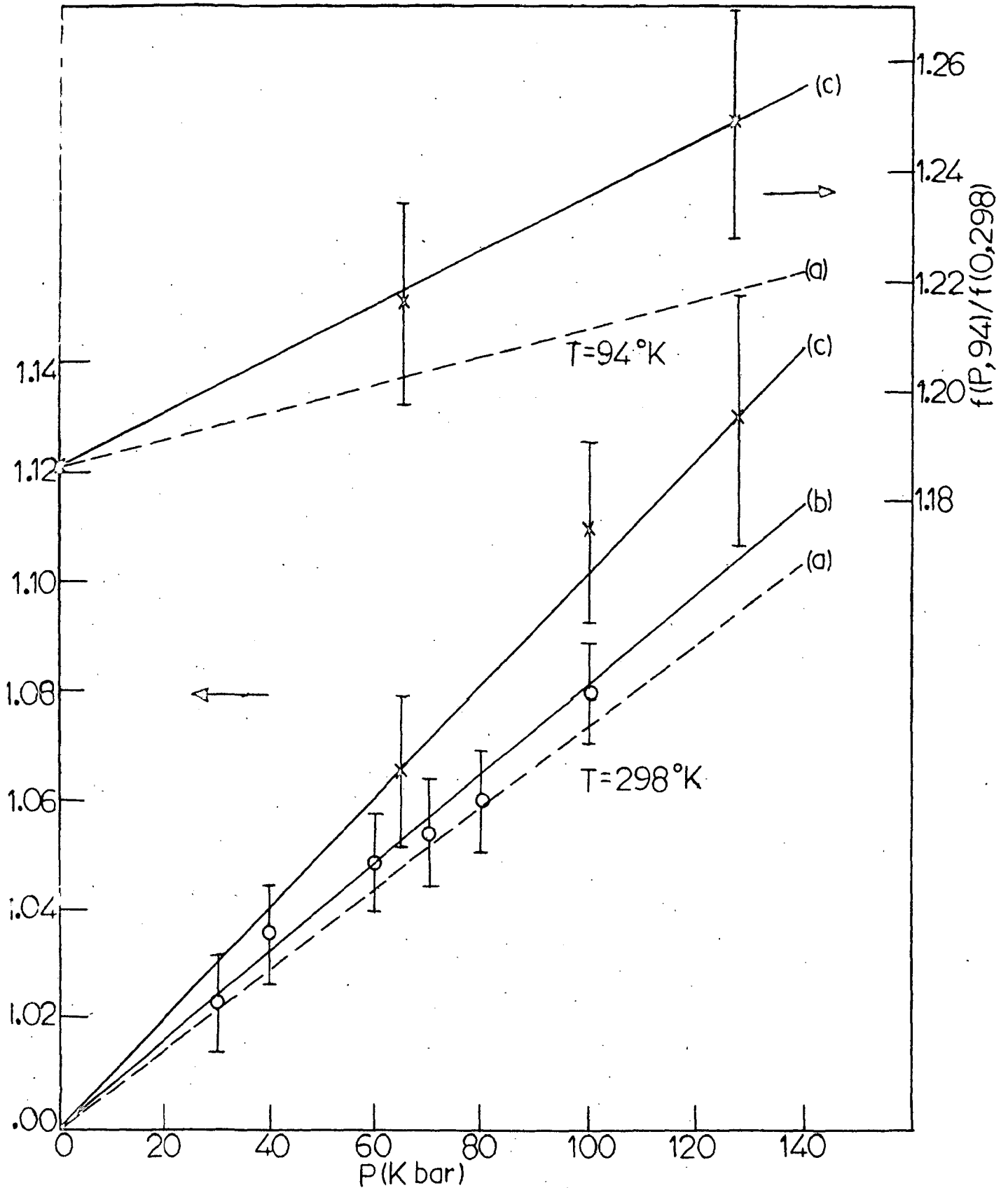


FIG.9.1- Variation of calculated f_P/f_0 versus pressure for Fe^{57} in Pt lattice for various q'/q values, along with the experimental results [230].

$$\delta E_2(P) = \frac{3kT}{2M'c} \left[1 + \frac{1}{20} \left(\frac{\theta'_{eff}}{T} \right)^2 \right] \quad \dots (9.1)$$

where all the quantities are defined already. The Mössbauer fraction and S.O.D. is calculated |237| at 94 and 298°K employing the input data given in Table (9.1). The force constant ratio q'/q was taken as 1.19|41,137,225| and the calculated results are tabulated in Table (9.2). Figure (9.2) represents the calculated f , (a), along with the experimental results (b and c). The solid lines (b and c) represent the least square fit given by the authors |236,218|. We have already derived |41| from the pressure studies, the force constant ratio q'/q at 298°K to be around 1.2. At 94°K the calculated slope $\frac{\partial}{\partial P} (f_{P,94}/f_{0,298}) = 2.58 \times 10^{-4}$ is to be compared with the experimental value $(5.0 \pm 2.4) \times 10^{-4} \text{ Kbar}^{-1}$ |236|. Because of the large error in the experimental value no conclusion is warranted regarding the change of force constant with temperature, what one expects normally. Miler and Brockhouse |240| from the inelastic neutron scattering of Pd at various temperatures have found that the dominant force constant decreases with increasing temperature. The similar conclusion has been derived by Nicklow et al. |215| in the case of Cu. However to get the clear conclusion about the temperature variation of force constant between Fe^{57} in Cu, more precise data on measurements of f is required.



9.2- Calculated relative f versus pressure for Fe^{57} in Cu at $T=94$ and $298^\circ K$ for $q'/q = 1.19$ (a) along with the experimental results (b and c). (O due to Moyzis et al. [218], X due to Williamson and Ingalls [236]).

In view of the higher accuracy of the available energy shift data [218,236] one can attempt to get meaningful information from its analysis. Figure (9.3) shows the calculated (a) S.O.D. shift (δE_2) versus pressure along with experimentally measured shift δE at both the temperatures (b and c). Again the solid lines (b) and (c) represent the least square fit given by them through their experimental points. Although the experimental energy shift δE does not change appreciably with temperature [236], the S.O.D. contribution changes appreciably with temperature (Fig.(9.3)). This implies that I.S. (δE_1) does vary with temperature. Figures (9.4a) and (9.4b) gives the plot of I.S. versus pressure at temperatures 298 and 94°K (normalised to that at 1 atm. and T=298°K). However, it is more instructive to plot the real I.S. versus pressure at these temperatures. The information about the actual value of I.S. at different pressures is easily obtained from Figs.(9.4a) and (9.4b) when the difference of I.S. at 94 and 298°K (at atmospheric pressure) is known from independent measurements. Using the total energy shift values as measured by Steyart and Taylor [38], with respect to Fe^{57} in iron, after correcting for the S.O.D., one gets $(\delta E_1)_{298} - (\delta E_1)_{94} \Big|_{P=1 \text{ atm.}} = +0.0068 \text{ mm/sec}$. Based on this value the actual I.S. variation with pressure at 94°K is reconstructed and is shown in Fig.(9.4c). The difference $(\delta E_1)_{298} - (\delta E_1)_{94}$, as shown in Fig.(9.5), decreases

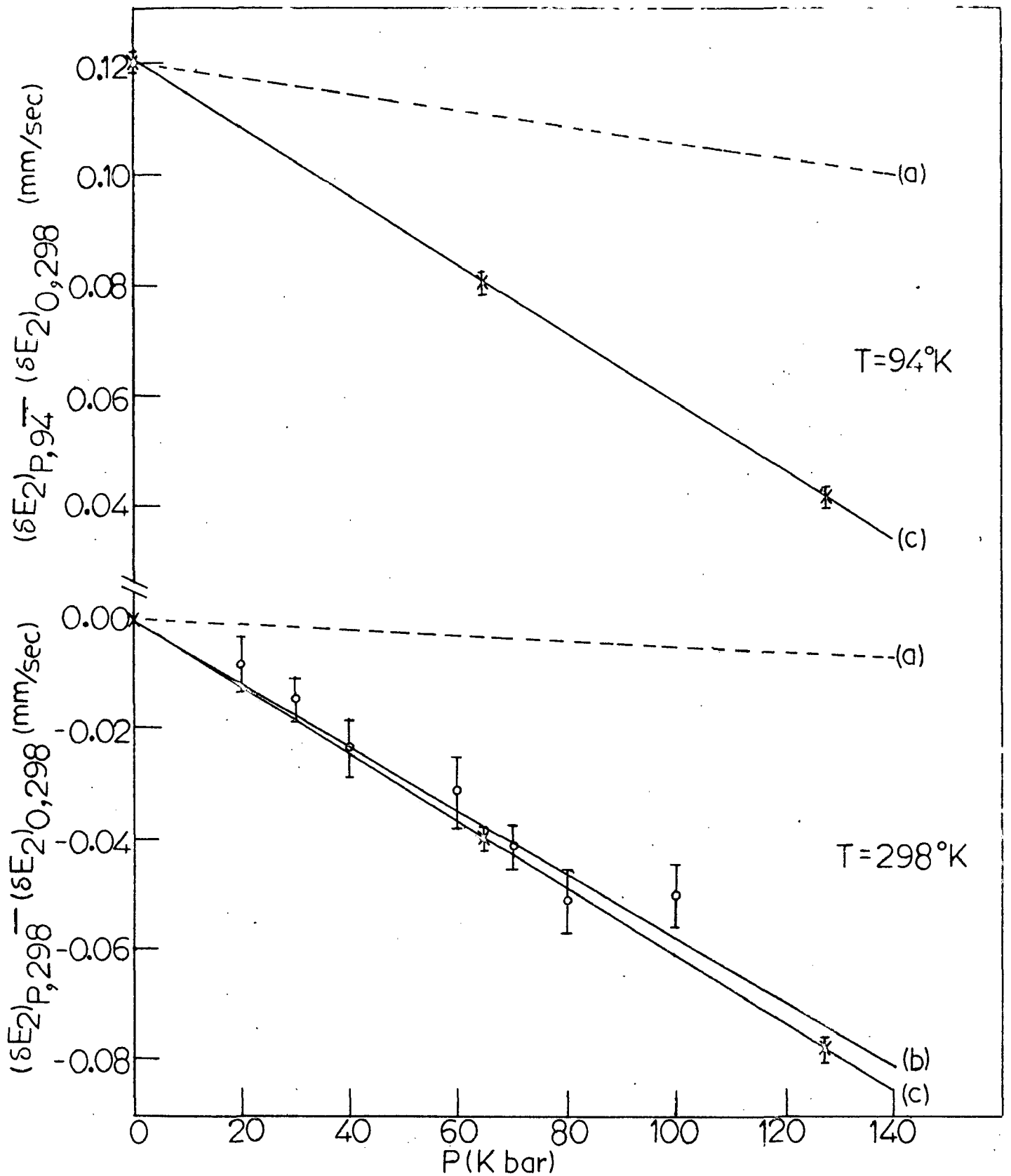


FIG.9.3- Second order Doppler Shift (δE_2) versus pressure (a) calculated curve; (b) and (c) experimental curves [218,236] for total energy shift δE .

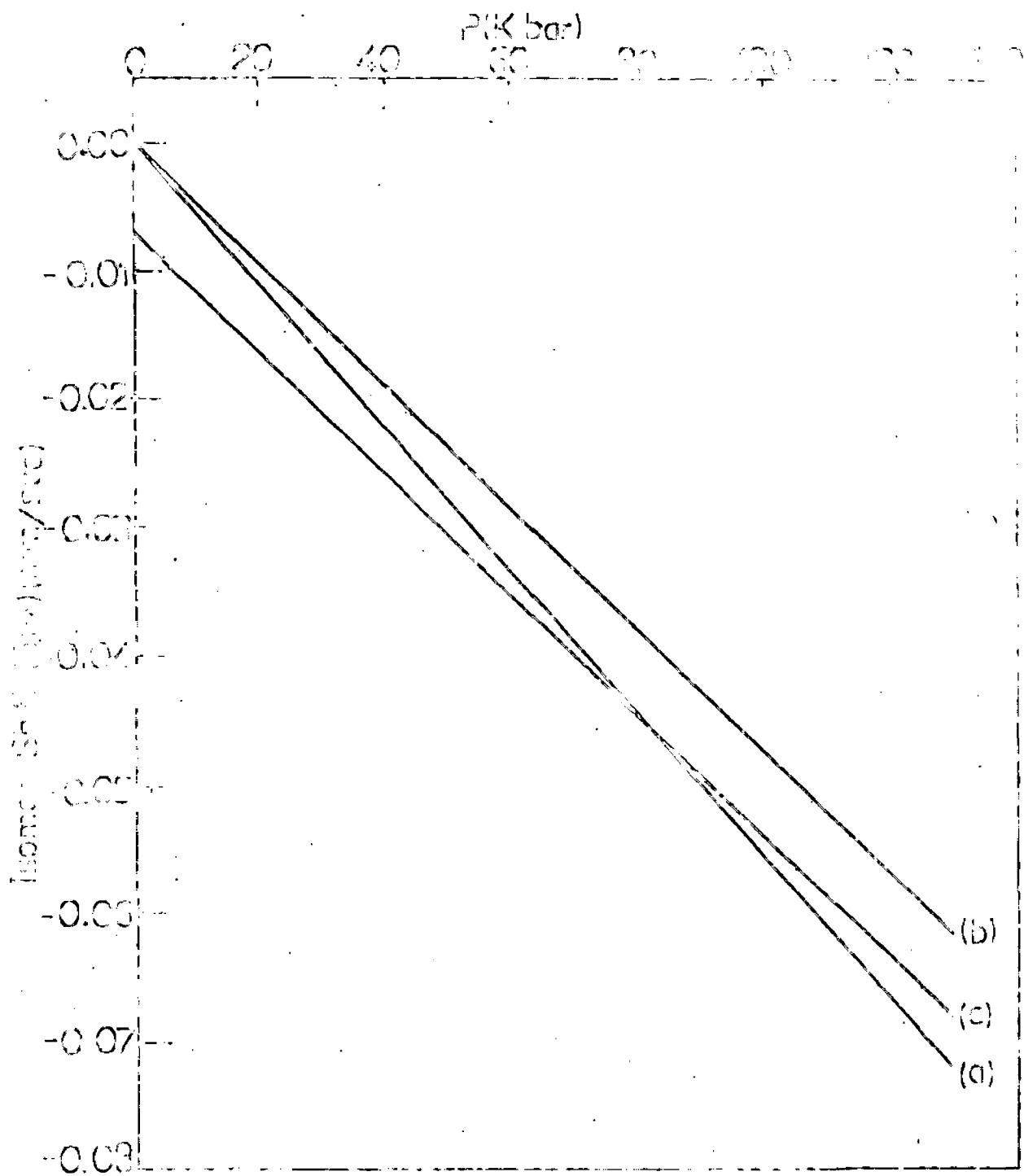


FIG.9.4 - Variation of the derived isomer shift ΔE_I with pressure at (a) 293 and (b) 94°K; (c) actual variation with pressure at 94°K as explained in the text.

Table 9.1- Input data, used in the calculation for the Mössbauer fraction f and second order Doppler shift energy δE_2

T °K	θ °K	C_{11} (10^{11} dyn/cm ²)	C_{12} dyn/cm ²	E_T 10^{-12} cm ² / dyne	C_V (cal/gm mol °K)	α ($10^{-6}/^\circ\text{K}$)	a Å	γ^*
94	0.315 229	17.434 238	12.358 238	0.712	3.610 229	9.75 167	3.604 239	1.916
298	324 41	-	-	0.750 41	-	-	-	2.00 41

* Gruneisen parameter $\gamma = 3\alpha V / K_T C_V$; molar volume $V = \frac{Na}{4}$ (for f.c.c. lattice) with 'a' the lattice constant.

Table 9.2- Results of the various calculations as explained in the text
 $(x=V_P/V_0)$

Quantity	T °K	Calculated results	Experimental results	
			(f, δE)	(f, δE)
$\frac{\partial}{\partial P} (f_{P,298}/f_{0,298})$	298	$7.38 \times 10^{-4} \text{ Kbar}^{-1}$	$(10.1 \pm 1.7) \times 10^{-4}$	$(8.14 \pm 0.65) \times 10^{-4}$
$\frac{\partial}{\partial P} (f_{P,94}/f_{0,94})$	94	$2.58 \times 10^{-4} \text{ Kbar}^{-1}$	$(5.0 \pm 2.4) \times 10^{-4}$	—
$\frac{\partial}{\partial P} ((\delta E_2)_P, 298)$	298	-5.44×10^{-5} (mm/sec.Kbar)	$-(6.11 \pm 0.49) \times 10^{-4}$ (mm/sec Kbar)	$-(5.78 \pm 0.28) \times 10^{-4}$
$\frac{\partial}{\partial P} ((\delta E_2)_P, 94)$	94	-1.415×10^{-4} (mm/sec.Kbar)	$-(6.16 \pm 0.49) \times 10^{-4}$ (mm/sec.Kbar)	—
$\frac{\partial}{\partial x} ((\delta E_2)_x, 298)$	298	0.0896 (mm/sec)	(1.0066 ± 0.0807) mm/sec.	(0.9522 ± 0.0461) mm/sec.
$\frac{\partial}{\partial x} ((\delta E_2)_x, 94)$	94	0.2331 (mm/sec)	(1.0148 ± 0.0807) mm/sec.	—

1120-

1120-

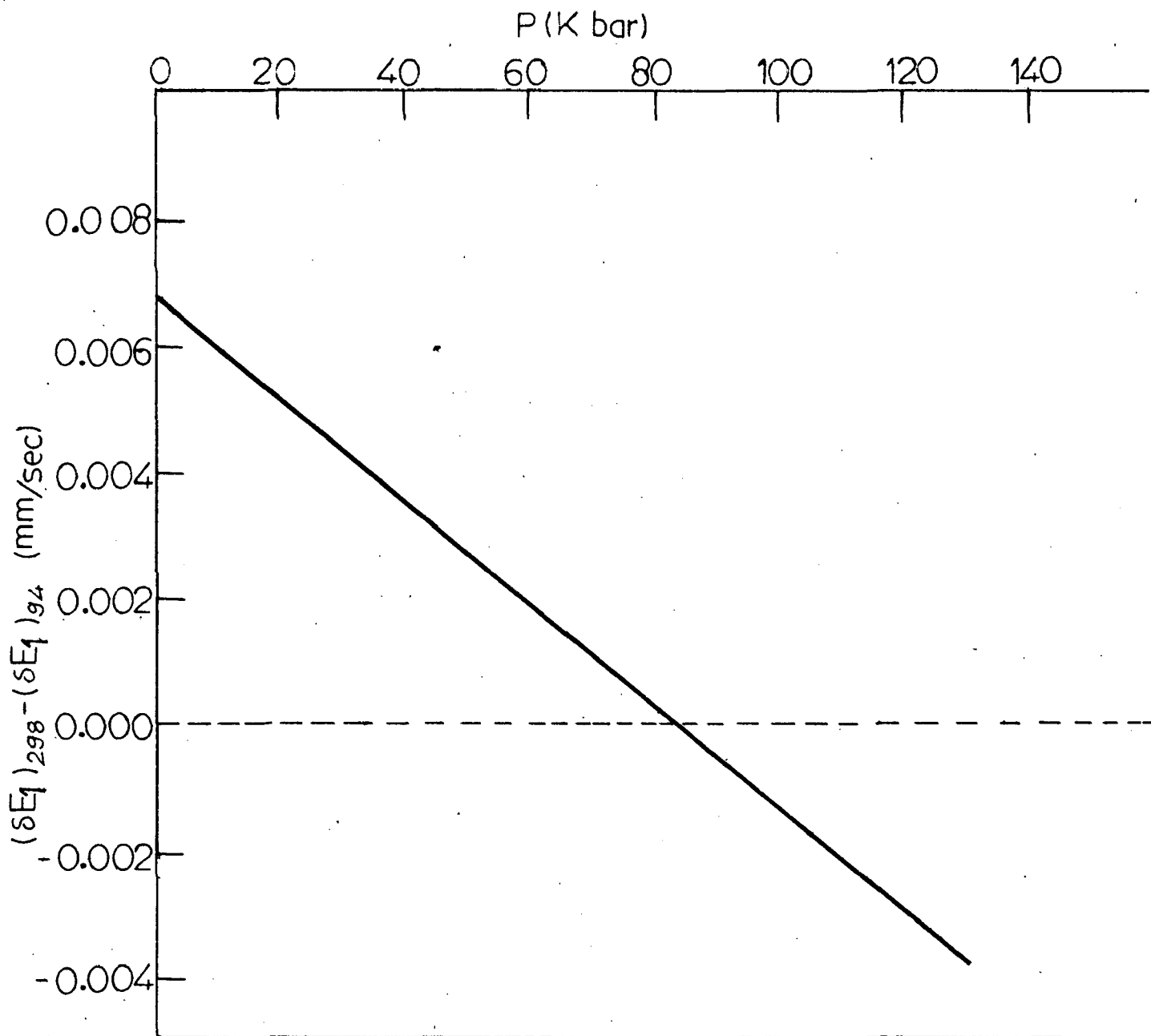


FIG.9.5- Variation of derived I.S., $(\delta E_1)_{298} - (\delta E_1)_{94}$ versus pressure.

with increase of pressure and at about 82 Kbar I.S. (hence s-electron density) at 298 becomes equal to that at 94°K and 1 bar. To explain this interesting result we consider the band structure of Cu lattice which has a rather broad 4s band overlapped by a narrow 3d band and the density of allowed energy states is much higher, in the latter one. The Fermi level lies somewhere within the 3d band. Due to the large difference in the density of states between the two bands, a small movement of the 3d band with respect to the 4s band caused by the change of pressure and temperature could result in a substantial redistribution of electronic population. Therefore the obtained results indicate that the transfer of electrons from 4s to 3d band caused by a pressure of 82 Kbar is probably counter balanced by the transfer of electrons caused by decrease in temperature. The quantitative estimation of the electronic transfer can be possible if α (proportionality constant between isomer shift and electron density at the nucleus, Eq.(7.5)) and X (s \leftrightarrow d electron transfer parameter) are known (Chapter VII). To calculate these we make use of Eq.(7.10) which gives the volume dependence of I.S. at some reference volume, say $V=V_1$. Although this equation is primarily derived for Fe^{57} in iron but we will assume that the same relation can also be applied to Fe^{57} in Cu as done by Moyzis et al. too [218]. Employing values of

the various quantities which are volume independent, the same as given in Eq.(7.12) and the volume dependent quantities as $|\Psi_{\uparrow\downarrow}(0)|^2 = 7.1a_0^{-3}$ and $7.2 a_0^{-3}$ at 298 and 94°K respectively [214] (as $|\Psi_{\uparrow\downarrow}(0)|^2 \sim CV^{-\gamma}1$ and $V(298^\circ\text{K}) = 80.0 a_0^3$, $V(94^\circ\text{K}) = 79.50 a_0^3$)

$$\left. \frac{\partial(\delta E_1)}{\partial \lambda nV} \right|_{298} = 0.917 \text{ mm/sec.} \text{ and } \left. \frac{\partial(\delta E_1)}{\partial \lambda nV} \right|_{94} = 0.782 \text{ mm/sec.,}$$

(Table (9.2), Cols. 5 and 6) in Eq.(7.10), we get the relations

$$0.917 = -4.869\alpha + 12.05\alpha X \quad \text{at } 298^\circ\text{K} \quad \dots (9.2)$$

$$0.782 = -4.935\alpha + 12.15\alpha X \quad \text{at } 94^\circ\text{K}, \quad \dots (9.3)$$

The values of I.S. variation, $\frac{\partial \delta E_1}{\partial \lambda nV}$ were obtained from converting the pressure variation of isomer shift data to volume variation through the Murnaghan equation for copper lattice [218],

$$\frac{V_P}{V_0} = \left(1 + \frac{P}{234}\right)^{-0.176} \quad \dots (9.4)$$

The relation (9.2) and (9.3) have been shown as α vs. X plots in Fig.(9.6), along with that obtained for Fe^{57} in iron at room temperature [212]. Thus the quantitative estimation of electronic transfer can be possible provided either α or X is known independently. However, from Stern's work [210], $X > 0$ so that this portion of curve would be physically meaningful region. Furthermore, it is obvious from Fig.(9.6), that the electron transfer

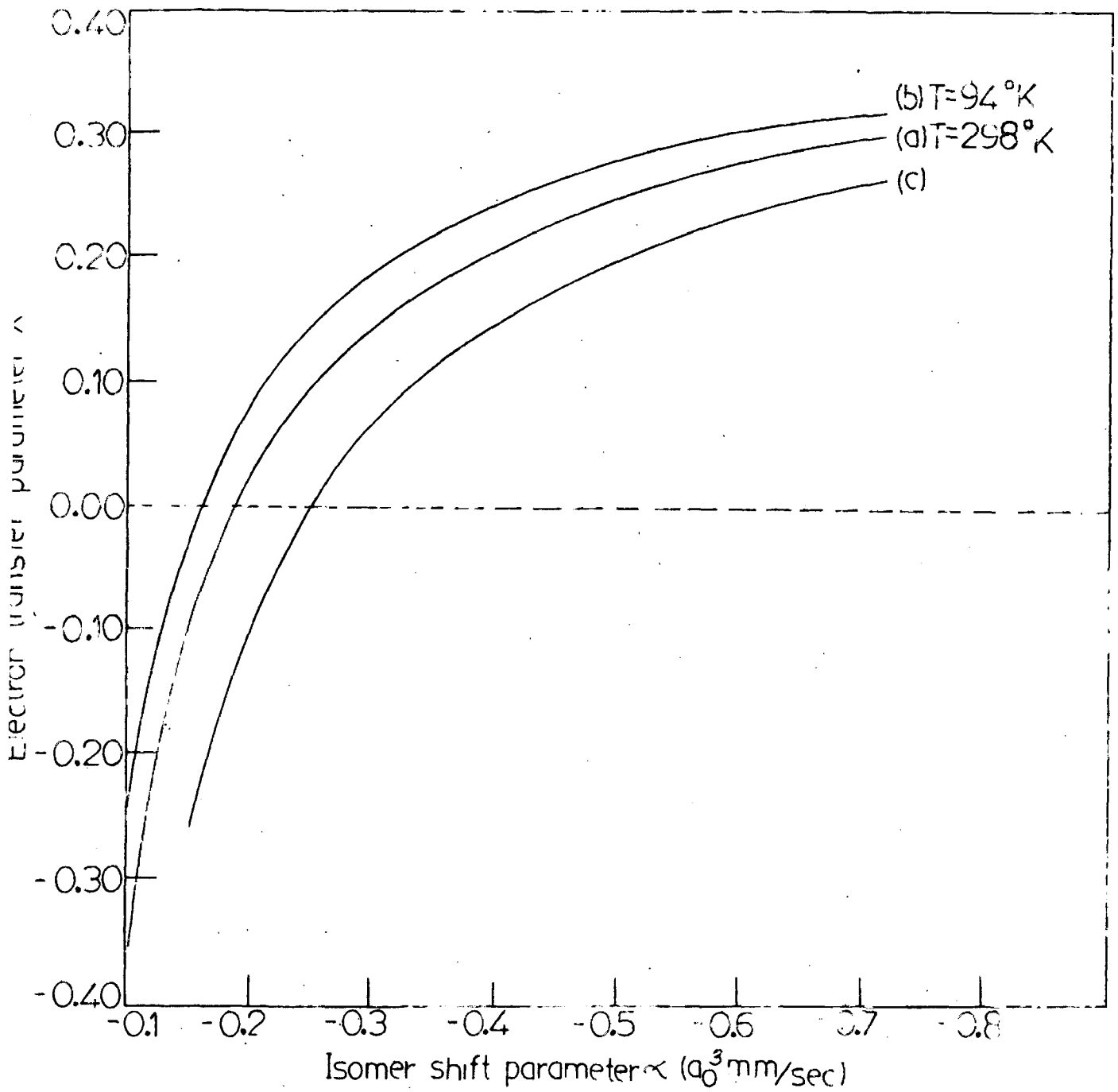


FIG.9.6- Calculated λ versus X for Fe^{57} in Cu at 298 and 94 °K (a, b) along with that obtained for Fe^{57} in Fe (c) at room temperature [2'2].

parameter X at 94°K is greater than at 298°K by about 25%. This conclusion is plausible since the decrease of temperature will cause a contraction in volume which will simulate the effect of increase of pressure.

9.4 14.4 keV TRANSITION OF Fe^{57} IN NATURAL IRON- In the previous cases the pressure studies of Mössbauer parameters at two temperatures were analysed. On the other hand Millet and Decker [241] reported Mössbauer measurements on iron at 88 Kbar and temperature upto 600°C . It was decided to analyse this data, in conjunction with the earlier measurements of Preston et.al. [205] at atmospheric pressure, in order to determine the temperature dependence of isomeric shift at 1 and 88 Kbar. [242].

Using p.f.d.f. of iron measured at room temperature by Minkiewicz et.al. [102], S.O.D. at 1 bar was calculated through Eq.(2.23). The calculations were repeated at 88 Kbar, the input p.f.d.f. having been modified through Eq.(6.3) with $V_P/V_0 = (1 + \frac{P}{275})^{-0.169}$ and $\gamma = 1.6$. The change in the calculated values of S.O.D. (δE_2) due to anharmonicity and magnetic ordering were incorporated through Eqs.(4.12), (5.7) and (5.9) with anharmonic parameter $A = 0.08052 \times 10^{-3}/^\circ\text{K}$ and magnetic ordering parameter $B_0 = 0.4$. The relative S.O.D. values at 1 and 88 K bar are shown in Figs.(9.7) and (9.8), along with the available measurements of energy shift δE at constant

volume |205,241|. The measured energy shift at constant pressure was converted to constant volume through Eq.(7.16). To quote the numerical values from Figs.(9.7) and (9.8); the energy shift $\frac{\partial}{\partial T}(\delta E)$ and S.O.D. variation $\frac{\partial}{\partial T}(\delta E_2)$ respectively are

$$7.528 \times 10^{-4} \text{ mm/sec.}^\circ\text{K} \quad |205|, \quad 6.993 \times 10^{-4} \text{ mm/sec}^\circ\text{K}$$

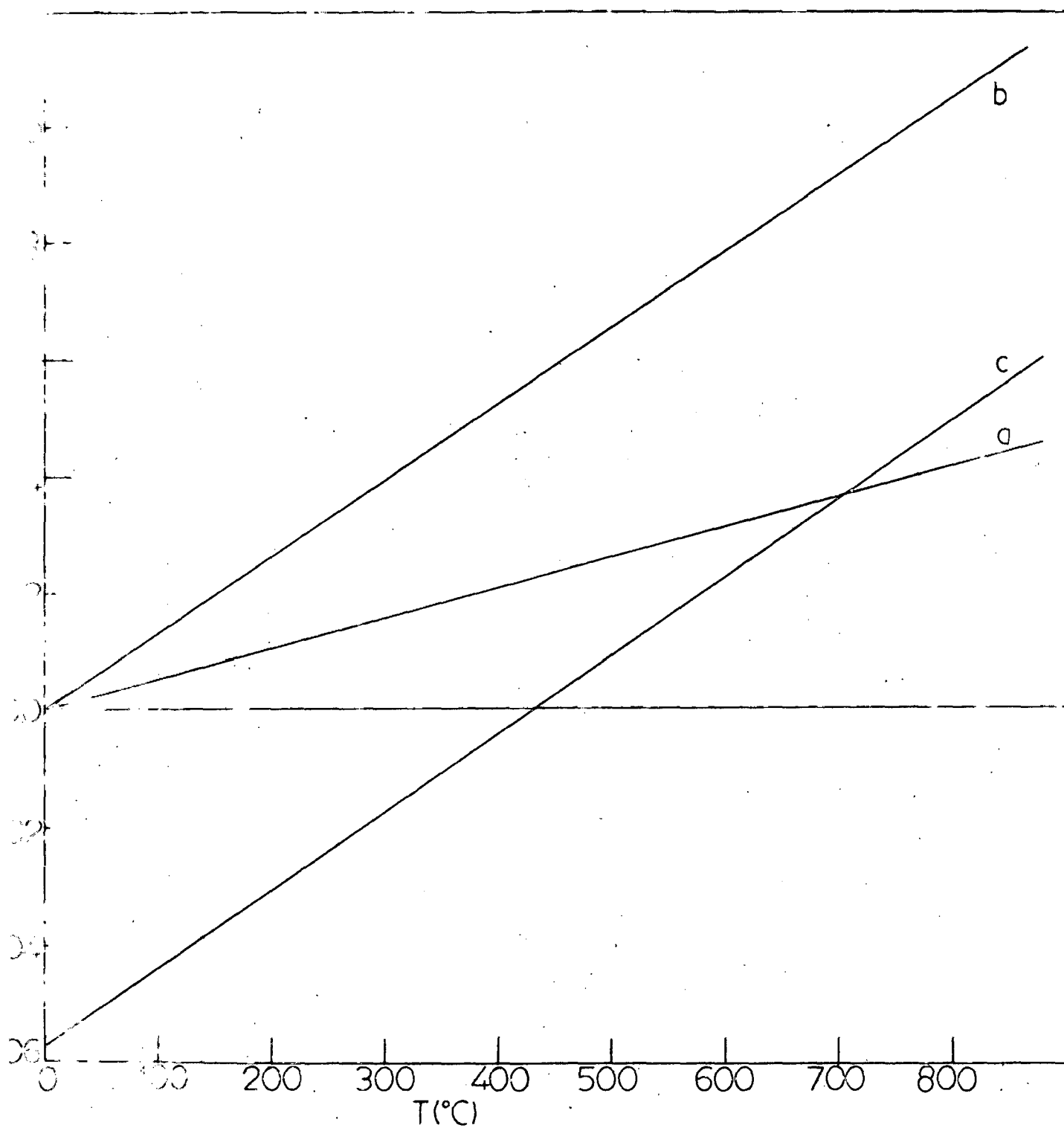
at 1 bar

and

$$8.275 \times 10^{-4} \text{ mm/sec}^\circ\text{K} \quad |241|, \quad 0.946 \times 10^{-4} \text{ mm/sec}^\circ\text{K}$$

at 88 Kbar.

Figure (9.9) gives the plot of relative variation of I.S. with temperature at these pressures. However to get meaningful information, it is more effective to plot the absolute I.S. versus temperature at these pressures. This can be obtained from Figs.(9.9a) and (9.9b) when the difference of I.S. at 1 and 88 Kbar is known from independent measurements. Employing the energy shift measurements of Moyzis and Drickamer|211|, the actual I.S. difference at 300°K comes out to be $(\delta E_1)_{88 \text{ Kbar}} - (\delta E_1)_{1 \text{ bar}} = -0.0585 + 0.0032 = -0.0553 \text{ mm/sec.}$ The resulting I.S. at different temperatures at 88 Kbar is depicted in Fig.(9.9c). The plot of $(\delta E_1)_{88 \text{ Kbar}} - (\delta E_1)_{1 \text{ bar}}$ versus temperature is shown in Fig.(9.10). It is obvious that at 700°C, the I.S. (and for that reason the s-electron density at the nucleus) at 88 Kbar becomes equal to that 1 bar and room temperature. Again



9.9. Variation of the derived i.S., ΔE_1 with temperature, (a) at 1bar and (b) at 88K. bar; (c) actual variation with temperature at 88K bar as explained in the text.

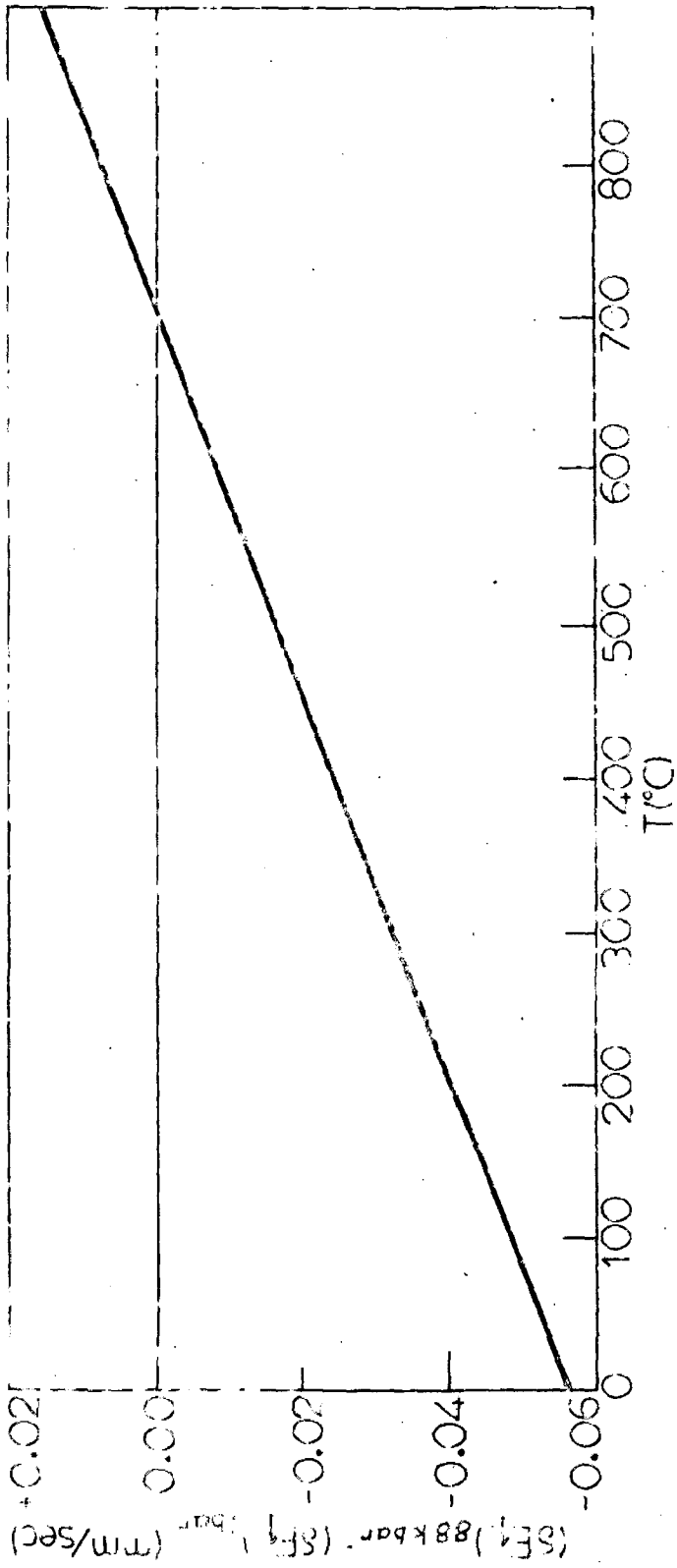


FIG.9.10- Variation of I.S. (SE)_{188kbar} - (SE)_{15cr} vs. temperature.

considering the band model of iron lattice, the above interesting result, viz. equality of s-electron at the iron nucleus at two different sets of temperature and pressure, indicates that the transfer of electrons from 4s to 3d band caused by a temperature of 700°C is probably counterbalanced by the increase in pressure. The quantitative estimation of electronic transfer can be done using Eq.(7.10) with the relation

$\frac{\partial \delta E_1}{\partial \lambda nV} = \frac{\partial \delta E_1}{\partial T} \cdot \frac{\partial T}{\partial \lambda nV}$ at the two pressures with volume expansion, $\partial \lambda nV / \partial T = 46.41 \times 10^{-6} / ^\circ K$. Employing the following set of values

$$\begin{aligned} |\Psi_{|1}(0)|^2 &= 7.10 a_0^{-3} \text{ at } P = 1 \text{ bar} \\ &= 7.57 a_0^{-3} \text{ at } P = 88 \text{ Kbar} \quad |214| \\ (V_{1\text{bar}} &= 80 a_0^3; V_{88\text{Kbar}} = 76.33 a_0^3) \end{aligned}$$

$$\begin{aligned} \frac{\partial \delta E_1}{\partial \lambda nV} &= 1.153 \text{ mm/sec at } 1 \text{ bar} \\ &= 2.864 \text{ mm/sec. at } 88 \text{ Kbar} \end{aligned}$$

with the other quantities in Eq.(7.10) which are volume independent, the same as given in Eq.(7.12), one obtains the following relations between α and X,

$$\begin{aligned} 1.153 &= -4.869\alpha + 12.05\alpha X \text{ at } 1 \text{ bar} \\ 2.864 &= -5.180\alpha + 12.52\alpha X \text{ at } 88 \text{ Kbar} \end{aligned}$$

which any independent measurement of α and X must satisfy. These are plotted in Fig.(9.11) and the plot

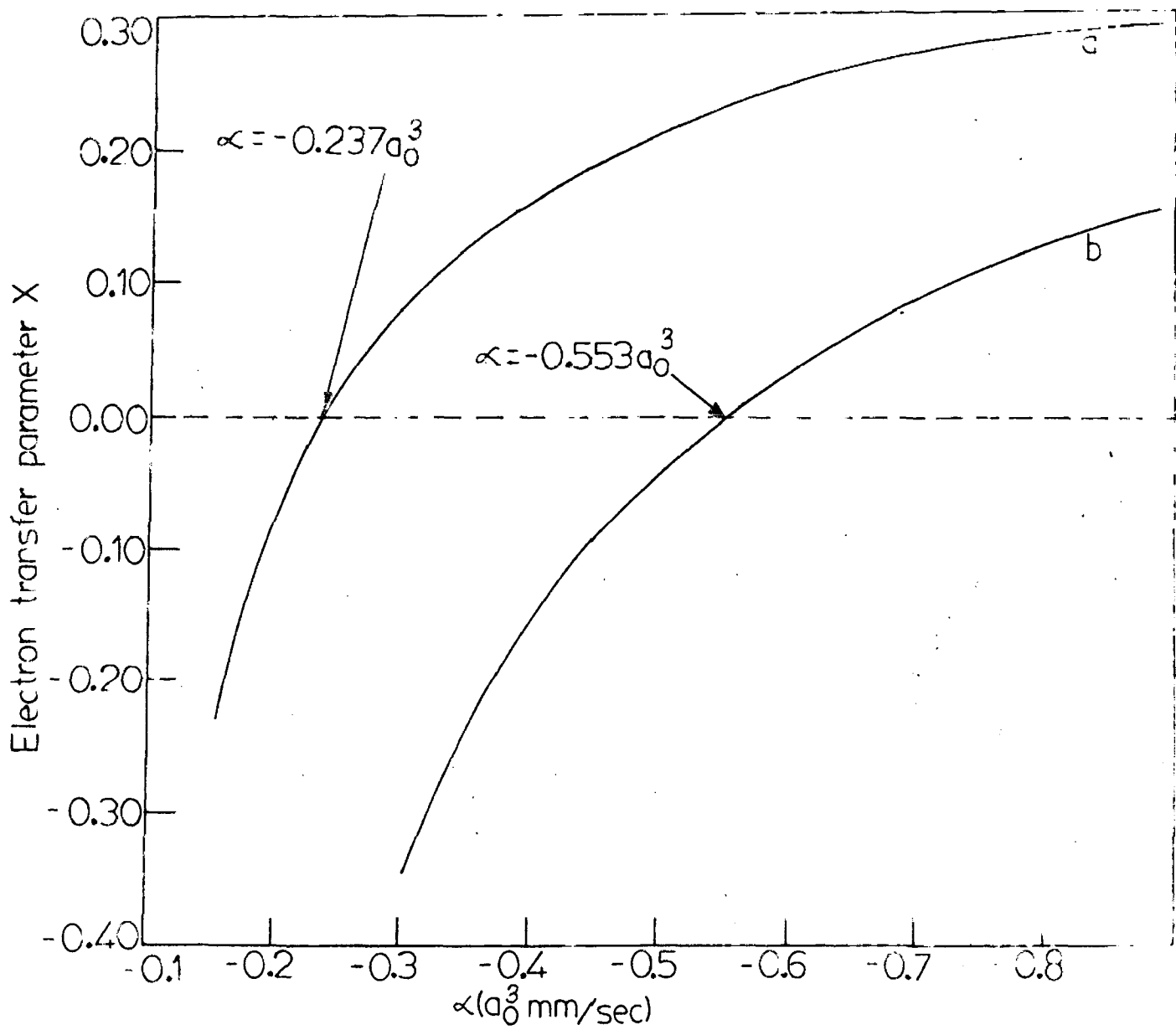


FIG.9.11- Calculated α vs. X for Fe^{57} in Iron at 1bar (a), and 88K bar (b).

gives value of $\alpha = -0.237$ and $-0.553 a_0^3$ at 1 bar and 88 Kbar respectively, for $X = 0$. i.e. assuming the s-electron density to scale with volume only without the change of shape of 4s wavefunction. The problem of quantitative estimation of electronic transfer then reduces to the problem of getting α from independent calculation.

Thus it is concluded that the combined effect of pressure and temperature on the centre shift values and Mössbauer fraction can yield useful informations.

REFERENCES

1. R.L.Mössbauer, Z. Physik 151(1958)124; Naturwissenschaften 45(1958)538; Z.Naturforsch 14A(1959) 211.
2. P.B. Moon, Proc. Phys. Soc.63(1950) 1189.
3. K.G.Malmfors in K.Siegbahn (ed.), 'Beta and Gamma ray Spectroscopy', North-Holland, Amsterdam, 1955, Chap. XVIII (II).
4. F.R.Metzger in O.R. Frisch (ed.), 'Progress in Nuclear Physics', Pergamon, New York, 1959, Vol.7.
5. F.C. Blake, Rev.Mod. Phys.5(1933) 69; R.W.James, 'Optical Principles and the Diffraction of X-Rays', Bell(1948).
6. W.E. Lamb, Phys.Rev.55(1939) 190.
7. R.L.Mössbauer, Ann.Rev.Nucl. Sci.12(1962) 123.
8. R.L. Mössbauer, in K.Siegbahn (ed.), ' α -, β and γ spectroscopy', North-Holland, Amsterdam, 1965, p.1293.
9. H.J.Lipkin, Ann.Phys.(N.Y.)9(1960) 332; 18(1962)182.
10. H.Franenfelder, 'The Mössbauer Effect', W.A.Benzamin, New York, 1962.
11. W.M. Visscher, Ann.Phys. 9(1960) 194.
12. K.S.Singwi and A.Sjolander, Phys.Rev.120(1960)1093.
13. V.I. Goldanskii and R.H.Herber, 'Chemical Applications of Mössbauer Spectroscopy' (ed.), Acad.Press, New York and London,1968. Chapt I.
14. N.N. Greenwood and T.C.Gibb, 'Mössbauer Spectroscopy', Chapman and Hall Ltd. London,1972.
15. D.E.Neagle, P.P. Craig and W.Keller, Nature,186(1960) 707.
16. Leopold May, Appl. Spectroscopy, 23(1969) 204.
17. R.Walker, G.K.Wertheim and V.Jaccarino, Phys.Rev. Letters, 6(1961) 98.

18. R.E.Watson; Tech.Rept.No.12; Solid State and Molecular Theory Group, M.I.T. (unpublished); Phys.Rev. 119(1960) 1934.
19. S.DeBenedetti, G.Lang and R.Ingalls, Phys.Rev.Letters, 6(1961) 60.
20. E.Fermi and E.Segre', Z.Physik 82(1933) 729; S.A. Goudsmit, Phys.Rev.43(1933) 636.
21. R.M. Golding in 'Applied Wave Mechanics', D.Von Nostrand Co.Ltd. London (1969), p.401.
22. R.V.Pound and G.A.Rebka, Phys.Rev.Letters 4(1960)274.
23. B.D. Josephson, Phys.Rev.Letters 4(1960)341.
24. M.H.Cohen and F.Reif, Solid State Physics 5(1957) 321.
25. E.Fluck, 'Adv. in Inorganic Chemistry and Radiochemistry' (ed.) H.J.Emoleous and A.G.Sharpe, Acad.Press, New York, 1964.
26. G.K. Wertheim, 'The Mössbauer Effect- Principles and Applications', Acad.Press 1964.
27. S.S.Hanna, J.Heberle, G.J. Parlow, R.S.Preston and D.H.Vincent, Phys. Rev.Letters, 4(1960) 513.
28. Leopold May, 'Introduction to Mössbauer Spectroscopy' (ed.), Plenum Press, New York, London,1971.
29. L.I.Schiff, 'Quantum Mechanics', McGraw Hill Book Co. Inc. New York, Toronto, London (1955), p.60.
30. H.J. Lipkin, Ann.Phys.23(1963) 28; 26(1964) 115.
31. A.A.Maradudin and P.A. Flinn, Phys.Rev.126(1962) 2059.
32. M.Lax and I.Waller, Phys.Rev.138(1965) A523.
33. M.A. Krivoglaz, Sovt. Phys.JETP. 19(1964)432.
34. A.H.Muir, in Tables and Graphs for computing Debye-Waller-Factors in Mössbauer Effect Studies, Rep.A1-6699. Atomic International, Calif.1962.
35. D.A.O'Conner, Nuclr. Instr.Methods.21(1963) 318.
36. G.A.Bykov and Pham.Zuy. Heim, Sovt. Phys.JETP.16 (1963), 646.

37. R.M. Housely, N.E.Erickson and J.G.Dash, Nuclr.Instr. Methods 27(1964) 29.
38. W.A.Steyart and R.D.Taylor, Phys.Rev.134(1964) A716.
39. B.Kolk and B.Harwig, Nuclr. Instr. Methods 94(1971) 211.
40. G.W.Lehman and R.E.DeWames, Phys.Rev.131(1963)1008.
41. S.S.Nandwani and S.P.Puri, Phys.Status, Solidi. 41(1970) 199.
42. D.Raj and S.P.Puri, J.Phys.Chem.Solids. 33(1972), 2177.
43. S.S.Nandwani and S.P.Puri, Phys. Letters.(In Press)1973.
44. D.P.Johnson and J.G.Dash, Phys.Rev.172(1968)985.
45. Y.Hazony, P.Hillman, M.Pasternak and S.L.Ruby, Phys. Letters 2(1962)337.
46. H.Shechter, J.G.Dash, G.A.Erickson and R.Ingalls, Phys.Rev.2B(1970)613.
47. W.M.Visscher, Phys.Rev.134(1964) A965.
48. K.Chandra and S.P.Puri, Phys.Rev.169(1968) 272;
V.K.Garg and S.P.Puri, J.Chem.Phys.54(1971) 209.
49. C.J.Meechan and A.H.Muir, Rev.Mod.Phys.36(1964) 438.
50. W.Kundig, K.Ando and H.Bömmel, Phys.Rev.139(1965)4889.
51. V.I.Goldanskii, E.F.Makarov and V.K.Kharapov, Phys. Letters.3(1963)344; Sovt. Phys. JETP.17(1963) 508.
52. H.A.Stockler and H.Sano, Phys.Rev.165(1968) 406.
53. R.H.Herber and S.Chandra, J.Chem.Phys.52(1970) 6045;
54(1971) 1847; R.H.Herber, S.Chandra and Y.Hazony,
J.Chem.Phys. 53(1970) 3330.
54. J.W.Burton, H.Frauenfelder and R.P.Goodwin, Proc. Vienna. Conf.on the Mössbauer Effect. (Tech.Report Series No.50) 1966, p.73.
55. P.A.Flinn, S.L.Ruby and W.K.Kehl, Science 143(1964)1434.
56. S.Anderson and B.Kasemo, Solid State Comm.8(1970) 1885.
57. M.Rich, Phys.Letter. 4(1963) 153.

58. U.Gonser, J.Phys.Chem.66(1962) 564.
59. G.K.Wertheim and R.H.Herber, J.Chem.Phys.38(1963) 2106.
60. S.Bukshan and R.H.Herber, J.Chem.Phys.46(1967) 3375; 48(1968) 4242.
61. Y.Hazony, J.Chem.Phys.45(1966) 2664.
62. Y.Hazony, Discussion of the Faraday Soc.48(1969)148.
63. J.Dlouha, Czech. J.Phys. B16(1966) 495; O.Litzman, ibid. 18(1968) 1587.
64. T.A. Kitchen and R.D.Taylor, Mössbauer Effect Methodology, Vol.5 (Plenum Press, 1969) p.123; R.D.Taylor and P.P.Craig, Phys.Rev.175(1968) 782.
65. D.Suganthy, R.Fatehally and T.M.Haridasan, Proc. Nuclr. and Solid State Phys.Symposium, 14C(1972)283.
66. P.P.Craig, T.A. Kitchen and R.D. Taylor, Phys.Rev., 1B (1970) 1103.
67. M.L. McMillan, Phys.Rev.167(1968) 331.
68. A.J.F. Boyle and H.E.Hall, Repts. Prog.Phys.XXV(1962) 441; A.A.Abrikosov, I.M.Khalatnikov, Sovt.Phys.JETP,14 (1962) 389.
69. S.P.Taneja, A.E.Dwight, L.Gilbert, W.C.Harper, C.W., Kimball and C.Wood, J.Phys.Chem.Glasses 13(1972)153; C.R.Kurkjian and E.A. Sigety, ibid 9(1968) 73.
70. V.G. Bhide in 'A Short Course in Solid State Physics' Vol.1 (ed.) F.C.Auluck, Thomson Press Ltd., Publication Division (N.Delhi, India), 1971; P.A.Montano, H.Shechter and U.Shimony, Phys.Rev.3B(1971) 858.
71. S.W.Marshall and R.W.Wilenzick, Phys.Rev.Letters. 16(1966) 219; D.Schroerer, 'Mössbauer Effect Methodology' Vol.5, 141, Plenum Press, 1969; R.Ruppin, Phys.Rev.2B (1970) (1970) 1229.
72. B.P. Srivastava, H.N.K.Sharma and D.L. Bhattacharya, Phys. Status Solidi 45b(1971), 647; 49b(1972) 329.
73. I.Dezsi, L.Keszthelyi, B.Molnar and L.Poes, Hung, Acad. Sci.Rept. KFKI 9/1967, Budapest; D.L.Uhrich, J.M.Wilson and R.A.Resch, Phys.Rev.Letters. 24(1970) 355.
74. Y.P. Varshni and R.Blanchard, Phys.Letters 30A(1969) 238.

75. S.S.Jaswal, Phys. Letters. 19(1965) 369; Phys.Rev. 144(1966) 353.
76. D.Raj and S.P.Puri, J.Phys.Soc. Japan 27(1969) 788; Phys. Letters 29A(1969) 510.
77. H.Schuster and I.Bostock, Phys.Letters 35A(1971)31.
78. J.J.Bara, Proc. Conf. on the Application of the Mössbauer Effect, Tihany, 1969, p.93(ed.I.Dezsi), Akademiai Kiado, Budapest 1971.
79. S.S.Nandwani, D.Raj and S.P.Puri, J.Phys.C.Solid State Physics. 4(1971) 1929.
80. S.S.Nandwani and S.P.Puri, J.Phys.Chem.Solids 33 (1972) 973.
81. S.S.Nandwani, Ram Munjal and S.P.Puri, Solid State Communications (communicated) 1973.
82. S.S.Nandwani and S.P.Puri, J.Phys.Chem.Solids(comm-unicated) 1973.
83. K.Gilbert and C.E. Violet, Phys.Letters. 28A(1968) 285.
84. B.Kolk, Phys. Letters. 35A(1971) 83.
85. J.S. Brown and G.K.Horton, Phys.Rev.Letters, 18(1967) 647.
86. W.B.Daniels, G.Shirane, B.C.Frazer, H.Umerbayashi and J.A. Leake; Phys.Rev.Letters 18(1967) 548.
87. N.P.Gupta and P.K. Gupta, Canad.J.Phys.47(1969) 617.
88. J.Walkley, J.Chem.Phys. 44(1966) 2417.
89. L.X.Finegold and N.E. Philips, Phys.Rev.177(1969) 1383.
90. N.P. Gupta, Czech. J.Phys. B22(1972) 1022.
91. N.P. Gupta, Aust. J.Phys. 22(1969) 471.
92. K.Mahesh and N.D. Sharma, Phys.Status Solidi:44b(1971) 167.
93. P.Vashishta and K.N. Pathak, Physica, 48(1970) 474.
94. T.A.Kovats and J.C. Walker, Phys. Rev.181(1969) 610.
95. E.A. Owen and E.W.Evans, Brit. J.Appl.Phys.18(1967) 611.

96. B. Sharan and L.M. Tiwari, Phys. Status. Solidi. 3(1963) 1408.
97. P.S. Mahesh and B. Dayal, Phys. Rev. 143(1966) 443.
98. J. Behari and B.B. Tripathi, J. Phys. Soc. Japan 33 (1972) 1207.
99. P. Schweiss, A. Furrer and W. Bührer, Helv. Phys. Acta. 40(1967), 378.
100. B.N. Brockhouse, H.E. Abou-Helai and E.D. Hallman, Solid State Comm. 5(1967), 211.
101. J. Bergsma, C. VanDijk and D. Tocchetti, Phys. Letters 24A(1967) 270.
102. V.J. Minkiewicz, G. Shirane and R. Nathans, Phys. Rev. 162 (1967) 528.
103. D.J. Erickson, L.D. Roberts, J.W. Burton and J.O. Thomson, Phys. Rev. 3B (1971) 2180.
104. N. Egede Christensen and B.O. Seraphin, Phys. Rev. 4B (1971) 3321.
105. B.W. Hafemeister, G. DePasquali and H. DeWaard, Phys. Rev. 135(1964) B1089.
106. A.J.F. Boyle and G.J. Perlow, Phys. Rev. 151(1966) 211.
107. R. Kamal, R.G. Mendiratta, S.B. Raju and L.M. Tiwari, Phys. Letters. 25A(1967) 503.
108. K. Mahesh and N.D. Sharma, Phys. Letters 28A(1968) 377.
109. T.M. Haridasan and R. Nandini, Phys. Letters 28A(1968) 301.
110. Yu. Kagan and Y.A. Maslov, Sovt. Phys. JETP 14(1962) 922.
111. E.W. Kellermann, Phil. Trans. R. Soc. A239(1940) 513.
112. A.D.B. Woods, B.N. Brockhouse and W. Cochran, Phys. Rev. 119(1960) 980.
113. W. Bührer and W. Halg, Phys. Status, Solidi 46b(1971) 679 (Private Communication with Dr. W. Bührer).
114. A.M. Karo, J. Chem. Phys. 31(1959) 1489.
115. E.R. Cowley and R.A. Cowley, Proc. R. Soc. A292(1966) 209.



116. G.Dolling, R.A. Cowley, C.Schittenhelm and I.M. Thorson, Phys. Rev.147(1966) 577.
117. Satya Pal, J.Chem.Phys.56(1972) 6234.
118. A.J.F. Boyle and G.J.Perlow, Phys.Rev.149(1966) 165.
119. M.Pasternak, A.Simopoulos and Y.Hazony, Phys.Rev. 140A(1965) 1892.
120. M. Pasternak and T.Sonnino, J.Chem.Phys.48(1968)2004.
121. G.Leibfried and W.Ludwig, Solid State Physics.(ed.) F.Scitz. and D.Turnbell (Academic Press Inc., New York), Vol.12 (1961) p.275.
122. A.A. Maradudin and P.A. Flinn, Phys.Rev.129(1963) 2529.
123. R.A. Cowley, Adv. Phys. 12(1963) 421.
124. K.N.Pathak, Phys. Rev.139A(1965) 1569.
125. T.R.Koehler, 'A New Theory of Lattice Dynamics at 0°K ', IBM Research Report.RJ457, 1967;
126. A.A. Maradudin and A.E.Fein, Phys.Rev.128(1962) 2589.
127. J.J. Kokkedde, **Physica** 28(1962) 374.
128. R.Stedman, L.Almquist and G.Nilsson, Phys.Rev.162, (1967) 549.
129. G.Gilat and R.M. Nicklow, Phys.Rev.143(1966) 487.
130. W.C.Overton in 'Lattice Dynamics', (ed.) R.F.Wallis (Oxford; Pergamon) 1965, p.287.
131. V.V.Goldman, Phys.Rev.174(1968) 1041.
132. J.S. Brown, Phys.Rev.187(1969) 401.
133. A.J. Leadbetter, J.Phys.C. Solid State Physics 1(1968) 1481, 1489.
134. D.L.Losee and R.O. Simmons, Phys.Rev.172(1968) 944.
135. T.H.K. Barron in 'Lattice Dynamics' (ed.) R.F.Wallis (Oxford, Pergamon) 1965, p.247.
136. L.S.Salter, Adv.Phys.14(1965) 1.
137. R.H.Nussbaum, D.G. Howard, W.L. Nees and C.F.Steen, Phys. Rev.173(1968) 653.

138. C.Feldman, M.L. Klein and G.K.Horton, Phys.Rev. 184(1969) 910.
139. E.Grüneisen, Ann.d.Physik 26(1908) 211.
140. W.C. Overton, J.Phys.Chem.Solids 29(1968) 711.
141. D.N. Batchelder, D.L. Losee and R.O.Simmons, Phys. Rev.162(1967) 767.
142. J.L. Feldman, G.K. Horton and J.B.Lurie, J.Phys.Chem. Solids 26(1965) 1507.
143. M.N.Saha and B.N.Srivastava in 'A Treatise on Heat', The Indian Press Publication Pvt. Ltd., Allahabad,1965, p.713.
144. D.C.Wallace, Phys. Rev.133(1963) 2046; 133(1964) A153.
145. R.H.Beaumont, H.Chihara and J.Morrison, Proc.Phys. Soc.78(1961) 1462.
146. J.L. Feldman and G.K.Horton, Proc. Phys.Soc.92(1967) 227.
147. L.X.Finegold and N.E.Philips, Phys.Rev.177(1969) 1383.
148. J.S.Brown, Phys.Rev.3B (1971) 21.
149. M.L.Klein, G.K. Horton and J.L.Feldman, Phys.Rev. 184(1969) 968.
150. D.L.Losee and R.O. Simmons, Phys.Rev.172(1968) 934.
151. D.L. Losee and R.O. Simmons, Phys.Rev. Letters 18 (1967) 451.
152. A.O.Urvas, D.L. Losee and R.O. Simmons, J.Phys.Chem. Solids 28(1967) 2269.
153. T.H.K. Barron and M.L. Klein, Proc. Phys.Soc. 85(1965) 533.
154. M.L.Klein and G.K. Horton, in 'Proc.Eleventh Int. Conf.on Low Temperature Phys', St.Andrews, Scotland 1968, p.553.
155. J.W. Leech and J.A. Reissland, J.Phys. C.Solid State Phys. 3(1970)987.
156. N.S.Gills, N.R.Werthamer and T.R.Koehler, Phys.Rev.165 (1968) 951.

157. V.V.Goldman, G.K.Hortan and M.L.Klein, Phys.Rev. Letters, 21(1968) 1527.
158. N.R.Werthamer, Ann. J.Phys. 37(1969)763.
159. J.A.Rayne and B.S.Chandersekhar, Phys.Rev.122(1961), 1714.
160. A.E.Lord and D.N.Besher, J.Appl.Phys.36(1965) 1620.
161. J.Lees and A.E.Lord, J.Appl.Phys.39(1968) 3986.
162. N.Ridley and H.Stuart, Brit.J.Appl.Phys.Ser.2, 1 (1968), 1291.
163. K.K.Kelley, J.Chem.Phys.11(1943) 16.
164. J.M.D. Coey, G.A. Sawatzky and A.H.Morrish, Phys.Rev. 184(1969) 334.
165. Sh.Sh. Bashkirow and G.Ya. Selyutin, Phys.Status Solidi 26(1968) 253.
166. T.H.Geballe and W.R.Giauque, J.Am.Chem. Soc. 74 (1952) 2368.
167. D.P. Fraser and A.C.Hollis-Hallett, Canad.J.Phys.43 (1965) 193.
168. F.F.Kos, Phys.Letters 28A(1968) 219.
169. J.R.Neighbours and G.A. Alers, Phys.Rev.111(1958)707,
170. L.A.Alekseev, P.L. Gruzin, M.N. Uspenskii and M.R. Gryaznov, JETP Letters 14(1971) 192.
171. Sh.Sh. Bashkirov, G.Ya. Selyutin and V.A.Chistyakov, Sovt. Phys. Doklady 13(1968) 449.
172. M.Hayase, M.Shiga and Y.Nakamura, Phys.Status Solidi 46b(1971) K 117.
173. Fred Masset and J.Callaway, Phys.Rev.2B (1970) 3657.
174. Sh.Sh. Bashkirov and G.Ya. Selyutin, Sovt. Phys.Solid State 9(1968) 2284.
175. A.A.Maradudin, P.A.Flinn and I.M. Radcliffe, Ann.Phys. 26(1964) 81.
176. G.K. Wertheim, D.N.E. Buchanan and H.J.Guggenheim, Phys.Rev.2B(1970) 1392.

177. R.M. Housley and F.Hess, Phys. Rev.164(1967) 340.
178. C.Kittel, Introduction to Solid State Physics, Wiley, 1956, p.154.
179. M.W.Zemansky, Heat and Thermodynamics, McGraw Hill Publ.Co., Inc. IV Edition, 1957, p.268.
180. Russel V.Hanks, Phys.Rev.124(1961) 1319.
181. J.Dlouha, Czech. J.Phys. 14B (1964) 571.
182. W.H.Southwell, D.L.Decker and H.B.Vanfleet, Phys. Rev.171 (1968) 354.
183. V.N.Panyushkin and F.F.Voronov, JETP Letters 2(1965) 97.
184. D.W. Hafemeister and E.B.Shera, Phys.Rev.Letters 14(1965) 593; Mossbauer Effect Methodology Vol.3(ed.) I.J. Gruverman (Plenum Press, New York) 1967,p.231.
185. S.N.Vaidya and G.C.Kennedy, J.Phys.Chem.Solids. 31 (1970) 2329.
186. R.G.McQueen and S.P.Marsh, J.Appl.Phys.31(1960) 1253.
187. P.W.Bridgman, Proc.Am.Acad.Arts.Sci.: 76(1945)1.
188. P.W.Bridgman, Proc.Am.Acad.Arts.Sci.: 76(1948) 55.
189. M.Sorai, J.Phys.Soc. Japan, 25(1968) 421.
190. N.F.Mott and H.Jones, 'The Theory of Properties of Metals and Alloys' (Dover Publ. Inc., New York), 1958.
191. V.G.Shapiro and V.S.Shipinel, Sovt. Phys. JETP 19 (1964) 1321.
192. M.J.P.Musgrave, Proc. Royal. Soc.A272(1963) 503.
193. A.J.F.Boyle, D.St. P.Bunbury, C.Edward and H.E.Hall, Proc. Phys.Soc.77(1961) 129.
194. J.L.Feldman and G.K.Horton, Phys.Rev.132 (1963) 644.
195. S.S.Nandwani and S.P.Puri, Phys.Status Solidi (Communicated) 1973.
196. P.W. Bridgman, Proc. Am.Acad. Arts.Sci.77(1949) 189.
197. R.A.Cowley, A.D.B. Wood and G.Dolling, Phys.Rev. 150(1966) 487.

198. S.N. Vaidya, I.C. Getting and G.C.Kennedy, J.Phys. Chem.Solids 32(1971) 2545.
199. R.S.Srivastava and K.Singh, Phys.Status Solidi, 39(1970) 25.
200. S.S.Nandwani and S.P.Puri, Phys.Status, Solidi. (Communicated) 1973.
201. H.K.Mao, William A.Bassett and T.Takahashi, A.Appl. Phys.38(1967) 272.
202. J.J.M. Franse, R.Winkel, R.J.Veen and G.deVries, Physica 33(1967) 475.
203. H.B.Vanfleet and D.L.Decker, Report No.9761-03, 1966; Grant No:AFOSR 708-65(unpublished) (cited from Ref.118).
204. R.V.Pound, Phys.Rev.140B(1965) 788.
205. R.S. Preston, S.S.Hanna and J.Heberle, Phys.Rev.128 (1962) 2207.
206. G.M. Rothberg, S.Guimard and N.Benczerkoller, Phys. Rev.1B (1970) 136.
207. A.Simpulos and I.Pelah, J.Chem.Phys.51(1969) 5691.
208. R.Ingalls, Phys.Rev.155(1967) 157.
209. E.Clementi, I.B.M., J.Res.Development. Suppl. 9(1965)2.
210. F.Stern, Phys.Rev.116(1959) 1399.
211. J.A.Moyzis and H.G.Drickamer, Phys.Rev.171(1968), 389.
212. S.S.Nandwani and S.P.Puri, J.Phys.Chem.Solids, 34(1973), 711.
213. Z.S.Basinski, W.H.Rothery and A.L.Sutton, Proc. R. Soc. London 229A(1955) 459.
214. Prof. R.Ingalls (Private communication).
215. R.M. Nicklow, G.Gilat, H.G.Smith, L.J. Raubernheimer and M.K. Wilkinson, Phys.Rev.164(1967), 922.
216. S.Alexander and D.Treves, Phys.Letters 20(1966) 134.
217. A.A.Maradudin, Solid State Physics (ed.) F.Seitz and D.Turnbell (Academic Press Inc., New York) Vol.18 (1966), 273.

218. J.A.Moyzis, G.DePasquali and H.G.Drickamer, Phys. Rev. 172(1968) 665.
219. W.M.Visscher, Phys. Rev.129(1963) 28.
220. P.D.Mannheim, Phys.Rev.165(1968) 1011.
221. J.Bara and A.Z.Hryniewicz, Phys. Status Solidi 15(1966) 205.
222. S.M. Qaim, J.Phys.F.Metal Phys.1(1971) 320.
223. P.D. Mannheim and A.Simopoulos, Phys.Rev.165(1968), 845.
224. D.G.Howard and J.G.Dash, J.Appl. Phys.38(1967)991.
225. D.Raj and S.P.Puri, Solid State Physics and Nuclear Physics Symp., Roorkee, 1969. Abs.No.20.
226. D.Raj and S.P.Puri, Phys.Letters, 33A(1970) 306.
227. R.H.Busey and W.F.Giaque, J.Am.Chem. Soc. 74(1952) 3157.
228. J.A. Rayne and W.R.G. Kemp, Phil.Mag.1(1956) 918.
229. D.L.Martin, Canad.J.Phys. 38(1960) 17.
230. John. L.Stokes, Ph.D. Thesis (Unpublished) 1972,p.76.
231. American Institute of Physics Handbook (McGraw Hill, New York, 1963), 2nd Edition.
232. R.E.Macfarlene, J.A.Rayne and C.K.Jones, Phys.Letters 18(1965) 91.
233. M.Shimizu and A.Katsuki, J.Phys.Soc.Japan 19(1964), 1135.
234. J.M.Walsh, M.H.Rice, R.G.McQueen and F.L.Yarger, Phys.Rev.108(1957), 196.
235. K.Patnaik and J.Mahanty, Solid State Comm.6(1968),899.
236. D.L.Williamson and R.Ingalls, Phys.Letters, 34A(1971), 33.
237. S.S.Nandwani and S.P.Puri, Phys.Status. Solidi , 57 (1973) 43.

238. W.C.Overton and J.Gaffney, Phys. Rev.98(1955), 969.
239. G.B.Mitra and S.K. Mitra, Ind.J.Phys.37(1963) 462.
240. A.P.Miller and B.N.Brockhouse, Canad.J.Phys.49(1971),
704.
241. L.E.Millet and D.L. Decker, Phys.Letters 29A(1967)7.
242. S.S.Nandwani and S.P.Puri, Phys.Status Solidi.
(communicated- revised manuscript),1973.

12. 'Pressure Variation of the Probability of Mössbauer Effect for 29.4 keV Transition in K^{40} ,' with S.P.Puri, Phys. Status Solidi (communicated), 1973.

13. 'Mössbauer Spectrum Shift in Spin Ordered System', G.C.Shukla and S.S.Nandwani, Presented at Nuclear Physics and Solid State Physics Symposium (Chandigarh), 1972 (Dec., 28-31).

